INVESTIGATION OF CELLULAR RESPONSES IN A PATIENT WITH STAT1
GAIN-OF-FUNCTION MUTATION SUCCESSFULLY TRANSPLANTED
WITH RUXOLITINIB BRIDGE THERAPY AND CHARACTERIZATION OF
ANTI-VIRAL IMMUNE RESPONSES IN DOCK8 DEFICIENCY

A THESIS SUBMITTED TO
THE GRADUATE SCHOOL OF NATURAL AND APPLIED SCIENCES
OF
MIDDLE EAST TECHNICAL UNIVERSITY

BY

BAŞAK KAYAOĞLU

IN PARTIAL FULFILLMENT OF THE REQUIREMENTS
FOR
THE DEGREE OF DOCTOR OF PHILOSOPHY
IN
BIOLOGY

JANUARY 2023

Approval of the thesis:

INVESTIGATION OF CELLULAR RESPONSES IN A PATIENT WITH STAT1 GAIN-OF-FUNCTION MUTATION SUCCESSFULLY TRANSPLANTED WITH RUXOLITINIB BRIDGE THERAPY AND CHARACTERIZATION OF ANTI-VIRAL IMMUNE RESPONSES IN DOCK8 DEFICIENCY

submitted by **BAŞAK KAYAOĞLU** in partial fulfillment of the requirements for the degree of **Doctor of Philosophy** in **Biology, Middle East Technical University** by,

Prof. Dr. Halil Kalıpçılar
Dean, Graduate School of **Natural and Applied Sciences**   _____

Prof. Dr. Ayşe Gül Gözen
Head of the Department, **Biological Sciences**   _____

Prof. Dr. Mesut Muyan
Supervisor, **Biological Sciences, METU**   _____

Examining Committee Members:

Prof. Dr. Mayda Gürsel
IBG, Dokuz Eylül University   _____

Prof. Dr. Mesut Muyan
Biological Sciences**,** METU   _____

Prof. Dr. Safa Barış
Pediatric Immunology, Marmara University   _____

Assoc. Prof. Dr. Erkan Kiriş
Biological Sciences**,** METU   _____

Asst. Prof. Dr. Banu Bayyurt Kocabaş
Biological Sciences, METU   _____

Date: 17.01.2023

I hereby declare that all information in this document has been obtained and presented in accordance with academic rules and ethical conduct. I also declare that, as required by these rules and conduct, I have fully cited and referenced all material and results that are not original to this work.

Name Last name : Başak Kayaoğlu

Signature :

ABSTRACT

INVESTIGATION OF CELLULAR RESPONSES IN A PATIENT WITH STAT1 GAIN-OF-FUNCTION MUTATION SUCCESSFULLY TRANSPLANTED WITH RUXOLITINIB BRIDGE THERAPY AND CHARACTERIZATION OF ANTI-VIRAL IMMUNE RESPONSES IN DOCK8 DEFICIENCY

Kayaoğlu, Başak
Doctor of Philosophy, Biology
Supervisor: Prof. Dr. Mesut Muyan

January 2023, 128 pages

Gain-of-function mutations (GOF) in the *STAT1* gene are associated with impaired STAT1 phosphorylation/dephosphorylation cycle and Th17 deficiency. A sporadic T835M mutation in the STAT1 gene was detected in a patient with chronic mucocutaneous candidiasis (CMC), viral and bacterial infections accompanied by autoimmunity. Here, we aimed to investigate the cellular level defects in the patient and how they were affected by Ruxolitinib treatment and hematopoietic stem cell transplantation (HSCT). We showed that Ruxolitinib treatment partially restored the dysregulated STAT1 phosphorylation dynamics but failed to improve Th17 deficiency, whereas both functions were normalized following HSCT. Furthermore, STAT1 GOF patient showed a dysregulated gene expression profile, which was partially improved with Ruxolitinib treatment and completely normalized with HSCT. Our results suggest that improved disease management and relatively normalized gene expression profile can be achieved with Ruxolitinib treatment

before transplantation and this would be beneficial to reduce the risk of adverse outcome of HSCT. Herein, we also investigated the underlying mechanisms leading to susceptibility to viral infections in DOCK8 deficiency. Differential gene expression analysis followed by principal component analysis (PCA) on 15 patients with DOCK8 deficiency revealed that the patients clustered into two distinct groups relative to healthy controls. One group of patients showed increased expression of interferon-stimulated genes (ISGs) and immune exhaustion markers but presented with compromised type I interferon response to stimulation with several different nucleic acid ligands. Our preliminary findings indicate that this dysregulated interferon response might be the consequence of the "exhausted phenotype" of innate immune cells caused by chronically elevated interferon signature.

ÖZ

RUXOLITINIB KÖPRÜ TERAPİSİ İLE BAŞARIYLA NAKLİ YAPILAN STAT1 İŞLEV KAZANIM MUTASYONLU BİR HASTADA HÜCRE YANITLARININ KARAKTERİZASYONU VE DOCK8 EKSİKLİĞİNDE BOZULMUŞ VİRAL İMMÜNİTE İLE İLİŞKİLİ SİNYAL YOLAKLARININ ANALİZİ

Kayaoğlu, Başak
Doktora, Biyoloji
Tez Yöneticisi: Prof. Dr. Mesut Muyan

Ocak 2023, 128 sayfa

STAT1 genindeki fonksiyon kazanımı mutasyonları (GOF), bozulmuş STAT1 fosforilasyon/defosforilasyon döngüsü ve Th17 eksikliği ile ilişkilidir. Otoimmünitenin eşlik ettiği kronik mukokutanöz kandidiyazis (CMC), viral ve bakteriyel enfeksiyonları olan bir hastada STAT1 geninde sporadik T835M mutasyonu tespit edildi. Bu çalışmada, bu mutasyon sonucunda ortaya çıkan hücresel düzeydeki bozuklukları ve Ruksolitinib tedavisi ile hematopoietik kök hücre transplantasyonunun (HKHT) bu bozuklukları nasıl etkilendiğini araştırmayı amaçladık. Ruksolitinib tedavisinin düzensiz STAT1 fosforilasyon dinamiklerini kısmen düzelttiğini, ancak Th17 eksikliğinin iyileşme göstermediğini saptarken, HKHT sonrasında bütün bozukların normale döndüğünü gösterdik. Ayrıca, STAT1 GOF hastası, Ruksolitinib tedavisi ile kısmen iyileştirilmiş ve HKHT ile tamamen normale dönmüş, düzensiz bir gen ekspresyon profili göstermiştir. Sonuçlarımız, transplantasyon öncesi Ruksolitinib köprü tedavisi ile iyileştirilmiş hastalık yönetimi ve kısmi olarak düzelmiş gen ekspresyon profilinin elde edilebileceğini ve bunun HKHT'nin oluşabilecek olumsuz sonuçlarını azaltmada faydalı olabileceğini

göstermektedir. Bunun dışında, DOCK8 eksikliğinde gözlenen viral enfeksiyonlara yatkınlığa yol açan mekanizmaları, nükleik asit ligandları ile stimülasyon üzerine tehlikeli bir tip I interferon salgılanmasını öneren önceki bulgularımızın ışığında araştırdık. DOCK8 eksikliği olan 15 hasta, diferansiyel olarak eksprese edilen genlerinin temel bileşen analizine (TBA) göre iki gruba ayrıldı. Bir grup hastada, interferon ile uyarılan genlerin ve bağışıklık tükenme belirteçlerinin ekspresyonunda artış saptandı. Ön bulgularımız, DOCK8 eksikliği olan hücrelerden bozulmuş interferon üretiminin, kronik olarak yüksek olan interferon imzasının neden olduğu doğuştan gelen bağışıklık hücrelerinin "tükenmiş fenotipinin" bir sonucu olabileceğini göstermektedir.

Anahtar Kelimeler: STAT1 GOF, Ruksolitinib, DOCK8 Eksikliği, viral bağışıklık, bağışıklık tükenimi

To my family,

ACKNOWLEDGMENTS

my daughter, Deniz Kayaoğlu, for giving me unlimited happiness and teaching me time management in an enjoyable way.

TABLE OF CONTENTS

LIST OF TABLES

TABLES

LIST OF FIGURES

LIST OF ABBREVIATIONS

AD	Autosomal dominant
AIM2	Absent in melanoma 2
ALP	Alkaline phosphatase
AP-1	Activator protein 1
APC	Antigen presenting cell
AR	Autosomal recessive
ASC	Apoptosis associated speck-like protein containing a CARD
BCR	B-cell Receptor
BDCA2	Blood dendritic cell antigen 2
CAP1	Cyclase Associated Actin Cytoskeleton Regulatory Protein 1
CARD	Caspase activation and recruitment domain
CCL	C-C Motif Chemokine Ligand
CD	Cluster of differentiation
CDS	Cytosolic DNA sensor
CDT	Carboxy-terminal domain
cGAMP	Cyclic GMP-AMP
cGAS	Cyclic GMP-AMP synthase
CLR	C-type lectin receptor
CMC	Chronic mucocutaneous candidiasis
CMV	Cytomegalovirus

CSTL	Cathepsin L
CTLA-4	Cytotoxic T lymphocyte antigen 4
CXCL	Chemokine (C-X-C) ligand
DAMP	Damage-associated molecular patterns
DC	Dendritic cell
DIDS	DOCK8 immunodeficiency syndrome
DOCK8	Dedicator of cytokinesis 8
EBV	Epstein–Barr virus
ELISA	Enzyme-linked immunosorbent assay
ERK	Extracellular signal-regulated kinase
FACS	Fluorescence-activated cell sorting
FBS	Fetal bovide serum
FCS	Forward scatter
GAS	Gamma interferon activation site
GBP	Guanylate-binding protein
GEF	Guanine nucleotide exchange factor
GOF	Gain-of-function
GvHD	Graft vs host disease
HIES	Hyper-IgE syndrome
HKCA	Heat-killed Candida albicans
HSCT	Hematopoietic stem cell transplantation
HSV	Herpes simplex virus

ICOS	Inducible T-cell co-stimulator
IFI	Gamma-interferon-inducible protein
IFIT	interferon-induced protein with tetratricopeptide repeats
IFN	Interferon
IFNAR	Interferon-alpha/beta receptor
IFNGR	Interferon-gamma receptor
IgE	Immunoglobulin E
IKK	Inhibitor of κB kinase
IL	Interleukin
IP-10	Interferon gamma-induced protein 10
IRAK	Interleukin-1 receptor associated kinase
IRF	Interferon regulatory factor
ISG	Interferon-stimulated gene
ISRE	IFN-stimulated response element
JAK	Janus Kinase
JNK	c-Jun N-terminal kinases
LAG-3	Lymphocyte-activation gene 3
LAMP	Lysosomal-associated membrane protein
LGP2	Laboratory of Genetics and Physiology 2
LPS	Lipopolysaccharide
LSM	Lymphocyte separation medium
MAPK	Mitogen-activated protein kinase

MAVS	Mitochondrial antiviral signaling protein
MDA5	Melanoma differentiation-associated protein 5
MHC	Major histocompatibility complex
MyD88	Myeloid differentiation factor-88
NEMO	NF-κB essential modulator
NFAT	Nuclear factor of activated T-cells
NF-κB	Nuclear factor- kappa B
NK	Natural kill
NLR	NOD-like receptor
NLRP	NLR family pyrin domain containing
NOD	Nucleotide oligomerization domain
OAS	2'-5'-Oligoadenylate Synthetase
ODN	Oligodeoxynucleotide
PAMP	Pathogen-associated molecular patterns
PBMC	Peripheral blood mononuclear cells
PCA	Principal component analysis
PD-1	Programmed cell death protein 1
pDC	Plasmacytoid dendritic cell
PD-L1	Programmed death-ligand 1
PID	Primary immunodeficiency disease
PKR	Protein kinase R
PMA	phorbol 12-myristate 13-acetate

PNPP	p-Nitrophenyl Phosphate
PRR	Pattern recognition receptor
PSMB	Proteasome subunit beta
PYHIN	Pyrin and HIN
R848	Resiquimod
RIG-I	retinoic acid-inducible gene I
RLR	RIG-like receptor
RPMI	Roswell Park Memorial Institute
SAVI	STING-associated vasculopathy with onset in infancy
SLE	Systemic lupus erythematosus
SOCS	Suppressor of cytokine signaling proteins
SSC	Side scatter
STAT	Signal transducer and activator of transcription
STING	Stimulator of interferon genes
TAK1	TGF-β activated kinase 1
TAP	Transporter associated with antigen processing
TBK1	TANK-binding kinase 1
TCL1A	T-cell leukemia/lymphoma protein 1A
TCR	T cell receptor
Th	Helper T-cell
TIGIT	T cell immunoreceptor with Ig and ITIM domains
TIM-3	T-cell immunoglobulin and mucin domain 3

TLR	Toll-like receptor
TNF	Tumour Necrosis Factor
TRAF	TNF-receptor associated factor
Treg	Regulatory helper T-cell
TREX1	Three prime repair exonuclease 1
TRIF	TIR-domain-containing adapter-inducing interferon-β
TYK2	Tyrosine kinase 2

CHAPTER 1

INTRODUCTION

1.1   Innate and Adaptive Immune System

The immune system is the body's defense mechanism against infectious agents and other harmful substances. The protection against a potential danger can be achieved by a complex network of effector cells and molecules collectively named as the immune system. First, the presence of a danger such as infection is detected by the white blood cells of the innate immune system. This innate immune recognition is achieved through a multitude of sensors specialized to specifically bind to molecular patterns expressed by certain groups of pathogens. Next, the effector function of immunity comes into play to eliminate the source of danger through the recruitment of leukocytes and the release of effector molecules such as proteins of the complement system. The innate immune response is rapidly generated following an encounter with a foreign molecule and eliminates the danger before it accumulates. Occasionally innate immunity fails to eliminate infection or other sorts of dangers, in which case the adaptive immune system takes the wheel to generate a more targeted and effective immune response through the specific recognition function of lymphocytes. The antigen receptors generated by somatic gene-segment arrangements can achieve the specific recognition function of T-cells and B-cells (Gellert, 1992). Therefore, they can recognize billions of different antigens of foreign origin. The self-recognizing T-cell and B-cells were mostly eliminated in the course of development by means of negative selection in the thymus and bone marrow, respectively (Stritesky et al., 2012). The generation of a proper adaptive immune response takes several days. However, once produced, long-lasting protection is acquired. Adaptive immunity enables the establishment of immunological memory,

providing a rapid and more effective memory response to secondary and subsequent encounters. The cell-mediated adaptive immunity is driven by the activation of T-lymphocytes through the recognition of specific antigens via T-cell receptors (TCR) expressed on their surface. Until the encounter of T-cells with their specific antigens, they are called naïve T-cells. The transformation of naïve T-cells to effector T-cells requires the presentation of processed antigens embedded in the major histocompatibility complex (MHC) on the surface of antigen-presenting cells (APCs). The signal coming from the interaction between MHC and TCR is not sufficient enough for the activation and differentiation of naïve T-cells. Additional stimuli including co-stimulatory molecules and cytokines are needed for this priming process. Cytotoxic (CD8$^+$) T-cells recognize cytosolic antigens presented on MHC Class I molecules on target cells. Conversely, antigens internalized and processed in the endosomal/lysosomal compartment are presented on MHC Class II molecules on the surface of APCs, which are recognized by the helper (CD4$^+$) T-cells (Guéguen & Long, 1996). Helper T-cells differentiate into a variety of subsets with distinct effector functions. In general, Th1 cells are responsible for activating the infected cells to facilitate the killing of intracellular pathogens, whereas Th2 cells activate B-cells to induce class switching and IgE antibody production to fight against parasitic infections. Th17 cells, on the other hand, function in the clearance of extracellular bacteria and fungi. In addition, regulatory helper T-cells (Tregs) play a pivotal role in restraining immune response to prevent autoimmunity (Reiner, 2007). Furthermore, specific antibody molecules secreted from plasma cells provide the humoral part of immunity. Upon binding an antigen to a B-cell receptor (BCR), B-cells proliferate and differentiate into plasma cells with help from previously activated helper T-cells. All the components of the immune system work in harmony by interacting with each other. However, any impairment in this regulated system leads to immune-related diseases, including allergies, autoimmunity and immunodeficiency diseases.

1.1.1 Innate Immunity and Pattern Recognition

Anatomical barriers, including epithelial cells and mucosal surfaces, prevent pathogens from entering and colonizing the body. If the pathogen can break through the first-line of defense, the antimicrobial peptides and complement system will come into play, limiting the colonization of pathogens. Simultaneously, the inflammatory response is initiated and effector cells are recruited to the site of infection (Murphy & Weaver, 2016). Innate immune cells include dendritic cells (DCs), monocytes, macrophages, granulocytes, natural killer (NK) cells and innate lymphoid cells (Marshall et al., 2018). Dendritic cells (DCs) are generally divided into two subsets according to their developmental lineages. The myeloid-derived DCs (mDCs) perform phagocytosis for the sampling of extracellular material to the T-cells, whereas lymphoid-originated ones, plasmacytoid dendritic cells (pDCs), are the professional IFN-α producers. The other phagocytotic cells of the immune system are monocytes, macrophages and granulocytes, which are essential in elimination of pathogens and apoptotic cells (Fond & Ravichandran, 2016). NK cells are derived from the common lymphoid progenitor but are considered as part of the innate immune system due to their invariant receptors. In other words, the immune recognition by NK cells does not occur specifically by recognizing an antigen, but depends on the altered expression of MHC Class I molecules on the infected or tumor cell (Raulet, 2006).

For the proper function of innate immunity, cells should be able to differentiate self from non-self both for the phagocytosis and the generation of an inflammatory response. This discrimination is provided by a variety of pattern recognition receptors (PRRs) that sense the presence of pathogen-associated molecular patterns (PAMPs) (Takeuchi & Akira, 2010). The pathogens harbor certain repetitive molecular structures such as lipopolysaccharides (LPS) found in the cell wall of Gram-negative bacteria. Similarly, viral and bacterial nucleic acids have distinct properties that are not shared by mammalian cells. Additionally, the host-derived damage-associate molecular patterns (DAMPs) released from the damaged or dying cells can be recognized by certain PRRs to activate the immune system (Roh & Sohn,

2018). The inflammatory response triggered upon the recognition of PAMPs/DAMPs by PRRs includes the regulation of transcription, cytokine and chemokine secretion, the release of antimicrobial peptides and the recruitment of phagocytes (Saxena & Yeretssian, 2014). Toll-like receptors are a family of membrane-bound PRRs that recognize extracellular PAMPs. TLRs are composed of two main domains: a ligand-binding ectodomain and a TIR domain involved in downstream signaling. The binding of a corresponding ligand to the ectodomain of TLR molecule results in the recruitment of adaptor molecules to the cytoplasmic TIR domain, to initiate a signaling cascade (O'Neill & Bowie, 2007). The plasma membrane-bound TLRs are mainly responsible for the detection of the cell wall or membrane components of infectious agents. For instance, lipopolysaccharide (LPS), the outer membrane component of Gram-negative bacteria, is recognized by TLR4, whereas flagellin, the major structural protein of bacterial flagella, is sensed by TLR5 (Kawai & Akira, 2006). In contrast, the recognition of pathogen-associated nucleic acids occurs in the endosomal compartments where the endosomal TLRs reside. General properties of TLR-mediated signaling is summarized in Figure 1-1.
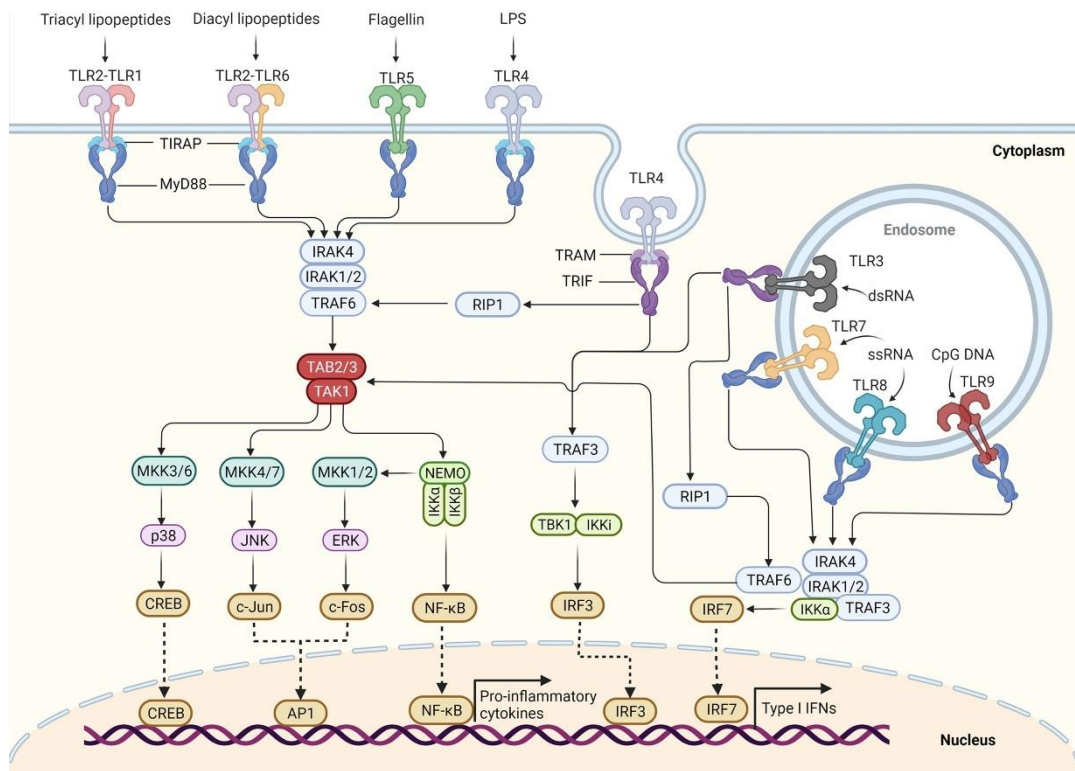
Figure 1-1: TLR signaling pathway in innate immune cells. (Duan et al., 2022)

Another transmembrane protein family, C-type lectin receptors (CLRs), primarily recognize fungal-derived PAMPs and modulate anti-fungal immune responses (Nikolakopoulou et al., 2020). The detection of cytoplasmic PAMPs is performed by three main families of cytosolic PRRs, including the NOD-like receptors (NLRs), RIG-like receptors (RLRs) and cytosolic DNA sensors (CDS). The presence of bacterial-derived molecules such as peptidoglycan or flagella in the cytosol is detected by NLRs which results in the generation of inflammatory response, autophagy and cell death (Ting et al., 2008). Additionally, RLRs and CDS function in the recognition of nucleic acids in the cytosol.

1.1.1.1 Nucleic Acid Sensing

The digestion of engulfed extracellular pathogen results in the localization of microbial nucleic acids in endosomal compartments where the nucleic acid sensing-TLRs reside. The microbial DNA fragments containing unmethylated CpG motifs bind to TLR9, triggering the NF-κB and IRF-mediated production of pro-inflammatory cytokines and type I interferons, respectively (Kumagai et al., 2008). The binding of unmethylated CpG-enriched DNA to TLR9 results in the dimerization and conformational change of TLR9, leading to the recruitment of an adaptor molecule, MyD88. Next, the interaction between MyD88 and TLR9 subsequently recruits IRAK1 and IRAK4, forming a complex to activate TAK1. The activated TAK1 further phosphorylates the IKK complex, subsequently inducing NF-κB activation. Ligand-induced TLR9 signaling in pDCs results in IRF7-mediated type I IFN production through the formation of TRAF6, IRAK1 and IRAK4 complex (Huang & Yang, 2010). In addition to TLR9, TLR7 is predominantly expressed in pDCs, whereas the expression of TLR8 is primarily observed in monocytes, macrophages and conventional DCs (Cervantes et al., 2012). Both TLR7 and TLR8 recognize single-stranded RNA molecules released into endosomes upon internalization of ssRNA viruses. The sequence-independent detection of ssRNA molecules by TLR7/8 triggers the transcription of pro-inflammatory cytokines and type I IFNs via IRAK4-dependent signaling, similar to TLR9 (Cushing et al., 2017). Following the digestion of dsRNA viruses in phagosomes, dsRNA strings bind to endosomal TLR3 and induce a TRIF-mediated inflammatory response. Different from other endosomal TLRs, ligand-induced dimerization of TLR3 is followed by the recruitment of adaptor molecule TRIF, which interacts with TRAF3 and TRAF6. The downstream of TRAF6-depending signaling involves induction of inflammatory cytokines through the sequential activation of TAK1 and NF-κB signaling, whereas the TRAF3-mediated signaling mainly depends on the phosphorylation-induced activation of TBK1 and IRF3, resulting in the production of type I IFNs (Kawasaki & Kawai, 2014).

Viral RNAs produced within the cytosol are detected by a protein family called RIG-like receptors (RLRs) with three members. The first identified member of the RLR family, RIG-I, bears a pocket in the carboxy-terminal domain (CDT) that senses the unmodified 5'triphosphate moieties on viral genomes. The recognition of the base-pairing portion of dsRNA by the helicase domain of RIG-I is also required to achieve full activation (Rehwinkel & Gack, 2020). The second RLR, MDA5, senses viral genomic dsRNA delivered and/or replicated in the cytoplasm. Conversely, the recognition of dsRNA molecules does not require a specific motif but rather relies on the cooperative assembly of MDA5 filaments along the length of dsRNA (Peisley et al., 2011). Upon ligand binding, RIG-I and MDA5 interact with the mitochondrial antiviral-signaling protein (MAVS) via their caspase activation and recruitment domains (CARD), triggering TBK1/IKKε signaling cascade which in turn activates NF-κB and IRF3-mediated transcription of type I IFN (Reikine et al., 2014). The last member of the RLR family, LGP2 does not possess signal-transducing activity due to its missing CARD domain. The high-affinity binding of LPG2 to dsRNA facilitates the interaction between dsRNA and MDA5, enhancing MAVS activation and anti-viral signaling (Bruns & Horvath, 2015). In contrast, LPG2 has been shown to negatively regulate the activity of RIG-I, independent from the dsRNA binding capability of LGP2 (Li et al., 2009).

Apart from the RLRs inducing antiviral immune response, there are several sensors with direct antiviral activity. For instance, the genomic viral ssRNA molecules bearing 5'ppp moieties are recognized by IFIT1, blocking its translation (Abbas et al., 2013). Another example for such a receptor is double-stranded RNA-dependent protein kinase R (PKR), which controls the replication of RNA viruses by negatively regulating mRNA translation in the host upon binding to dsRNA strings (García et al., 2006). The RNA recognition by anti-viral protein OAS1 promotes the generation of secondary messenger 2′-5′-oligoadenylate, which in turn activates RNase L, inducing the degradation of viral and host RNAs (Hornung et al., 2014).

The recognition of cytosolic RNA molecules by NLRP3 inflammasomes plays a pivotal role in anti-viral and anti-bacterial immunity. NLRP3 inflammasomes are

capable of sensing a variety of RNA molecules, including bacterial mRNAs, tRNA and rRNAs, viral-originated RNAs and RNA:DNA hybrids, triggering inflammasome assembly and caspase 1-dependent pro-inflammatory cytokine secretion (Choudhury et al., 2021; Kailasan Vanaja et al., 2014; Sha et al., 2014). The principles of RNA recognition by endosomal TLRs and cytosolic sensors is outlined in Figure 1-2.
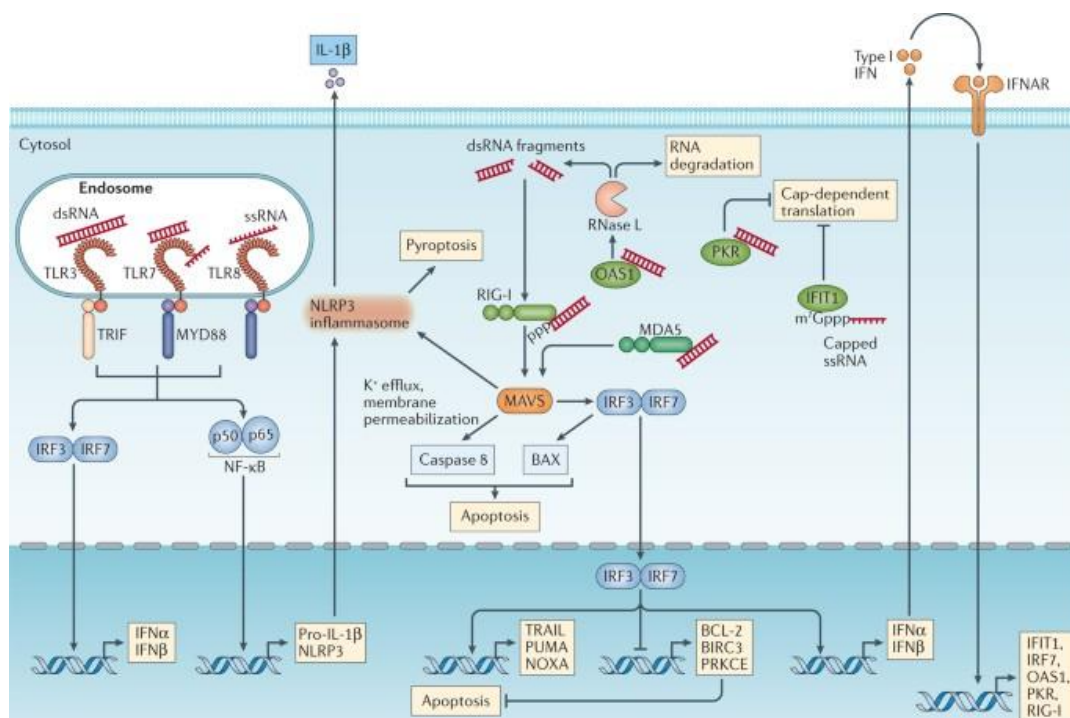
Figure 1-2: RNA sensing receptors (Schlee & Hartmann, 2016)

Presence of dsDNA in the cytoplasm is observed under certain conditions, including endogenous DNA leakage from nucleus caused by damage and during infections with an intracellular pathogen. Cytoplasmic DNAs are sensed by a variety of DNA receptors within the cell inducing an immune response. The detection of dsDNA in cytoplasm induces the activation of several cytosolic DNA sensors, cGAS, IFI16 and DDX41, leading to STING-mediated interferon response and autophagy (Gui et al., 2019). The most predominantly found cytosolic DNA sensor, cyclic GMP-AMP

(cGAMP) synthase, cGAS, binds to DNA in the cytosol and catalyze the synthesis of cyclic GMP-AMP (cGAMP) from ATP and GTP. The endoplasmic reticulum (ER) membrane-associated adaptor molecule STING senses this secondary messenger cGAMP, leading to the activation of type I interferon production in a TBK1/IRF3-dependent manner (Chen et al., 2016). Additionally, cGAMP-induced LC3 lipidation, a hallmark of autophagy, occurs through the cGAS-STING signaling pathway, resulting in the clearance of DNA viruses and intracellular bacteria (Gui et al., 2019).

The DNA-induced inflammasome activation involves the recognition of cytosolic long dsDNA strings by AIM2, IFI16 and NLRP3. The PYHIN family protein, AIM2, interacts with the adaptor molecule ASC upon binding to dsDNA, inducing pyroptosis (Hornung et al., 2009). Another PYHIN family member, IFI16, can also induce the inflammasome assembly upon dsDNA binding, in addition to its role in the induction of interferon response (Kerur et al., 2011). The DNA sensing molecules and mechanisms are summarized in Figure 1-3.
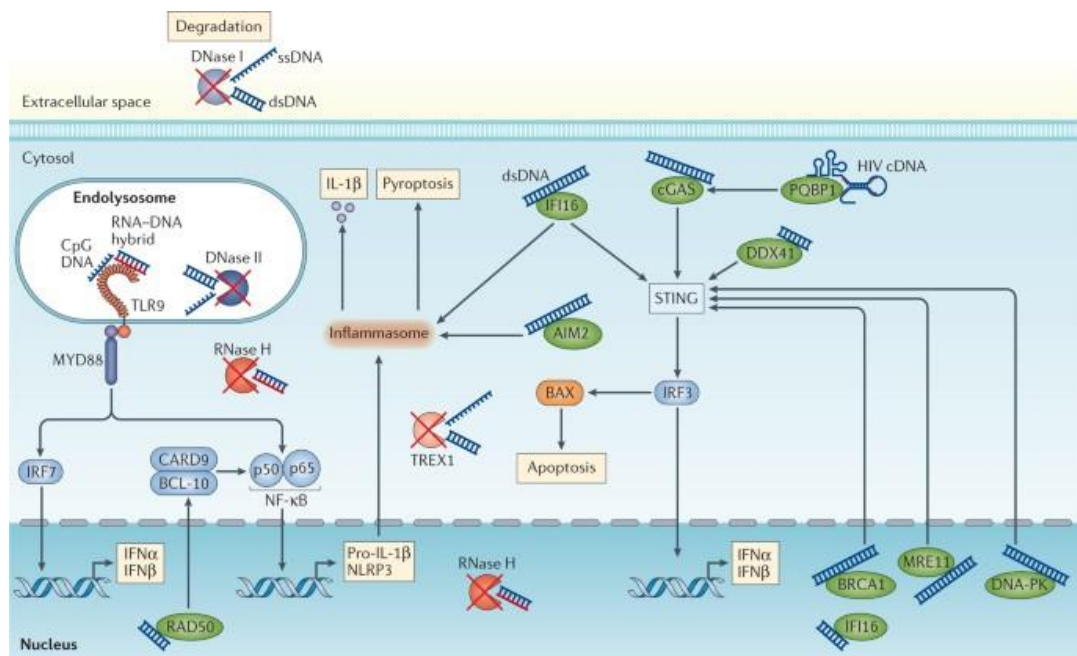
Figure 1-3: DNA sensing receptors (Schlee & Hartmann, 2016)

1.1.1.2   JAK/STAT Signaling

In the previous section, the generation of cytokine response following PRR activation was covered. The cytokines can be defined as secreted effector molecules that regulate major cell functions including survival, proliferation, differentiation, immune response and cell death. Cytokines that bind to the largest class of cytokine receptors, the type I/II cytokine receptor, include most of the interleukins (ILs), growth hormones, colony-stimulatory factors and interferons (O'Shea et al., 2019). Each of these cytokines binds to a distinct receptor inducing diverse outcomes but they all use the same signal transduction mechanism, the JAK/STAT pathway.

Type I/II cytokine receptors lack the intrinsic enzymatic activity that can drive signaling events. Ligand-induced dimerization of these receptors brings the Janus Kinases (JAKs) into close proximity and allows the auto and transphosphorylation (Jamilloux et al., 2019). Activated JAKs phosphorylate the cytoplasmic tail of cytokine receptors, creating a docking site for the recruitment of other signaling proteins, most importantly the members of STAT family (O'Shea et al., 2019). The members of JAK family, JAK1, JAK2, JAK3 and TYK2, selectively associate with certain cytokine receptors, leading to the recruitment of specific STAT molecules. The phosphorylated STATs dimerize and translocate to the nucleus, where they regulate the expression of target genes (Murphy & Weaver, 2016). There are seven members of the STAT family, STAT1, STAT2, STAT3, STAT4, STAT5A, STAT5B and STAT6, each with diverse target genes. All JAKs and STATs play a pivotal role in the regulation of cellular events which can be understood from the defects of these signaling molecules leading to a variety of conditions including immunodeficiency, autoimmunity and cancer (O'Shea et al., 2013). The cytokines, their corresponding receptors, their signaling partners and the expected outcomes of their defects are outlined in Figure 1-4.
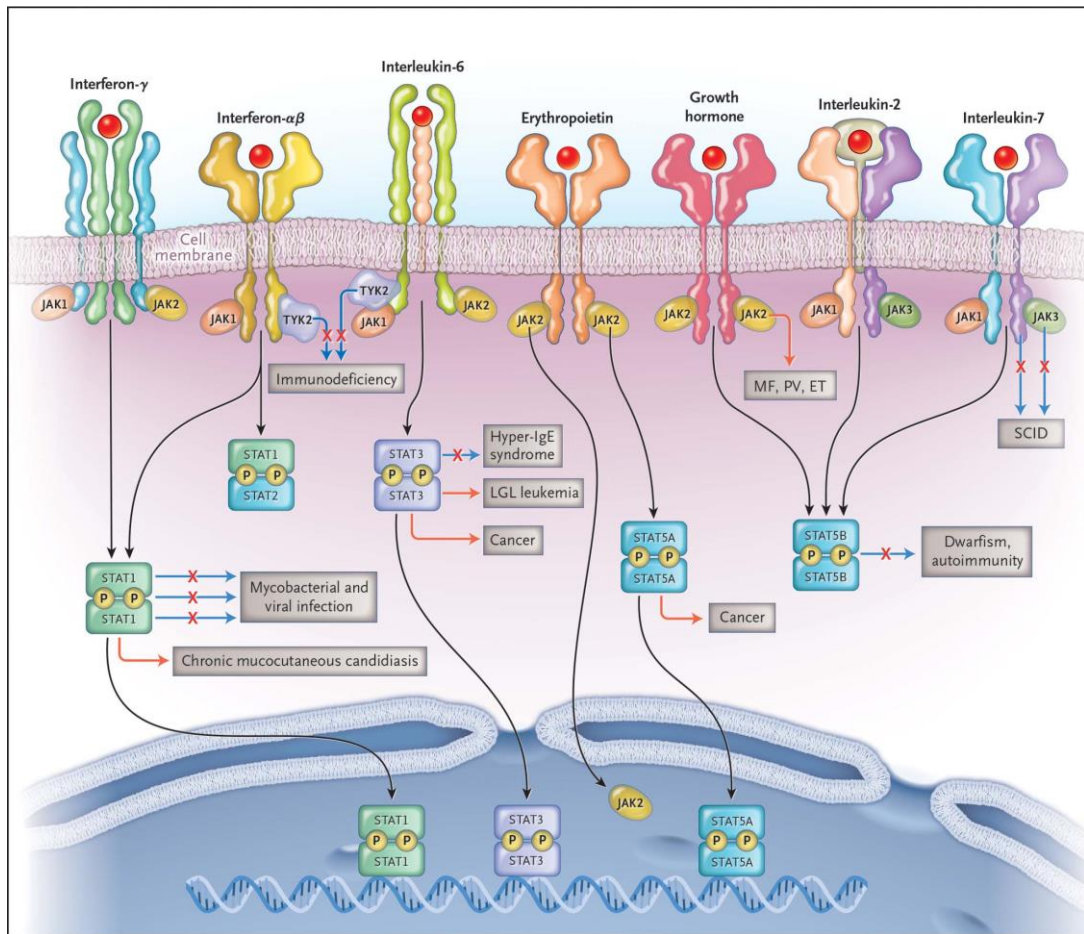
Figure 1-4: JAK/STAT signaling and disorders associated with the pathway (O'Shea et al., 2013)

One such signaling event is the binding of interferon-α/β to IFNAR1 and IFNAR2, inducing phosphorylation of JAK1 and TYK2, resulting in the phosphorylation-induced dimerization of STAT1 and STAT2. The STAT1/2 heterodimer complex with IRF9 and translocate to the nucleus, where the complex binds to the IFN-stimulated response element (ISRE) triggering the expression of antiviral genes (Pestka et al., 2004). Similarly, the binding of IFN-γ (type II IFN) to IFNGR1/IFNGR2 induces the JAK1/2-dependent STAT1 phosphorylation, resulting in the binding of STAT1 homodimer to IFN-γ activated sequence (GAS) to induce the expression of antiviral genes (Schneider et al., 2014). Interferon signaling pathway is summarized in Figure 1-5.
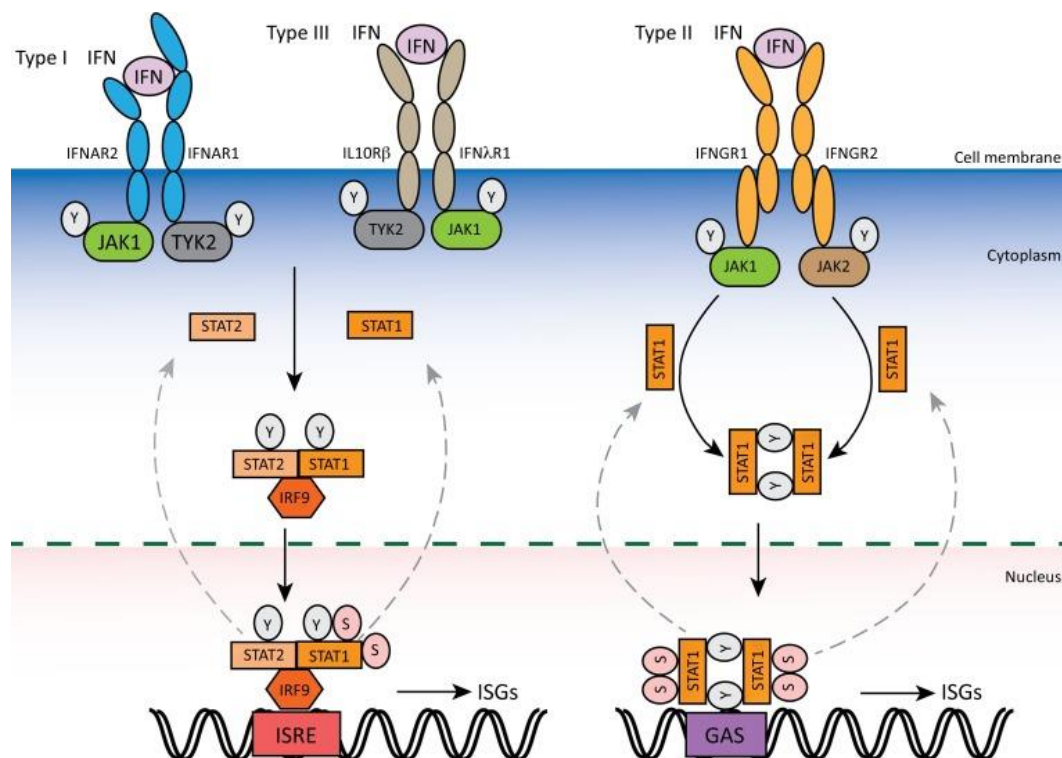
Figure 1-5: Interferon signaling cascade (W. Wang et al., 2017).

1.1.1.3   Interferon Stimulated Genes (ISGs) and Interferon Signature

The power of interferons stems from the diverse effector function of ISGs. Interferons can induce the expression of ISGs in both an autocrine and a paracrine manner, limiting the viral infection in already infected cell and providing resistance against infection in neighboring cells, respectively (Crosse et al., 2018). The OAS and IFIT family proteins, a group of ISGs, are involved in the degradation of viral RNAs, whereas certain ISGs, including ISG15, ISG20, GBP and IFI proteins inhibit viral translation and replication (Goraya et al., 2020). Apart from the mechanism limiting the viral infection in the already infected cells, another group of ISGs, IFITM proteins prevent the entry of virus into the host cell by inhibiting the membrane fusion between the viral envelope and cellular membranes (Bailey et al.,

2014). MX1, one of the first identified ISGs, interacts with viral components including, nucleocapsid and capsid proteins, restraining the infection (Verhelst et al., 2013). Furthermore, several ISGs, including ISG15 also play a role in the inhibition of viral packaging and egress (Perng & Lenschow, 2018). ISGs and their targets in viral life cycle are summarized in Figure 1-6. In general, interferon signaling triggered by viral infection results in the transcription of ISGs, providing anti-viral immunity. However, a variety of immune-system related diseases lead to persistent expression of ISGs, and are depicted to have an elevated interferon signature. This interferon signature serves as a relevant biomarker of certain diseases including, rheumatoid arthritis, and systemic lupus erythematosus (SLE) and monogenic type I interferonopathies. TREX1 deficiency is an example of a single gene defect leading to the accumulation of cytosolic DNA, inducing continuous interferon signaling (Rodero & Crow, 2016). Similarly, gain-of-function (GOF) mutations in *STING1* and *IFIH1* (MDA5) result in enhanced cytosolic nucleic acid recognition and interferon signature (Jang et al., 2015; Rice et al., 2014).

Apart from ISGs with direct anti-viral activity, interferon signaling also enhances the expression of MHC Class I and facilitates antigen processing in newly infected cells to make these cells the target of cytotoxic T cells (Keskinen et al., 1997). Furthermore, type I interferons also play a pivotal role in the maturation and activation of NK cells during viral infections (Müller et al., 2017). Additionally, type I IFNs can enhance the expansion of NK cells, providing resistance to viral infection-induced fratricide (Madera et al., 2016). However, the chronically elevated interferon signature in NK cells impairs their effector functions (Krämer et al., 2021).
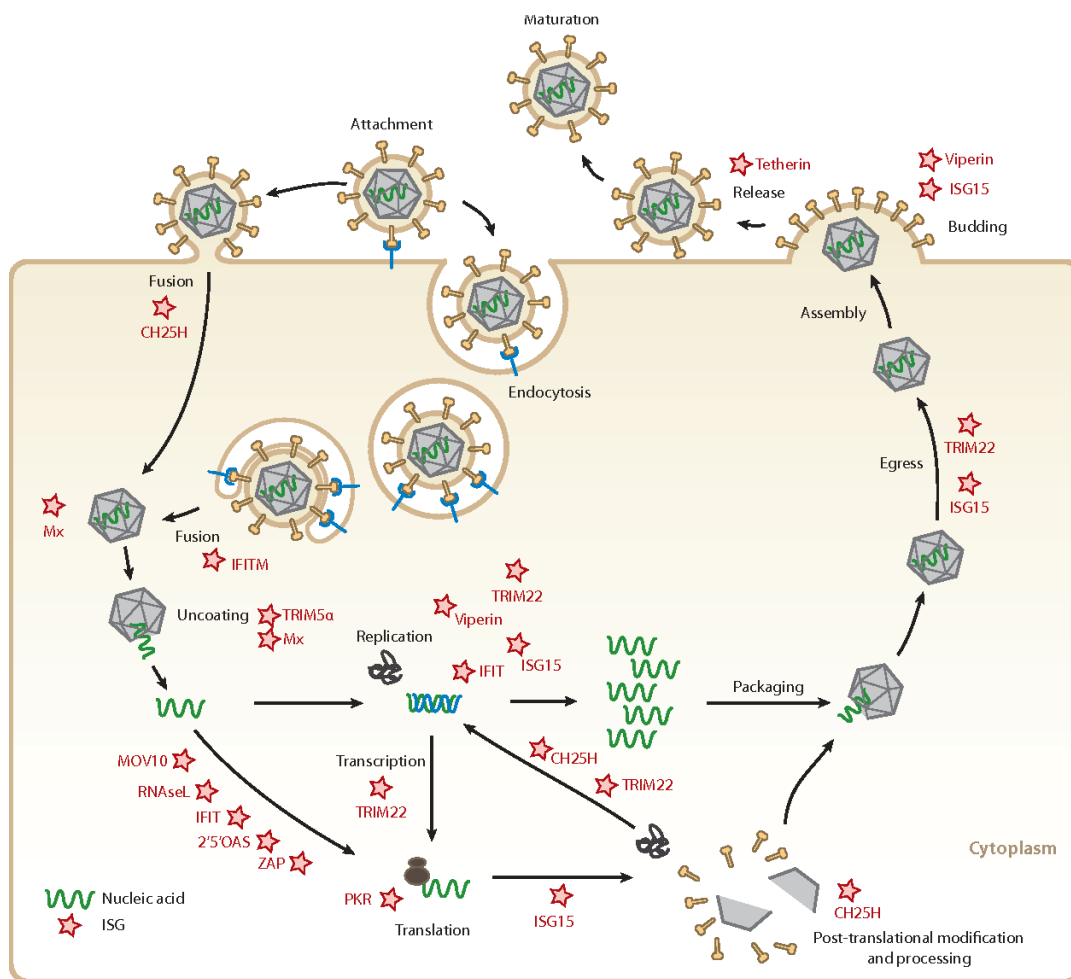
Figure 1-6: Targets for interferon-stimulated genes within viral life cycle (Schneider et al., 2014b)

1.2 Inborn Errors of Immunity

Primary immunodeficiency diseases (PIDs) are a heterogenous group of inherited disorders that are characterized by increased susceptibility to infections, autoimmunity, allergy and/or malignancy. To date, defects in nearly 500 genes have been shown to cause PIDs and this number is growing by leaps and bounds (Tangye et al., 2022). Identifying the genetic cause of an immune-related disease is not only important for development of targeted therapies but also guides us uncovering unknown or partially known molecular and immunological mechanisms.

1.2.1 PIDs Leading to Increased Susceptibility to Viral Infections

Multiple mechanisms are involved in inhibition and/or clearance of viral infections. First, the anatomical barriers and anti-viral factors prevent the entry and localization of viruses in the host's cells. If this is breached, the PRRs come into play to trigger an anti-viral immune response to call all effector cells such as NK cells to kill infected cells. If the innate immune cells fail to eliminate the infection, the established anti-viral response drives the generation of an adaptive immune response, activating cytotoxic T cells and inducing neutralizing antibody production from plasma cells. Almost all viral infections can be controlled by this complex anti-viral network unless a defect is present in this web.

Increased susceptibility to viral infections is primarily associated with inborn errors of both innate and adaptive immunity. Depending on the compromised component/s of the immune system, susceptivity may vary from a specific virus to multiple families of viruses. One such defect is the IRF7 deficiency, resulting in impaired type I interferon production from pDCs in response to viral, predominantly influenza, infections (Ciancanelli et al., 2015). The viral susceptibility in common variable immunodeficiency (CVID) stems from defective B-cell differentiation and lack of antibody production accompanied by T-cell defects (Dropulic & Cohen, 2011). Recurrent and persistent herpes simplex virus (HSV) infections are commonly observed in a variety of PIDs including STAT1 GOF and deficiencies of DOCK8, NEMO, GATA2, CARMIL2, TYK2 and STAT1 (Jouanguy et al., 2020).

1.2.1.1 PID associated with STAT1 Gain-of-function (GOF) Mutations

Gain-of-function mutations in *STAT1* gene result in elevated phosphorylated STAT1 levels and delayed dephosphorylation, inducing amplified STAT1-dependent gene expression. This enhanced STAT1 signaling overrides the STAT3 pathway, which is required for Th17 differentiation, resulting in Th17 deficiency. As a consequence of impaired Th17 immunity, STAT1 GOF patients suffer from chronic mucocutaneous candidiasis (CMC) (Van De Veerdonk et al., 2011). Recent findings

also suggest that augmented Th1 responses caused by enhanced STAT1 signaling contributes to susceptibility to cutaneous candida infections (Break et al., 2021). Furthermore, autoimmunity and increased viral susceptibility are the other well-known characteristics of STAT1 GOF mutations. The most frequently observed viral infections in patients with STAT1 GOF mutations are HSV, Varicella-zoster, molluscum contagiosum, CMV and EBV (Toubiana et al., 2016) Although the underlying causes of viral infections and autoimmune manifestations are less understood, the involvement of chronically elevated interferon signaling has been speculated by multiple groups (Weinacht et al., 2017). As reviewed earlier, the increased interferon signature is associated with type I interferonopathies, manifesting diverse autoinflammatory and autoimmune diseases. At the end of a long-standing debate, in the last review on the subject, STAT1 GOF was classified as a type I interferonopathy (Crow & Stetson, 2021). However, direct evidence of the link between elevated interferon signature and autoimmunity is still missing. Furthermore, the increased interferon signature and susceptibility to viral infection are two contradictory concepts. One proposed mechanism for increased viral susceptibility is the defective NK cell function in STAT1 GOF patients (Tabellini et al., 2017). Of note, it has been shown that the chronically elevated interferon signaling impairs NK cell functions (Krämer et al., 2021). Therefore, this consistently elevated interferon signature may lead to increased viral susceptibility in STAT1 GOF patients in a NK-cell-dependent and possibly independent manner.

The most prevalent treatment modality in STAT1 GOF is the utility of Ruxolitinib, a JAK1/2 inhibitor (Olbrich & Freeman, 2018). Ruxolitinib inhibits JAK activity by competitively occupying the ATP-binding site on JAK1 and JAK2 (Mascarenhas & Hoffman, 2012). Studies emphasize the importance of long-term use for a successful outcome however possible adverse side effects and drug sensitization pose a danger in long-term administration (Weinacht et al., 2017; Zimmerman et al., 2017). Another treatment option is hematopoietic stem cell transplantation (HSCT). However, the success rate of HSCT in STAT1 GOF has been reported to be low due to increased incidence of graft versus host disease (GvHD) (Leiding et al., 2018).

Therefore, treatment strategies for STAT1 GOF patients require further optimization.

1.2.1.2   DOCK8 Deficiency

Hyper immunoglobulin E syndrome (HIES) is a primary immunodeficiency characterized by recurrent infections, eczema and elevated concentration of serum IgE. The autosomal dominant hyper IgE syndrome (AD-HIES) is caused by dominant-negative mutations in *STAT3* genes, whereas mutations in *DOCK8*, *IL6ST*, *PGM3* and *ZNF431* result in the autosomal recessive form of hyper IgE syndrome (AR-HIES) (Al-Shaikhly & Ochs, 2019; Bergerson & Freeman, 2019). Apart from other forms of HIES, the Dedicator of Cytokinesis 8 (DOCK8) immunodeficiency syndrome (DIDS) is classified as a combined immunodeficiency due to defects in both innate and adaptive immune systems of the patients. Furthermore, increased viral susceptibility is a distinctive characteristic of DOCK8 deficiency among other forms of HIES (Su, 2010). More than half of the patients with DIDS have large deletions in one or both alleles of DOCK8 whereas some have point mutations and small indels (Su et al., 2019). Most of the mutations in *DOCK8* gene have been shown to lead to complete loss of expression but there are some reported cases with low but detectable levels of DOCK8 expression (Engelhardt et al., 2015). Furthermore, somatic reversion, spontaneous correction of a germline pathogenic allele, is commonly observed in DOCK8 deficiency, leading to subsequent re-expression of a functional protein (Pillay et al., 2021a). Depending on the nature of mutations and the presence or absence of residual DOCK8 expression, disease manifestations in DIDS range from mild to severe.

DOCK8 protein is a member of the DOCK180-related family of atypical guanine nucleotide exchange factor (GEF) highly expressed in immune cells. DOCK8 specifically regulates the activity of the Rho family of small GTPases including CDC42 and RAC1, controlling a variety of processes such as migration, adhesion and phagocytosis. Therefore, the absence of a functional DOCK8 protein causes diverse cellular defects in different immune cells (Su et al., 2011). The immune

synapses are tight appositions formed between APCs or target cells and lymphocytes and are required for establishing a proper immune activation in lymphocytes. Immune synapse formation is linked to actin cytoskeleton re-organization which is controlled by CDC42, downstream of DOCK8. Therefore, DOCK8 deficiency results in defective immune synapse formation in B-cells, cytotoxic T-cells and NK-cells, impairing long-lived antibody production from plasma cells, cytotoxic activity of CD8^{+} T-cells and NK-cells, respectively (Kearney et al., 2017). Furthermore, it has been shown that DOCK8-deficient lymphocytes exhibit normal chemotaxis but they get elongated and shattered during migration within dense environments such as a synthetic collagen matrix or dermal layer of skin (Q. Zhang et al., 2014). Additionally, DOCK8 deficiency causes a defect in STAT3 signaling, impairing Th17 differentiation since it regulates the STAT3 phosphorylation and translocation to the nucleus (Keles et al., 2016). Apart from its tasks associated with GEF activity, the DOCK8 protein has been shown to have an adaptor role in the TLR9-MyD88 signaling pathway. Due to its adaptor function, DOCK8 deficiency has been speculated to attenuate type I interferon production following TLR9 ligand stimulation and to weaken TLR9-driven B-cell proliferation, consequently impairing antibody production (Jabara et al., 2012).

The underlying cause of the increased viral susceptibility in DOCK8 deficiency has been studied extensively from the day it was first identified. One clue is that interferon alpha-2b treatment clears persistent infections in DOCK8 deficiency, implying a defect in type I interferon production in these patients. The decreased number of pDCs in DOCK8 deficiency has been proposed to cause viral susceptibly whereas the most commonly observed infections are HSV infections, where the impact of pDC depletion on HSV infections was shown to be partial (Swiecki et al., 2013). Given the diverse consequences of DOCK8 deficiency at the cellular level, the involvement of a possible defect of innate immunity leading to enhanced susceptibility to viral infections should be explored.

1.3 Immune Exhaustion

During certain conditions such as cancer and chronic infections, T-cells are chronically exposed to antigen and inflammatory signals, inducing a state of T-cell dysfunction, called exhaustion. The exhausted T-cells are characterized by poor effector function accompanied by elevated surface expression of co-inhibitory receptor (Wherry, 2011). T-cells require two simultaneous signals from APCs or target cells for optimal activation. The first signal is received from antigen recognition through the TCR whereas the second one is the co-stimulatory signal engaging CD28 on T-cells (Murphy & Weaver, 2016). Nuclear factor of activated T-cells (NFAT), downstream of TCR, is activated in a calcium-dependent manner and translocated to the nucleus. Simultaneously, the AP-1 signaling pathway is initiated by a co-stimulatory signal, inducing its nuclear transport. NFAT and AP-1 interact with each other in the nucleus and as a complex, bind to a composite DNA motif responsible for the transcription of activation-related genes such as interleukin-2. However, in the absence of AP-1, NFAT alone binds to a monomeric motif on DNA, inducing the expression of co-inhibitory receptors such as PD-1, TIM-3, LAG-3 and CTLA4 (Martinez et al., 2015). The expression of co-inhibitory receptors on T-cells results in an "exhausted phenotype" with reduced effector function including, IL-2 production and cytotoxicity, resulting in the ineffective clearance of viruses or tumor cells (Saeidi et al., 2018). One critical point regarding T-cell exhaustion is that the phenotype is not terminal, blockage of co-inhibitory receptor signaling has been shown to reverse this state of dysfunction (Nguyen & Ohashi, 2014).
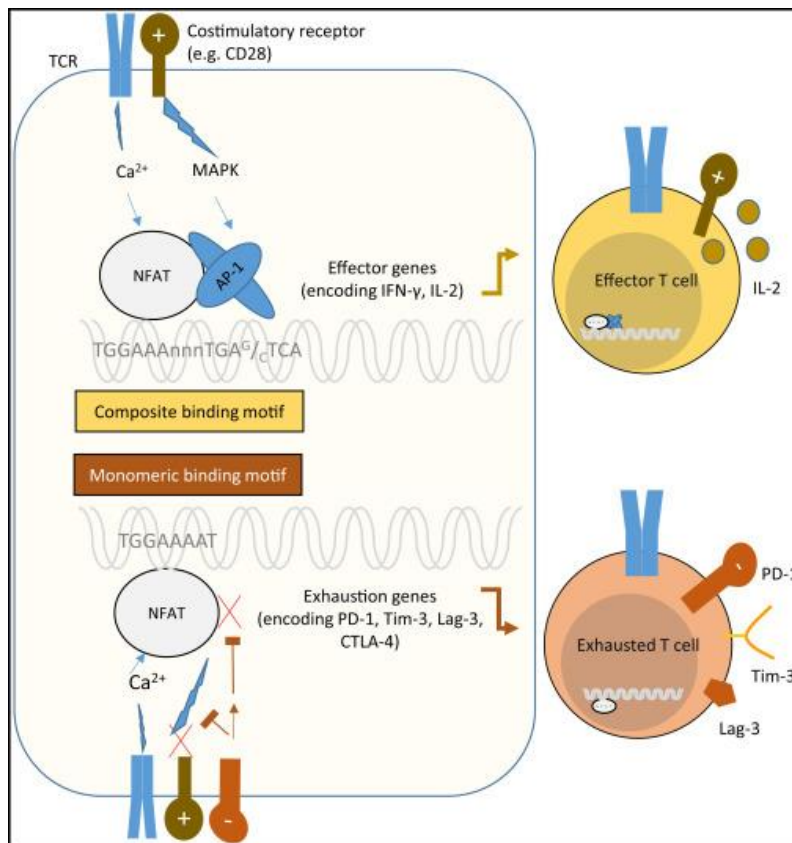
Figure 1-7: Effector T-cell activation vs T-cell exhaustion (Bengsch & Wherry, 2015)

Immune exhaustion is well-studied in T-cells, however, more recently, exhaustion in other cells, particularly innate cells, have also been considered. Similar to T-cells, elevated interferon signature has been suggested to induce exhausted phenotype, impairing the effector functions of innate immune cells including, type I interferon production (Greene et al., 2021). However, the exact mechanisms leading to "exhausted phenotype" in innate cells are largely unknown. It has been known that co-inhibitory receptor expression is not restricted to T-cells. For instance, expression of LAG-3 in plasmacytoid dendritic cells has been shown to be 10-fold higher than in any type of T-cells (Workman et al., 2009). Furthermore, TIM-3 is known to be expressed by a variety of innate immune cells, negatively regulating immune responses (Yang et al., 2013). However, to date, the link between immune exhaustion in innate cells and co-inhibitory receptor expression has not been addressed. By

20

deciphering the underlying mechanisms and the molecules playing a role in this process, new targeted therapy options can be explored.

1.4   Aim of the Study

STAT1 GOF patients are characterized by CMC and increased susceptibility to viral and bacterial infections accompanied by autoimmune manifestations. The underlying cause of CMC has been shown to stem from as Th17 deficiency. However, mechanisms leading to immunodeficiency and autoimmunity are less clear. Here, we aimed to investigate the gene expression profile of immune-related pathways to expand our knowledge of the underlying mechanisms contributing to disease progression. Furthermore, treatment options in STAT1 GOF are limited to long-term use of JAK inhibitors and HSCT. However, both have distinct drawbacks. Due to the possible complications including adverse side effects and drug desensitization in long-term use, patients are unlikely to use Ruxolitinib throughout their lifetime. Alternatively, HSCT, providing a definite solution, is a practice with a very low success rate in STAT1 GOF patients. Therefore, we proposed to develop a strategy combining both options for optimal patient treatment. Herein, we first verified the cellular level defects in the patient including impaired STAT1 phosphorylation dynamics and Th17 deficiency. Next, we investigated the impact of Ruxolitinib treatment and HSCT following Ruxolitinib bridge therapy on cellular-level defects. Furthermore, we utilized the PanCancer Immune Profiling gene expression panel to assess immune-related gene expression profiles of the patient, prior to, during Ruxolitinib treatment and post-HSCT. To this extent, we identified the dysregulated pathways in the patient and their improvement in the course of treatment.

Herein, we also aimed to investigate the defects related to interferon signaling and viral infections in DOCK8 deficiency. In our preliminary work, we observed this impaired type I IFN production in DOCK8-deficient patients in response to various cytoplasmic and endosomal nucleic acid ligand stimulation. Therefore, we planned to explore the underlying cause of impaired type I interferon response. For this, we

performed immune-related transcriptome analysis using the Host Response Panel in 15 patients with DOCK8 deficiency. According to principal component analysis, as the patients were clustered into two distinct groups. We identified the dysregulated pathways in these two groups and associated certain pathways with compromised type I IFN response and increased viral susceptibility. Additionally, we investigated the normalization of dysregulated immune-related gene expression profile in one DOCK8-deficient patient post-HSCT.

CHAPTER 2

MATERIALS & METHODS

2.1   Materials

2.1.1   Chemicals

RPMI 1640 with L-glutamine (Biological Sciences, Isreal, cat. # 01-100-1A) was used as cell culture media for all experiments. Cell culture grade water (cat. # 03-055-1A), DPBS (cat. # 02-023-1A) and media supplements; heat-inactivated Fetal Bovine Serum (FBS, cat. # 04-121-1A), HEPES buffer (cat. # 03-025-1B), MEM non-essential amino acid solution (cat.# 01-340-1B), Sodium pyruvate solution (cat. # 03-042-1B), Penicillin/Streptomycin solution (cat. # 03-031-1B) were purchased from Biological IIndustries(Isreal). Lymphocyte separation medium (LSM-A) was purchased from Capricon (Germany).

2.1.2   Antibodies and Related Reagents

Fluorochrome-conjugated antibodies targeting cell surface or intracellular antigens used in flow cytometric analysis are listed in Table 2-1. Fixation Medium (cat. # GAS001S-100) and Permeabilization Medium (cat. # GAS002S-100) were purchased from Thermo Fisher Scientific (USA). Methanol was purchased from Merck (Germany).

Table 2-1: List of fluorochrome-conjugated antibodies used in flow cytometry

Antibody	Fluoro-chrome	Company	Cat. #	Working Conc.
Anti-human CD3	FITC	Immunostep	3F1-100T	5μl/test
Anti-human CD4	PE	Immunostep	4PE-100T	5μl/test
Anti-human CD4	APC/Cy7	Biolegend	300517	2μl/test
Anti-human CD8a	FITC	Biolegend	300905	2μl/test
Anti-human CD14	APC	Biolegend	301808	1μl/test
Anti-human CD19	PE	Immunostep	19PE1-100T	5μl/test
Anti-human CD123	PerCP/Cy5.5	Biolegend	306016	5μl/test
Anti-human CD303(BDCA2)	FITC	Biolegend	354208	5μl/test
Anti-human CD45RA	PE/Cy7	Biolegend	304125	5μl/test
Anti-humanCD45RO	PE	Biolegend	304205	5μl/test
Anti-human IL-17A	Alexa Fluor® 488	Biolegend	512307	10μl/test
Anti-human IFN-γ	APC	Biolegend	502511	5μl/test
Anti-human pSTAT1(pY701)	Alexa Fluor® 488	Bioscience	612596	5μl/test
Anti-human pSTAT1(pY701)	Alexa Fluor® 647	Bioscience	612597	5μl/test
Anti-human pSTAT3(pY705)	Alexa Fluor® 647	Bioscience	557815	5μl/test
Anti-human IP-10	PE	Bioscience	555049	10μl/test
Anti-human ISG15	PE	R&D systems	IC8044P	5μl/test

Enzyme-Linked Immunosorbent Assay (ELISA) was performed using 96-well, flat bottom, maxibinding Immunoplates (SPL Life Sciences, Korea, cat. # 32296). Antibody pairs utilized in sandwich ELISA were from Mabtech (Sweden) (summarized in Table 2-2). Alkaline phosphatase-conjugated streptavidin (Strep-ALP, cat. # 3310-8-1000) were purchased from Mabtech (Sweden). 4-Nitrophenyl phosphate disodium salt hexahydrate (pNPP, cat. # 4264-83-9) was obtained from VWR Life Sciences (Ireland). Diethanolamine substrate buffer for pNPP (cat. # 34064) and Tween 20 detergent (cat. # BP-337-500) were purchased from Thermo Fisher Scientific, USA. Buffer recipes for ELISA are given in Appendix A.

Table 2-2: List of cytokine ELISA kits

Cytokine	Company	Kit	Cat. #
IFN-γ	Mabtech	ELISA Flex: Human IFN-γ (ALP)	3420-1A-6
IL-17A	Mabtech	ELISA Flex: Human IL-17A (ALP)	3520-1A-6
IL-10	Mabtech	ELISA Flex: Human IL-10 (ALP)	3430-1A-6
IFN-α	Mabtech	ELISA Flex: Human IFN-α (ALP)	3425-1A-6
TNF-α	Mabtech	ELISA Flex: Human TNF-α (ALP)	3512-1A-6
IL-1β	Mabtech	ELISA Flex: Human IL-1β (ALP)	3416-1A-6

2.1.3   Stimulants and Related Reagents

Opti-MEM^{TM} Reduced Serum Medium (cat. # 31985070) and Lipofectamine^{TM} 2000 Transfection Reagent (cat. # 11668019) were purchased from Thermo Fisher Scientific (USA). Protein transport inhibitors monensin (cat. # 554724, BD Bioscience, USA) and Brefeldin A (cat. # 420601, Biolegend, USA) were purchased from) were used for intracellular cytokine stainings. Identity of stimulants and their working concentrations used in cell stimulation experiments are given in Table 2-3.

Table 2-3 List of stimulants utilized in cellular activation experiments

Stimulant	Pathway	Working Concentration	Company	Cat. #
PMA	PKC	50ng/ml	Invivogen	tlrl-pma
Ionomycin	NFAT	1µg/ml	Invivogen	Inh-ion
HKCA	Dectin-1	4×10^6 cell/ml	Invivogen	tlrl-hkca
Zymosan	TLR2/Dectin-1	10µg/ml	Invivogen	tlrl-zyn
IFN-β	IFNAR1/2-JAK/STAT	100ng/ml	Merck-Serono	-
R848	TLR7/TLR8	5µg/ml	Invivogen	tlrl-r848
D-ODN (D35)	TLR9	3µM	-	-
HSV-60	CDS	5µg/ml	Invivogen	tlrl-hsv60n
PolyI:C	TLR3/RIG-I/MDA5	10µg/ml	Invivogen	tlrl-pic

2.1.3.1 Materials Used in RNA Isolation and Gene Expression Analysis

Reagents and Kits used for RNA isolation and Gene Expression Analysis are given in Table 2-4. RNA purity and quantity were assessed via BioDrop (BioChrom, UK) or NanoDrop™ 2000 (Thermo Fisher Scientific, USA).

Table 2-4 List of Reagents and Kits used in RNA isolation and Gene Expression

Product	Company	Cat. #
TRIzol^{TM} Reagent	Thermo Fisher Scientific	15596026
RNaseZAP^{TM}	Merck	R2020-250ML
Chloroform	Merck	102431
Isopropanol	Merck	101040
Ethanol	Merck	32221
RNA Clean & Concentrator	Zymo Research	R1018
DNase I (RNase-free)	NEB	M0303S
nCounter Human PanCancer Immune Profiling Panel	NanoString	XT-CSO-HIP1-12
nCounter Human Host Response Panel	NanoString	XT-HHR-12

2.2 Methods

2.2.1 Isolation of Human Peripheral Blood Mononuclear Cells (hPBMC) from Whole Blood

Experiments involving human participants have been approved by the Ethics Committee of Marmara University, School of Medicine. Blood samples from patients and healthy controls were collected in EDTA-coated blood collection tubes (BD Bioscience, USA). Blood collection process was carried out at Marmara University, Pendik Training and Research Hospital, Pediatric Allergy and Immunology Department. Blood samples were diluted with an equal volume of PBS and then slowly layered on top of Lymphocyte Separation Medium (LSM) at a ratio of 3:2. Centrifugation was performed at 1800 rpm for 30 minutes at room temperature with the brake-off, to maximize layer separation. Then, PBMC layer in between LSM and plasma fraction was harvested and transferred into a clean Falcon

tube with the help of a sterile Pasteur Pipette. Recovered PBMCs were washed twice with 2% FBS containing RPMI 1640 Medium (wash medium) by centrifugation at 1800 rpm for 10 minutes. Final PBMC pellet was resuspended in 1ml of 10% FBS containing RPMI 1640 Medium (complete medium). To determine PBMC count, 20µl of cell suspension was diluted in 1ml of PBS and 20µl of diluted sample was acquired using a flow cytometer (Novocyte 2060, Agilent Technologies, USA). PBMCs were gated according to forward and side scatters, based on their size and granularity. Event number in PBMC gate was multiplied with dilution factor (2500X) to find the number of cells in 1ml.

2.2.2   Stimulation of PBMCs

For determination of STAT1 phosphorylation/dephosphorylation cycles, PBMCs (1×10^6 cells/ml) were stimulated with IFN-β for 15, 60 and 120 minutes or left as such. For the assessment of STAT1 and STAT3 phosphorylation in T and B-cells, PBMCs (1×10^6 cells/ml) were stimulated with IFN-β for 30 minutes or left as such. Following incubations, PBMCs were centrifuged at 300g for 10 minutes. Cell pellets were resuspended in 100µl Fixation Medium (Medium A; containing formaldehyde) and incubated for 15 minutes at room temperature. Cells were washed twice with FACS buffer (Appendix A) by centrifugation at 400g for 10 minutes and stored at +4°C until utilized in further experiments. For the intracellular assessment of T-cell specific cytokines, PBMCs (1×10^6 cells/ml) were stimulated with PMA and Ionomycin. Simultaneously, unstimulated and stimulated PBMCs were treated with protein transport inhibitor Monensin (1000X) and incubated for 6-hour at 37°C. At the end of the incubation, cells were fixed and stored as explained above. Similarly, for the measurement of intracellular IP-10 amounts, PBMCs (1×10^6 cells/ml) were stimulated with Lipofectamine 2000 transfected HSV-DNA for 5 hours. At the end of the 5-hour incubation at 37°C, cells were treated with Brefeldin A (1000X) and incubated further for 3 hours at 37°C. Next, cells were fixed and stored as explained above. PBMCs (1×10^6 cells/ml) were stimulated with various PRR ligands for the assessment of intracellular ISG15. After overnight incubation, cells were fixed and

stored as explained above. For the measurement of secreted cytokine levels, PBMCs ($4x10^5$ cells/well) were layered into flat bottom 96-well tissue culture plates and stimulated with various PRR ligands or PMA/Ionomycin for 24 hours at 37°C. Culture supernatants were collected and stored at -20°C for ELISA.

2.2.3 Flow Cytometric Analysis

2.2.3.1 Determination of pDC population within PBMCs

Cell surface staining was performed with live cells on ice. PBMCs ($1x10^6$ cells/ml) were centrifuged at 300g for 10 minutes at 4°C. The live cell pellet was resuspended in 100µl FACS buffer containing fluorochrome-conjugated anti-CD123 and anti-CD303 (BDCA2). Cells were incubated for 30 minutes on ice and washed twice. A minimum of 20,000 events were acquired and cells were analyzed in the CD123$^+$ CD303$^+$ gate on a Novocyte 2060 Flow cytometer.

2.2.3.2 Intracellular Phospho-STAT Staining

Fixed PBMCs (unstimulated or IFN-β stimulated) were permeabilized with 95% ice-cold methanol for 20 minutes on ice. Permeabilized cells were washed twice with FACS buffer to recover from residual methanol prior to the addition of fluorochrome-conjugated antibodies. Next, the cell pellet was resuspended in 100 µl FACS buffer containing fluorescent-labeled anti-pSTAT1 (pY701) or anti-pSTAT3 (pY705) antibodies together with antibodies against cell surface markers and incubated for 45 minutes at room temperature in dark. Labeled cells were washed twice and final cell pellet was resuspended in 300µl of FACS buffer. A minimum of 20,000 events were acquired and cells were analyzed in the CD4$^+$ gate on a Novocyte 2060 Flow cytometer. Gating strategies are given in Appendix B.

2.2.3.3   Intracellular Cytokine Staining

For T-cell specific cytokine measurements, unstimulated and PMA/ionomycin stimulated PBMCs were treated with protein transport inhibitor and fixed as described above. The fixed cell pellet was resuspended in 100µl of fluorochrome-conjugated antibody (anti-IL-17A or anti-IFN-β) containing Permeabilization Medium (Medium B; containing saponin) and incubated for 45 minutes at room temperature in dark. Next, labeled cells were washed twice and cell surface staining was performed with fluorescent-labeled antibodies against CD4, CD45RA and CD45RO molecules. A minimum of 40,000 events were acquired and cells were analyzed in the $CD4^+CD45RO^+CD45RA^-$ gate on a Novocyte 2060 Flow cytometer. Gating strategies are given in Appendix B.

For intracellular IP-10 staining, PBMCs treated with protein transport inhibitor were fixed as described above. The fixed cell pellet was resuspended in 100µl of fluorochrome-conjugated anti-IP-10 containing Permeabilization Medium (Medium B; containing saponin) and incubated for 45 minutes at room temperature in dark. Then, IP-10 labeled cells were washed twice and monocytes were stained with fluorochrome-conjugated anti-CD14 for 30 minutes. A minimum of 20,000 events were acquired and cells were analyzed in the $CD14^+$ gate on Novocyte 2060 Flow cytometer. Gating strategies are given in Appendix B.

2.2.4   Cytokine Measurement from Cell Culture Supernatant

The amounts of secreted cytokines were determined using ELISA kits described in Table 2-2. First, capture antibodies were diluted in PBS as suggested in the manufacturer's protocol. Next, SPL immunoplates were coated with 50µl/well monoclonal capture antibody specific to the target cytokine. Following overnight coating at +4°C, plates were emptied by gentle flicking. Then, plates were blocked with the addition of 200µl/well of blocking buffer and incubated for 2 hours at room temperature. After the blocking buffer was discarded, plates were washed 4 times each for 3 minutes by soaking in wash buffer. Plates were left to air-dry and then

50µl/well samples or 50µl/well recombinant cytokine standards (prepared by 2-fold serial dilution in PBS) were added to corresponding wells. Culture supernatants were diluted with PBS for the detection of IFN-γ (1:2), whereas for other cytokines, undiluted supernatants were used. Plates were incubated for 2 hours and washed as described previously. Next, 50µl/well biotinylated detection antibodies diluted in T-cell buffer (at a concentration suggested in the manufacturer's protocol) were added and left for overnight incubation at +4°C. Streptavidin conjugated alkaline phosphatase (ALP) was prepared in T-cell buffer at a dilution of 1:1000. Following washing steps, streptavidin-AP solution was distributed to wells and incubated for 1 hour at room temperature. After a final wash cycle, 50µl/well enzyme substrates were added to each well and color development was monitored. For the preparation of PNPP solution, 1 PNPP tablet was dissolved in 4 ml of distilled water and 1 ml of diethanolamine substrate buffer was added to the solution. For color development, freshly prepared PNPP solution was used and absorbances were recorded at 405nm with 30 minutes intervals.

2.2.5 RNA Isolation and Quantification for Gene Expression Analysis

Freshly isolated PBMCs (2-4 × 10^6 cells) were centrifuged at 300g for 10 minutes. Cell pellets were suspended in 1 ml of TRIzol^{TM} reagent with vigorous pipetting. and stored at -80°C. Prior to RNA isolation procedure, all surfaces and equipment were cleaned with RNaseZAP^{TM} to avoid RNase contamination. One week before the Nanostring Assay, homogenized samples were thawed and incubated for 5 minutes at room temperatures. After the incubation, 200µl of chloroform was added to each tube and mixed by vortexing until a homogenous mixture was achieved. Tubes were left for incubation for 2-3 minutes at room temperature and centrifuged at 12,000g for 15 minutes at +4°C. The clear upper aqueous phase containing RNA was collected and transferred into a new RNase-free Eppendorf tube. An equal volume of isopropanol was added to each tube and incubated for 10 minutes at room temperature. Next, tubes were centrifuged at 12,000g for 10 minutes at +4°C and supernatants were decanted. RNA pellets were washed with 1ml of pre-chilled 70%

ethanol at 8,000g for 6 minutes. Washing step was repeated with 1ml of cold 100% ethanol. Ethanol was removed carefully and RNA pellets were air-dried. RNA pellets were then dissolved in 20µl of DNase/RNase-free water. Alternatively, RNA isolation after phase separation was achieved by using RNA Clean & Concentrator™ kit. For this, the clear upper aqueous phase was mixed with an equal volume of absolute ethanol. The mixture was applied to the column and centrifuged at 16,000g. Flow-through was discarded and in-column DNase I digestion was performed according to the manufacturer's protocol. Next, 400µl of RNA Prep Buffer was added to each tube and centrifuged. Flow-through was discarded again and filters were washed twice with RNA Wash Buffer. Columns were centrifuged to remove residual ethanol. Finally, 25µl of DNase/RNase-free water was applied to the columns and elution was performed by centrifugation.

2.2.6 Gene Expression Analysis using Nanostring nCounter® panel

The nCounter Human PanCancer Immune Profiling and the nCounter Human Host Response panels were used for gene expression analysis. All the components of the nCounter® XT Assay were removed from the freezer to thaw at room temperatures. RNA samples were adjusted to 50ng/5µl with the addition of an appropriate volume of DNase/RNase-free water. Master mix was obtained by the addition of 70µl hybridization buffer to thawed Reporter CodeSet. 8µl of Master Mix was introduced to each tube and mixed with 5µl of sample. Next, 2µl of Capture ProbeSet was added and final volume reached to 15µl/tube. Tubes were sealed and hybridization reaction was performed at 65°C for 18 hours. Following overnight hybridization, samples and cartridge were transferred to nCounter Analysis System for the fully automated process of cartridge loading. After immobilization and alignment of hybridized probes were achieved in Prep Station, the cartridge was transferred to Digital Analyzer for probe counting. The raw count data were normalized via housekeeping gene expression with the use of nSolver Analysis Software version 4.0. Logarithmic transformation was performed on GraphPad Prism 8 (GraphPad Software Inc, USA). The nSolver Analysis Software version 4.0 and nCounter Advanced Analysis

Software 2.0 were used to obtain fold change values of differentially expressed genes, pathway z scores and cell type scores.

2.2.7 Statistical Analysis

Statistical analysis was performed using GraphPad Prism 8. Student unpaired two-tailed t test, one-way ANOVA with Tukey posttest analysis and two-way ANOVA with Tukey posttest analysis were performed for the comparisons between healthy controls and patient groups as indicated in figure legends. Student paired two-tailed t-test was preferred for the comparisons within STAT1 GOF patient groups. Differences in means were accepted as statistically significant at a p value of less than 0.05 or q value (Bonferroni corrected p-value) of less than 0.05 as indicated in figure legends.

CHAPTER 3

RESULTS & DISCUSSION

PART ONE

The antiviral immune response is largely driven by STAT1-mediated IFN signaling. Upon binding to their receptors, interferons initiate the phosphorylation-dependent activation of Janus Kinases (JAKs), which in turn phosphorylates STAT1 at tyrosine residue (Lurie & Platanias, 2005). The activated forms of STATs dimerize and are translocated to the nucleus where they regulate the transcription of target genes, mainly IFN-stimulated genes with antiviral activity (Tolomeo et al., 2022). The pivotal role of STAT1 in host defense can be appreciated based on microbial susceptibilities of patients with three types of primary immunodeficiencies that result from diverse inborn errors in the *STAT1* gene. Autosomal recessive and dominant versions of STAT1 deficiency were commonly characterized by persistent mycobacterial and/or viral infections (Mizoguchi & Okada, 2021). Autosomal dominant (AD) gain-of-function (GOF) *STAT1* mutations are predominantly characterized by chronic mucocutaneous candidiasis (CMC). Additionally, patients with *STAT1* GOF mutations may suffer from various forms of autoimmunity as well as viral, bacterial and fungal infections (Toubiana et al., 2016).

3.1 Assessment of STAT1 Phosphorylation/Dephosphorylation Levels in Healthy and Patient PBMCs

A patient with GOF mutation in the *STAT1* gene presented with CMC, viral and bacterial infections accompanied by autoimmune manifestations. Next-generation sequencing (NGS) revealed a de novo heterozygous mutation in the DNA-binding domain (DBD) of *STAT1* (c.1154C > T; p.T385M). This amino acid substitution has previously been shown to induce hyperphosphorylation at Tyr701 and impair the dephosphorylation of STAT1 (Sampaio et al., 2013). Enhanced phosphorylation and

delayed dephosphorylation of STAT1 observed in these patients likely contribute to the pathogenesis of this disease. Ruxolitinib usage and benefits have been reported in multiple studies for the treatment of patients with *STAT1* GOF mutations (Weinacht et al., 2017). Additionally, multiple groups emphasized that Hematopoietic stem cell transplantation (HSCT) can be considered for these patients, but post-transplant complications are very severe and difficult to manage (Leiding et al., 2018). In this thesis, we planned to investigate the potential use of Ruxolitinib treatment as a bridge therapy for HSCT in a STAT1 GOF patient. With the use of Ruxolitinib treatment, we anticipated to normalize the STAT1 phosphorylation kinetics and consequently manage the infections and autoinflammatory manifestations in the patient, which would provide a better outcome after HSCT.

For this purpose, first, we aimed to confirm the defect in STAT1 phosphorylation/dephosphorylation cycle in patient helper T-cells. To assess the STAT1 phosphorylation kinetics, patient and control PBMCs were stimulated with IFN-β for 15, 60 and 120 minutes. Typically, STAT1 phosphorylation starts immediately after IFN stimulation, which would be followed by dephosphorylation. In the first 15 minutes upon IFN stimulation, phosphorylation will predominate in the environment and over time, phosphorylated Tyr701 residues would be dephosphorylated, resulting in a reduction in the amount of phosphorylated STAT1. Therefore, we would expect to observe maximal phosphorylation at 15 minutes followed by a gradual decline of levels at 60 and 120 minutes. By the end of 2 hours, as the interferon in the environment is depleted, the phosphorylated STAT1 levels recede to basal levels. This expected phosphorylation/dephosphorylation cycle in helper T cells was confirmed in PBMCs obtained from healthy controls (Figure 3-1A and B). In contrast, when patient-derived PBMCs were stimulated with an equivalent dose of IFN-β, STAT1 phosphorylation in helper T-cells at 15 minutes was robust (~5-fold higher than healthy controls) and dephosphorylation was delayed. Specifically, by 120 minutes, pSTAT1 levels in patient cells persisted (~6.3-fold higher than the unstimulated baseline level) whereas in healthy controls,

dephosphorylation was almost complete (1.7- and 1.9-fold above basal levels of HC1 and HC2, respectively; Figure 3-1A and 3.1B).

Figure 3-1: Representative flow cytometric analysis of STAT1 phosphorylation kinetics in the patient (P-Baseline) CD4+ T-cells compared to controls

PBMCs ($1x10^6$) were stimulated with IFN-β (100ng/ml) for 15, 60 and 120 minutes. Time-dependent change in pSTAT1 levels were analyzed within CD4+ T-cell gate via flow cytometry. (A) Phosphorylation/dephosphorylation patterns are presented as overlays of the mean fluorescence intensity (MFI) histograms in the patient compared to healthy controls. (B) Enhanced phosphorylation and delayed dephosphorylation in the patient are illustrated as line graph of pSTAT1 (MFI) at different time points compared to healthy controls (P-Baseline: Patient before Ruxolitinib treatment and HSCT, HC: Healthy Controls).

3.2   Assessment of IL-17 Production in Healthy and Patient PBMCs

The balance between STAT1 and STAT3 signaling is pivotal in regulation of helper T-cell differentiation. STAT1 and STAT3 activation is reciprocally regulated and impairments in this balance may lead to various conditions including immunodeficiency, autoimmunity and cancer (Regis et al., 2008a). As a consequence of gain-of-function mutations in the *STAT1* gene, it is speculated that hyperactivation of STAT1, negatively regulates the STAT3-dependent signaling. Enhanced STAT1 signaling in response to IL-17 inducer cytokines IL-6, IL-21 and IL-23 antagonize with STAT3 activation which results in impaired Th17 differentiation. A reduced number of circulating IL-17 producing helper T-cells has been associated with the pathogenesis of CMC disease in STAT1 GOF patients (Liu et al., 2011). Here, we aimed to confirm the IL-17 deficiency in helper T-cells in patient PBMCs to account for the disease manifestations, including CMC and susceptibility to various infections. For this, PBMCs from patient and controls were treated with PMA (50ng/ml) and Ionomycin (1µg/ml) for 6 hours in the presence of protein transport inhibitor monensin. IFN-γ production in patient's CD4$^+$ T-cells was similar to healthy controls whereas the frequency of IL-17 producing CD4$^+$ T-cells in the patient was severely compromised when compared to healthy controls (Figure 3-2).
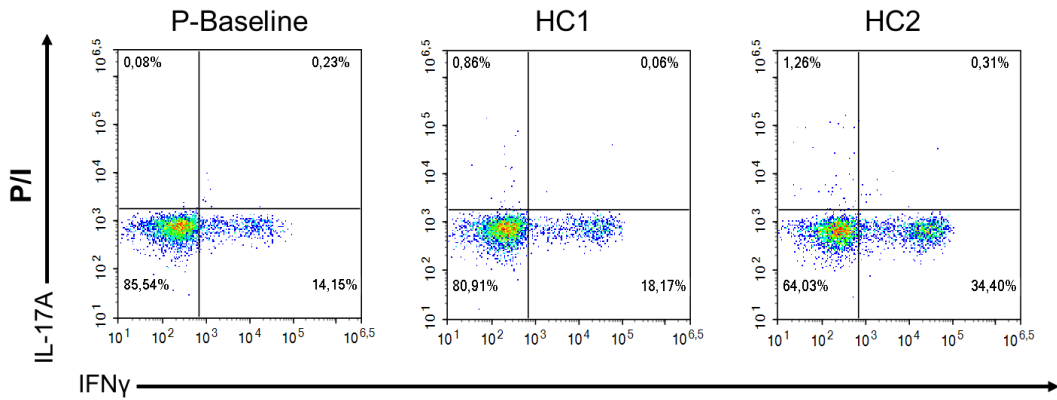
Figure 3-2: Flow cytometry density plots illustrating IL-17 deficiency in patient CD4+ T-cells

PBMCs (1x10^6) were stimulated with PMA (50ng/ml) and ionomycin (1μg/ml) for 6 hours in the presence of Monensin. IL-17 and IFN-γ producing CD4+ T-cells were assessed via intracellular cytokine staining from the PBMCs of patient (P-Baseline) and healthy controls (HC).

3.3 Assessment of Therapeutic Benefit of Ruxolitinib Treatment and Hematopoietic Stem Cell Transplantation (HSCT) on Dysregulated STAT1 Dephosphorylation

Dysregulated STAT1 phosphorylation/dephosphorylation cycles and deficiency in IL-17 producing helper T-cells were confirmed with comprehensive functional assays as discussed before. Following confirmation of these defects, the use of Ruxolitinib, a JAK inhibitor, was decided due to the severity of clinical manifestations and dependency on immunosuppressant agents in this patient. The initial dose for oral Ruxolitinib was determined as $5mg/m^2$/dose twice a day. After 1 month of the therapy, the Ruxolitinib dose was increased to $10mg/m^2$/dose twice a day due to the persistent dysregulation in STAT1 dephosphorylation and lack of adverse side effects of Ruxolitinib. By the end of 6 months under Ruxolitinib therapy, delayed dephosphorylation of STAT1 was normalized and pSTAT1 levels were comparable to those observed in healthy controls (Figure 3-3).
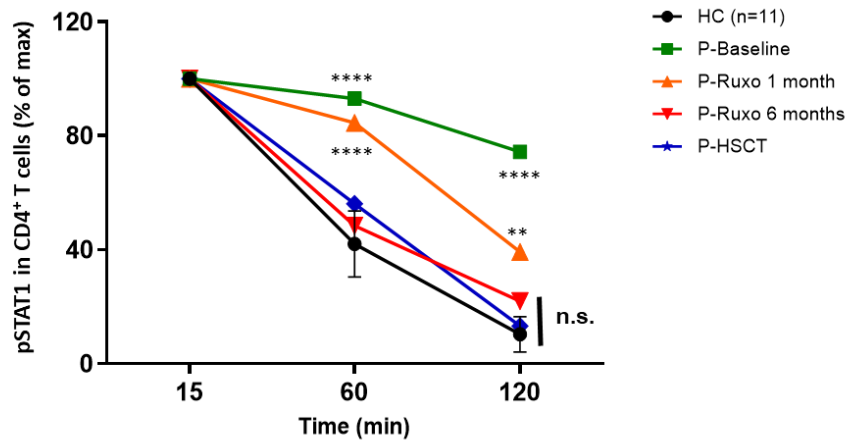
Figure 3-3: Line graph illustrating the change in STAT1 phosphorylation/ dephosphorylation pattern during Ruxolitinib treatment and following HSCT

PBMCs ($1x10^6$) were stimulated with IFN-β (100ng/ml) for 15, 60 and 120 minutes. Change in pSTAT1$^+$ cell percentages in CD4$^+$ T-cell population in the patient, before (P-Baseline), 1 month and 6 months after Ruxolitinib treatment (P-Ruxo 1 month and P-Ruxo 6 months) and 6 months post-transplantation (P-HSCT) in comparison to healthy controls (HC) were assessed via flow cytometry. Two-way ANOVA with Tukey's posttest was used to compare patient groups to healthy controls. (n.s., not significant, **p < 0.01 and **** p < 0.0001)

The patient benefited greatly from Ruxolitinib treatment. However, since long-term use of ruxolitinib can cause complications such as adverse side effects or induction of drug desensitization, it was decided that the patient would benefit from a hematopoietic stem cell transplantation in the long term. While the patient was under Ruxolitinib treatment, HSCT was conducted from a full-matched unrelated donor and thus, Ruxolitinib was utilized as a bridge therapy for transplantation and was discontinued one day after HSCT. 100% donor chimerism was achieved within one month after transplantation. The patient experienced mild complications of HSCT which were resolved with commonly administered interventions. 6 months after the transplant, delayed dephosphorylation and enhanced phosphorylation of STAT1

were resolved and levels returned to those comparable to healthy controls (Figure 3-3 and Figure 3-4).

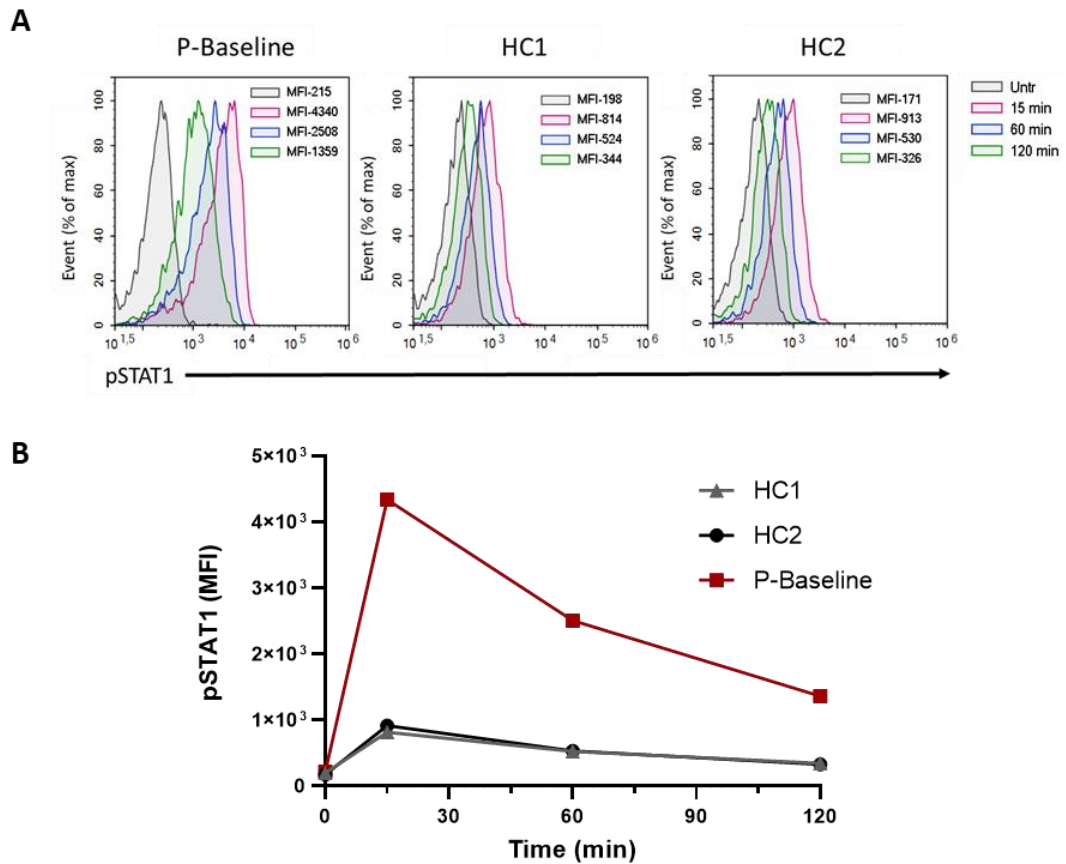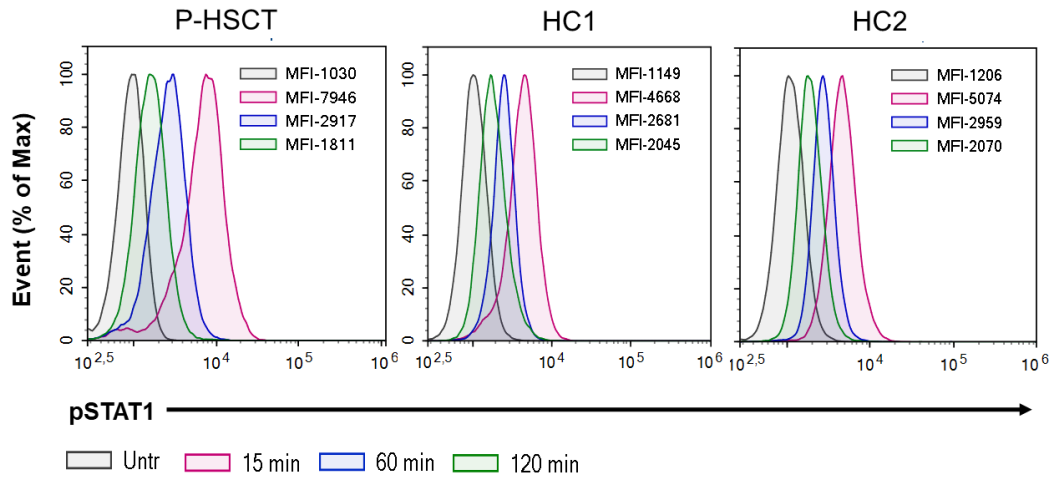*Figure 3-4: Representative flow cytometric analysis of STAT1 phosphorylation kinetics in patient (P-HSCT) CD4⁺ T-cells after transplantation compared to healthy controls*

PBMCs (1x10⁶) were stimulated with IFN-β (100ng/ml) for 15, 60 and 120 minutes. Time-dependent change in pSTAT1 levels was analyzed via flow cytometry. The data are presented as overlays of the mean fluorescence intensity (MFI) histograms. (P-HSCT: Patient post-HSCT, HC: Healthy Control)

3.4 Assessment of Therapeutic Benefit of Ruxolitinib Treatment and Hematopoietic Stem Cell Transplantation (HSCT) on Dysregulated Th17 differentiation

At the beginning of the study, we assessed the percentage of IL-17 producing cells in CD4⁺ T-cells from patient versus healthy control PBMCs and confirmed the absence of circulating Th17 cells in the patient. However, as expected, the frequency of IL-17 producing helper T-cell population in healthy controls was also very low. To better evaluate this population, we included additional cell surface markers to differentiated naïve versus memory cells, using anti-CD45RA and anti-CD45RO,

respectively. With the use of CD45RO together with CD4, we have determined memory Th-cells within the PBMC fraction. This gating strategy, enriched the intended target population and enabled more sensitive identification of the Th17 population frequency. Based on this method, analysis of the Th17 population even after 6 months of Ruxolitinib treatment, showed no improvement in IL-17 production (Figure 3-5, Figure 3-6A and Figure3-6B).
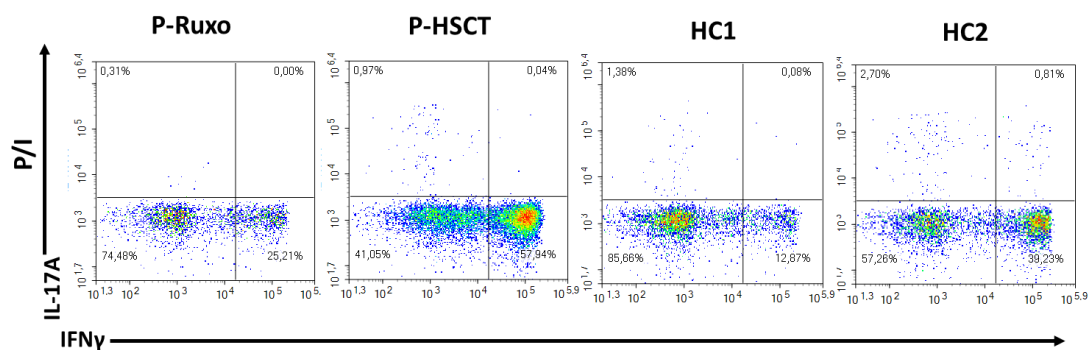
Figure 3-5: Representative flow cytometry density plots showing persistent IL-17 deficiency in patient CD4$^+$CD45RO$^+$ T-cells at 6 months of Ruxolitinib therapy and recovery after transplantation

PBMCs (1x10^6) were stimulated with PMA (50ng/ml) and ionomycin (1µg/ml) for 6 hours in the presence of Monensin . IL-17 and IFN-γ producing CD4$^+$CD45RO$^+$ T-cells were assessed via intracellular cytokine in PBMCs of the patient, after 6 months of Ruxolitinib treatment (P-Ruxo) and post-transplantation (P-HSCT), and healthy controls (HC).

To confirm the intracellular cytokine staining results, we also investigated the secreted IL-17 from overnight culture of PMA (50ng/ml) and Ionomycin (1µg/ml) stimulated PBMCs. The amount of IL-17 in the culture supernatant was lower than detectable levels for the patient before and after Ruxolitinib treatment (Figure 3-6C & D), indicating that long-term management of all symptoms would not be possible through ruxolitinib treatment alone, justifying the decision to administer HSCT.

The success of HSCT has also been proven by its effect on the IL-17 deficiency in patient's helper T-cells. We have shown an increase in the frequency of circulating IL-17 producing memory T-cells after transplantation (Figure 3-5, Figure 3-6A & B). We have also detected normal levels of secreted IL-17 from PMA/Ionomycin stimulated PBMCs of the patient post-HSCT (Figure 3-6C & D). Collectively, these results suggest that Ruxolitinib treatment would be a viable choice in maintenance treatment of STAT1 GOF patients until a suitable bone marrow donor is identified.
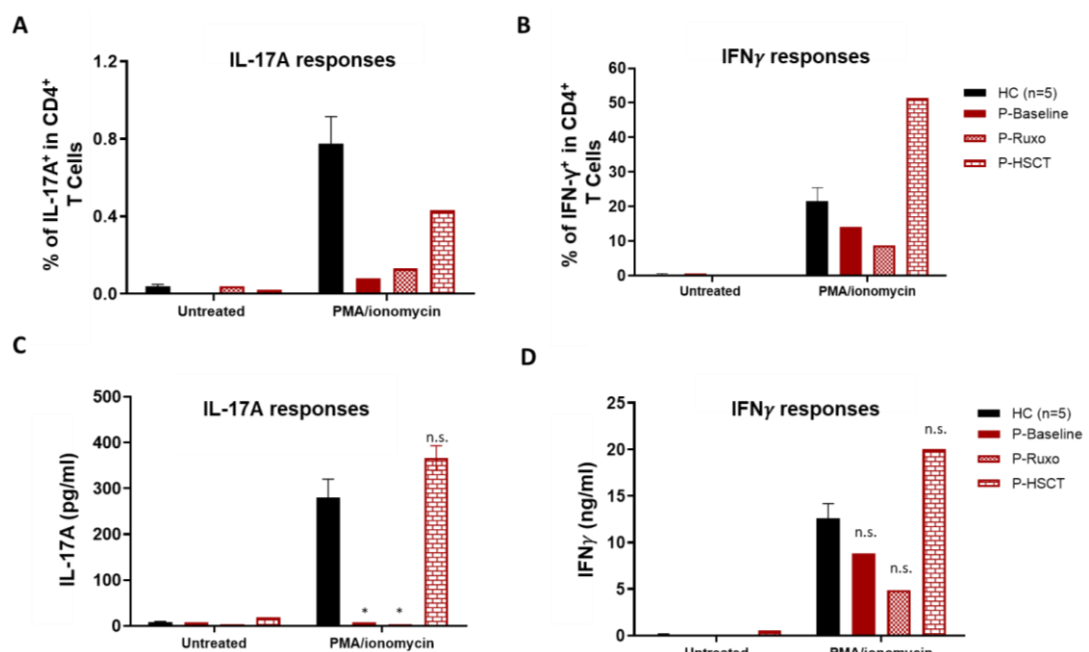
Figure 3-6: Bar graphs showing persistent IL-17 deficiency in patient at 6 months of Ruxolitinib therapy and recovery after transplantation

(A) The percentage of IL-17A producing CD4+ T cells before and after PMA (50ng/ml) and ionomycin (1μg/ml) stimulation was determined by intracellular cytokine staining. (B) Percentage of IFN-γ producing CD4+ T cells before and after PMA (50ng/ml) and ionomycin (1μg/ml) stimulation was determined by intracellular cytokine staining (C) IL-17A secretion from PBMCs stimulated with PMA (50ng/ml) and ionomycin (1μg/ml) for 24 hours was detected by sandwich ELISA. (D) IFN-γ secretion from PBMCs stimulated with PMA (50ng/ml) and ionomycin (1μg/ml) for 24 hours was detected by sandwich ELISA. One-way ANOVA with Tukey's posttest was used to compare patient groups to controls. (n.s., not significant, **p < 0.01 and **** p < 0.0001)

3.5 The Effect of Ruxolitinib Treatment and HSCT on Dysregulated Gene Expression

Defect in Th17 immunity has been considered the main reason for the CMC pathogenesis in STAT1 GOF patients (Huppler et al., 2012). However, underlying mechanisms causing the susceptibility to viral infections and autoimmune phenomena remained unexplored. To expand our knowledge of disease pathogenesis, we studied the differential expression of immune-related genes in the patient in comparison to healthy controls. For this, transcriptome analysis of 730 genes found in the nCounter PanCancer Immune Profiling Panel was performed using total RNA samples isolated from healthy controls versus the patient prior to or 7 months post-Ruxolitinib treatment in addition to 6 months post-HSCT. Using the gene expression analysis, we also aimed to investigate the effect of Ruxolitinib treatment and HSCT at the transcriptional level. Figure 3-7 presents volcano plots depicting the differential expressed genes in patient samples (Baseline, Ruxo and HSCT) in comparison to healthy controls. These results imply that, Ruxolitinib treatment ameliorated dysregulated gene expression but HSCT essentially normalized the dysregulated expression pattern back to healthy control levels.

A similar pattern of amelioration and normalization could be observed when the immune-related pathway z-scores were compared between untreated versus Ruxolitinib and HSCT groups, respectively (Figure 3-8). A few immune-related pathways returned to normal levels upon Ruxolitinib therapy, whereas HSCT pathway scores were similar to healthy controls, confirming the success of this treatment.
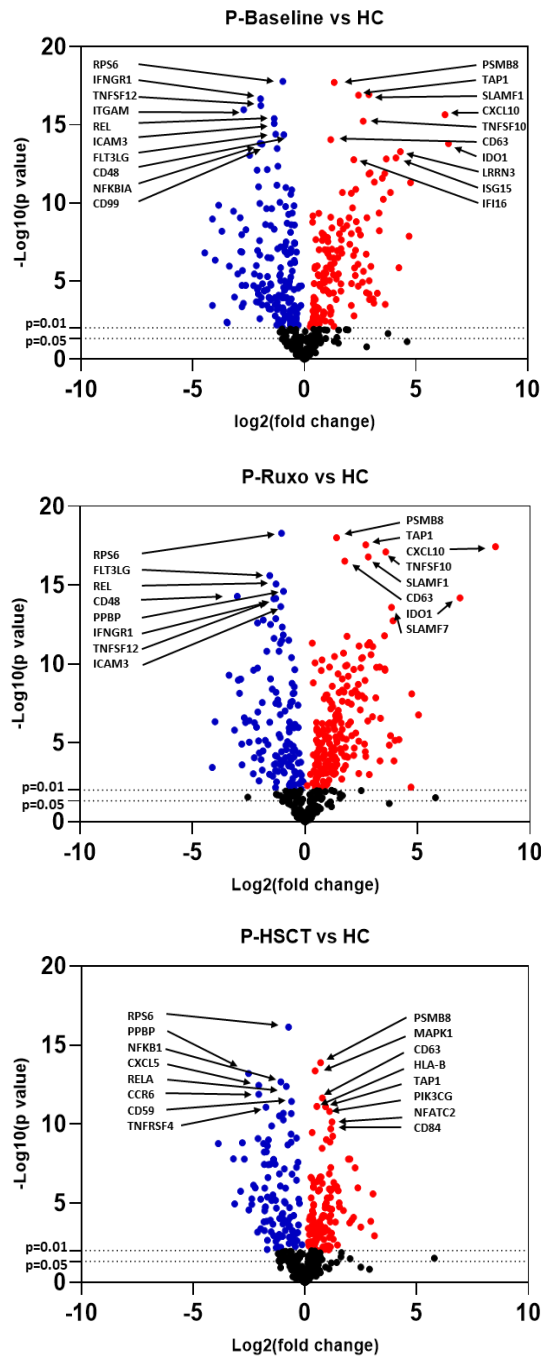
Figure 3-7: Volcano plots illustrating differentially expressed PanCancer Immune Profiling panel genes between patient and controls (n=3) before (P-Baseline vs HC), after 7 months of Ruxolitinib treatment (P-Ruxo vs HC) and 6 months post-HSCT (P-HSCT vs HC)

Upregulated genes with log2(fold change) ≥ 1and p < 0.01 (red) and downregulated genes with log2(fold change) ≤ -1and p <0.01 (blue) are shown. Names of the most differentially expressed genes are given on the plot.

Dysregulated STAT1 signaling resulted in the upregulation of multiple pathways related to regulation, cytokine and chemokine signaling, pathogen defense, antigen processing, T- and B-cell functions (Figure 3-8). Relatively fewer pathways were found to be downregulated in the patient compared to healthy controls. These pathways were related to NK-cell function, cytotoxicity, adhesion, senescence and cell cycle.
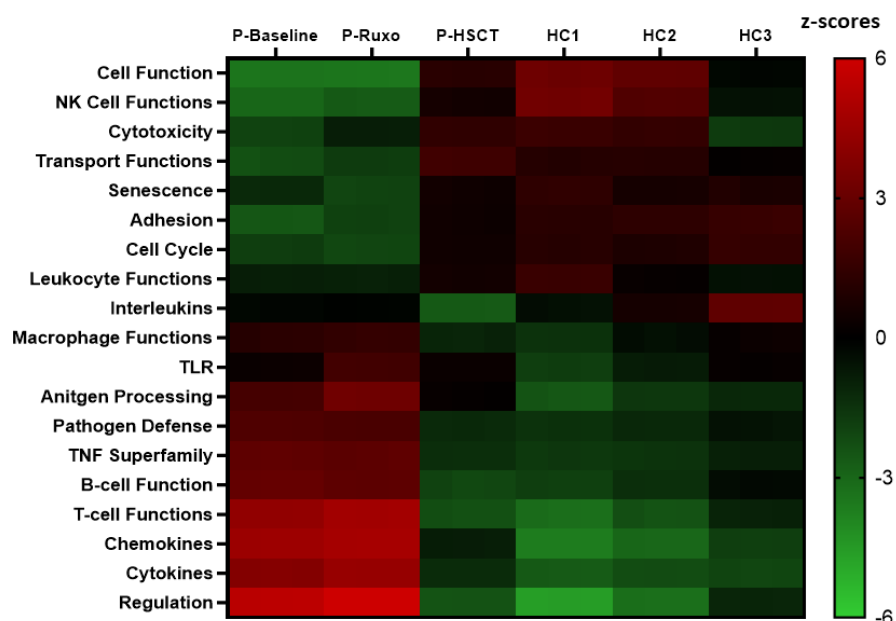
Figure 3-8: Heatmap illustrating the changes in z-score for immune-related pathways in the patient, before (P-Baseline), at 7 months of Ruxolitinib therapy (P-Ruxo) and 6 months post-transplantation (P-HSCT), and controls (HC) relative to mean of healthy controls

Z-scores were obtained from the differential expression of corresponding genes for each immune-related pathway presented above.

In addition to these pathways classified by the Nanostring nSolver software, we identified a global upregulation in genes related to type I IFN signaling. Consistent with the enhanced STAT1 signaling, most of the type I IFN-related genes found in our panel have been determined to be upregulated in the patient (Figure 3-9).
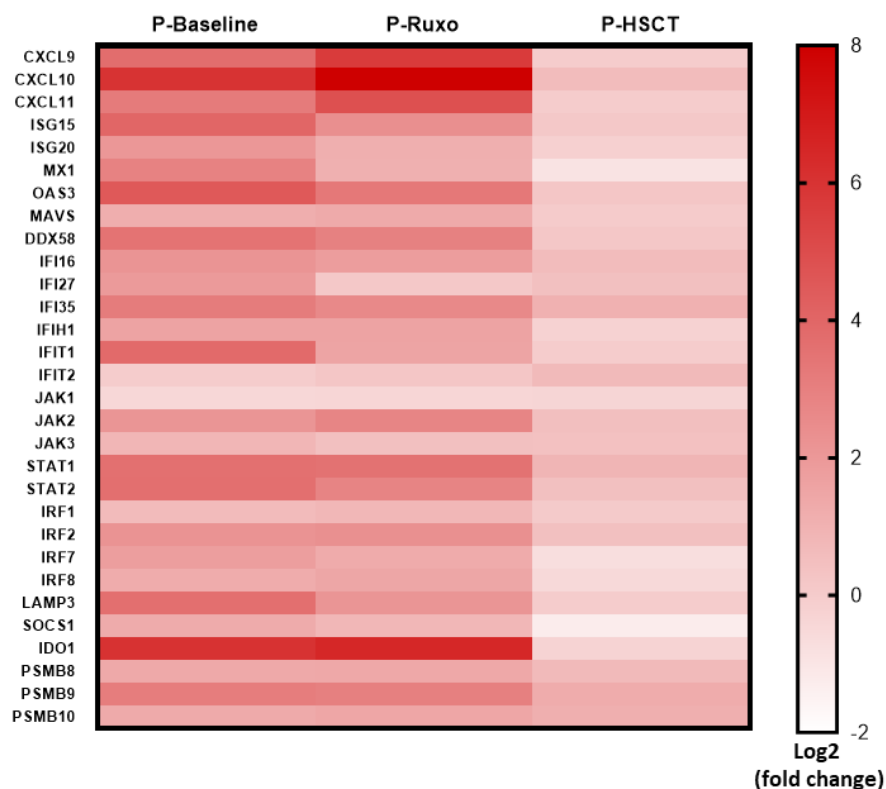
Figure 3-9: Heatmap illustrating the log2(fold change) of differentially expressed interferon-related genes in the patient, before (P-Baseline), at 7 months of Ruxolitinib therapy (P-Ruxo) and 6 months post-transplantation (P-HSCT), relative to healthy controls (n = 3)

Upon 7 months of Ruxolitinib therapy, certain interferon-related genes including, *ISG15*, *ISG20*, *MX1*, *OAS3*, *IFIT1* and *LAMP3* were partially downregulated compared to baseline, however, they had higher expression levels when compared to controls. In contrast, dysregulated expression of almost all type I IFN-related genes was completely normalized after HSCT.
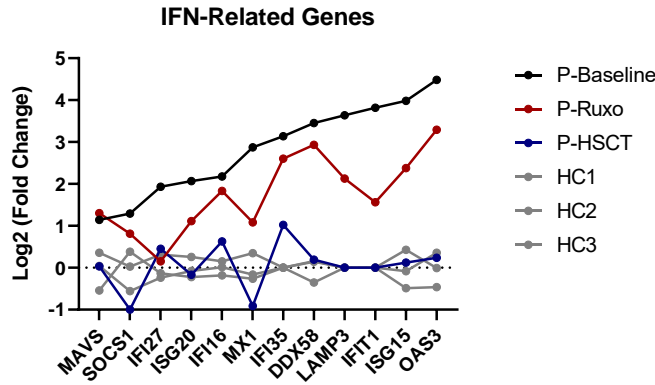
Figure 3-10: Line graph illustrating the log2(fold change) of differentially expressed interferon-related genes in the patient, before (P-Baseline), at 7 months of Ruxolitinib therapy (P-Ruxo) and 6 months post-transplantation (P-HSCT), and healthy controls (HC1, HC2 and HC3)

In addition to these IFN-related genes, T- and B- cell function and antigen processing related genes were found to be upregulated in the patient. Proteins encoded by these upregulated genes include the surface molecules CD19, MS4A1 (CD20), CD27, CD79B, CD274 (ICOS), CD80 and IL12RB2, which are required for the activation and differentiation of T- and B- cells (Figure 3-11).

Figure 3-11: Heatmap illustrating the log2(fold change) of differentially expressed B- and T- cell function related genes in the patient, before (P-Baseline), at 7 months of Ruxolitinib therapy (P-Ruxo) and 6 months post-transplantation (P-HSCT), relative to healthy controls (n = 3)

TAP complex (TAP1 and TAP2) function in peptide transport from cytosol to ER for processing and loading onto MHC Class I molecules. Expression of *TAP1* and *TAP2* genes are enhanced upon IFN stimulation under normal circumstances to increase antigen presentation (Ritz & Seliger, 2001). In this context, immunoproteasome genes *PSMB8*, *PSMB9* and *PSMB10* are pivotal for the generation of peptides suitable for loading onto MHC Class I molecules. These PSMB genes are considered as interferon-stimulated genes (ISG) since their expression is mostly regulated by IFN signaling (Tripathi et al., 2016). All these TAP and PSMB genes, together with certain HLA genes encoding MHC Class II molecules were found to be upregulated in the patient (Figure 3-12).
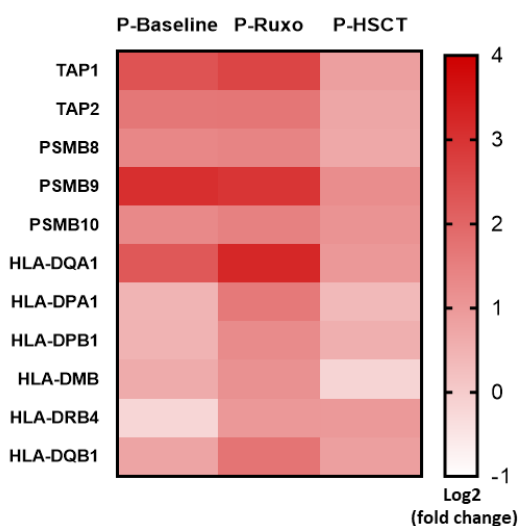
Figure 3-12: Heatmap illustrating the log2(fold change) of differentially expressed antigen processing related genes in the patient, before (P-Baseline), at 7 months of Ruxolitinib therapy (P-Ruxo) and 6 months post-transplantation (P-HSCT), relative to healthy controls (n = 3)

These results indicate that the patient has an elevated ISG signature. In order to assess whether this upregulation is statically significant, we calculated the IFN scores using the expressions of 30 genes in the patient and healthy controls (Mistry et al., 2019). The IFN scores of patient samples before and after Ruxolitinib treatment were significantly higher than healthy controls (Figure 3-13A). Although the IFN score after Ruxolitinib therapy was still higher than the healthy controls, when we perform a comparison within patient groups, we observed that the IFN score of the patient samples obtained 7 months after Ruxolitinib treatment was significantly lower than baseline. These findings suggest that Ruxolitinib therapy provided a partial improvement in dysregulated IFN-related gene expression. In addition to IFN scores, we also investigated the z-scores of antigen processing, T- and B-cell function pathways. Z-scores of these pathways were also significantly elevated in the patient and remain unchanged upon Ruxolitinib therapy (Figure 3-13B, C and D). Z-scores of antigen processing, T- and B-cell function pathways were normalized post-HSCT, indicating that HSCT but not Ruxolitinib treatment improved T- and B-cell related functions.
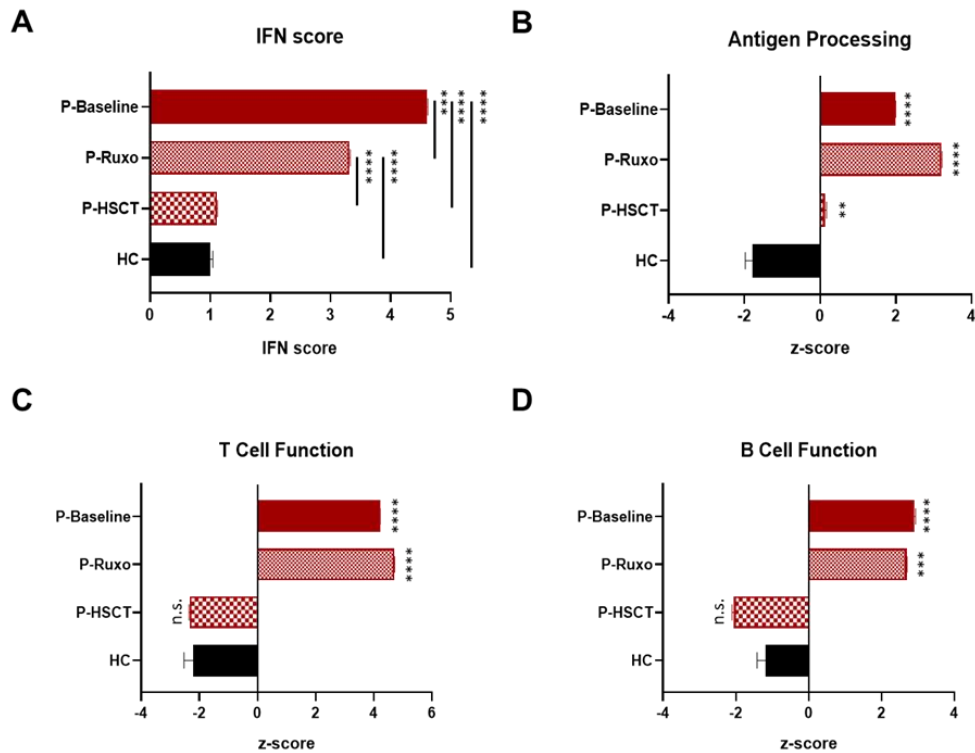
Figure 3-13: Bar graphs illustrating the IFN score (A), antigen processing (B), T-cell function (C) and B-cell function (D) pathway z-scores in the patient, before (P-Baseline), at 7 months of Ruxolitinib therapy (P-Ruxo) and 6 months post-transplantation (P-HSCT), versus healthy controls (HC, n = 3)

IFN score was calculated using median fold change relative to healthy controls for the expression of 30 interferon-related genes given in Figure 3-9 Paired two-tailed t-test for comparison within patient groups and unpaired two-tailed t-test for comparison between patient and healthy controls were used. Comparison between patient groups and controls was indicated with asterisks (*) on bars. (n.s., Not significant, **p <0.01, ***p <0.001 and ****p<0.0001)

The main aim of our study was to investigate the mechanisms that could account for the autoimmune/autoinflammatory manifestations observed in the patient. Collectively, our results demonstrated a global upregulation in type I IFN-related genes, antigen processing, T- and B-cell function pathways. The elevated expression of IFN-related genes can be considered an IFN signature which may be speculated to contribute to autoimmune manifestations observed in the patient.

A number of monogenic disorders characterized by persistent upregulation of type I IFN related genes and autoimmunity are classified under the umbrella of Type I interferonopathies. Some well-known examples of Type I interferonopathy are associated with the Loss-of-function (LOF) mutation in *TREX1* and *RNASEH2B* genes, which cause a disease phenotype better known as the Aicardi-Goutières syndrome (AGS) (Rodero & Crow, 2016a). Another example is the STING-associated vasculopathy with onset in infancy (SAVI), which is caused by GOF mutations in the *TMEM173* gene. Unusual neurological manifestations are commonly observed in AGS, but not SAVI. Neurological dysfunction is not observed in STAT1 GOF patients. Presence of a high type I interferon signature coupled with various autoimmune/autoinflammatory manifestations, suggest that STAT1 GOF could be classified as an interferonopathy. However, some researchers oppose this idea since a link between ISG upregulation and disease phenotype has not been experimentally proven (Rodero & Crow, 2016a). In this respect, our findings provide preliminary evidence for this link since autoimmunity seen in the patient regressed with the use of Ruxolitinib. This regression is consistent with partial improvement in the IFN signature upon Ruxolitinib treatment. Indeed, in his recent review of Type I interferonopathy, Crow et. al. have finally classified the STAT1 GOF as a Type I interferonopathy with the accumulation of evidence showing the link between IFN signature and disease pathogenesis in STAT1 GOF (Crow & Stetson, 2021).

Antigen processing is another pathway that shows a significant increase in the z-score in the patient compared to controls (Figure 3-13B). This increment in z-score is consistent with the IFN signature since the upregulated genes (*TAP1*, *TAP2*, *PSMB8*, *PSMB9* and *PSMB10*) in this pathway are largely controlled with IFN-dependent STAT1 signaling (Satoh & Tabunoki, 2013). Interestingly, we did not observe any improvement in the z-score of the antigen processing pathway after Ruxolitinib therapy. This was unexpected since the expressions of these genes are regulated by STAT1 signaling and we have shown that Ruxolitinib inhibits this signaling pathway. Furthermore, z-scores of T- and B-cell function pathways are

elevated in the patient compared to healthy controls (Figure 3-13C & D). All of these upregulations, which were normalized after HSCT, might be relevant in understanding of the mechanisms underlying autoimmune manifestations in STAT1 GOF patient.
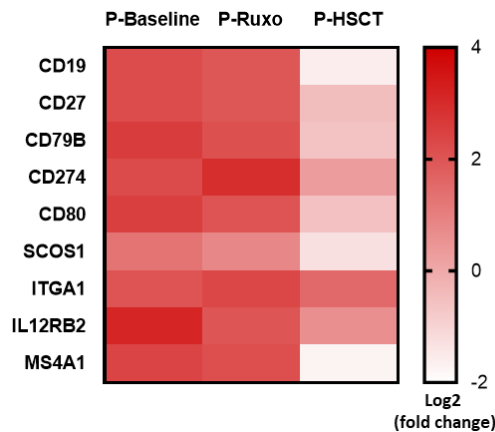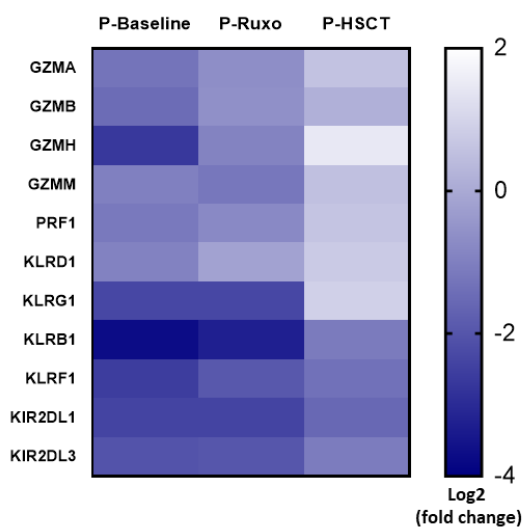

Figure 3-14: Heatmap illustrating the log2(fold change) of differentially expressed NK cell function and cytotoxicity related genes in the patient, before (P-Baseline), at 7 months of Ruxolitinib therapy (P-Ruxo) and 6 months post-transplantation (P-HSCT), relative to healthy controls (n = 3)

Transcriptome analysis has also demonstrated downregulation in NK cell function and cytotoxicity pathway related genes (Figure 3-14). The expression of genes encoding the cell surface molecules found on NK cells as well as the effector molecules mostly secreted from NK cells were downregulated in the patient. Our findings were in line with previous studies showing impaired effector function of NK cells and its relevance to viral susceptibility in STAT1 GOF patients (Tabellini et al., 2017, Vargas-Hernández et al., 2018). At baseline, z-scores of NK-cell function and cytotoxicity pathways were significantly low compared to healthy controls (Figure 3-15A & B). Ruxolitinib treatment significantly upregulated the expression of genes related to cytotoxicity which might contribute to the resolution

of persistent viral infections observed in patient following Ruxolitinib therapy (Figure 3-15B). Moreover, after transplantation, z-scores of NK-cell function and cytotoxicity pathways were recovered and become similar to healthy controls.
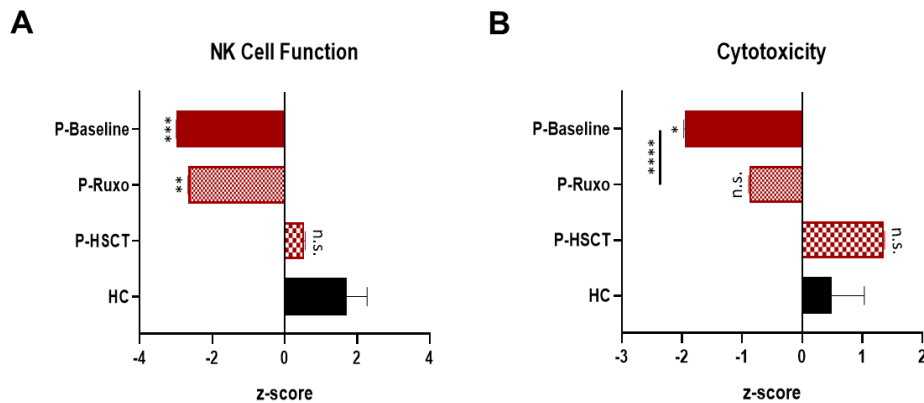
Figure 3-15: Bar graphs illustrating NK cell function and cytotoxicity pathway z-scores in the patient, before (P-Baseline), at 7 months of Ruxolitinib therapy (P-Ruxo) and 6 months post-transplantation (P-HSCT), and controls (HC, n = 3)

Paired two-tailed t-test for comparison within patient groups and unpaired two-tailed t-test for comparison between patient and healthy controls were used. Comparison between patient groups and controls was indicated with asterisks (*) on bars. (n.s., Not significant, *p <0.05, **p <0.01 ***p<0.001 and ****p<0.0001)

In addition to pathway specific analysis of gene expression, dysregulated expression of two genes; *SOCS1* and *PD-L1* has intrigued us. *SOCS1* is known as the negative regulator of STAT1 signaling (Liau et al., 2018). *SOCS1* was upregulated in response to hyperactivation of STAT1 signaling in the patient, possibly to suppress this hyperactivation (Figure 3-16A). Dysregulated *SOCS1* expression partially benefitted from Ruxolitinib treatment and was completely normalized upon HSCT (Figure 3-16A). Similarly, *PD-L1* was also upregulated in patient at baseline (Figure 3-15B). It is known that overexpression of *PD-L1* can inhibit Th17 differentiation (Y. Zhang et al., 2017). Our initial findings suggested a persistent Th17 deficiency upon Ruxolitinib treatment. In line with this, *PD-L1* expression did not decrease with

54

Ruxolitinib therapy. However, both dysregulated *PD-L1* expression and Th17 deficiency were normalized post-HSCT.
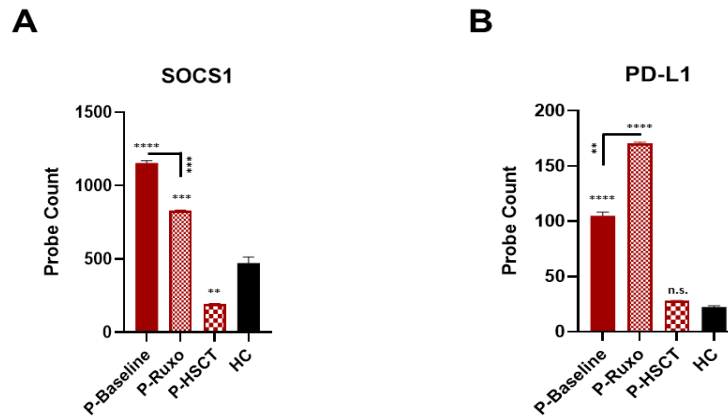
Figure 3-16: Bar graphs illustrating the number of probes detecting SOCS1 and PD-L1 mRNAs in the total RNA samples of the patient, before (P-Baseline), at 7 months of Ruxolitinib therapy (P-Ruxo) and 6 months post-transplantation (P-HSCT), and controls (HC, n = 3)

Paired two-tailed t-test for comparison within patient groups and unpaired two-tailed t-test for comparison between patient and healthy controls was used. Comparison between patient groups and controls was indicated with asterisks (*) on bars. (n.s., Not significant, **p <0.01 ***p<0.001 and ****p<0.0001)

In this study, the reversal effect of Ruxolitinib treatment and transplantation on impaired STAT1 phosphorylation/dephosphorylation cycle, defective IL-17 production from helper T-cells and dysregulated gene expression profiles observed in STAT1 GOF patient were investigated. We demonstrated the utility of Ruxolitinib as a bridge therapy to stabilize the STAT1 GOF patient before HSCT. While Ruxolitinib treatment partially corrected the impaired STAT1 phosphorylation kinetics, HSCT fully corrected this impairment. However, the defect in IL-17 production persisted after Ruxolitinib treatment, but was normalized post-transplantation. Immune transcriptome analysis revealed that upregulation in the genes related to interferon signaling were partially normalized upon Ruxolitinib

treatment and completely recovered after HSCT. Pathways related to antigen processing, T- and B-cell function were also upregulated, which were normalized after HSCT. These upregulations were considered the underlying reason for the autoimmunity in the patient which is resolved with Ruxolitinib treatment and HSCT. Transcriptome analysis also showed downregulation in the genes related to NK-cell function and cytotoxicity pathways. These pathways are important to constitute a proper immune response to viral infections and dysregulated expressions in these pathways can be related to the persistent viral infections observed in the patient. Upon Ruxolitinib treatment, persistent viral infections were resolved which is consistent with the normalized expression of NK-cell function and cytotoxicity related genes after Ruxolitinib therapy.

CHAPTER 4

RESULTS & DISCUSSION

PART TWO

Hyper-IgE syndrome (HIES) is a primary immunodeficiency characterized by recurrent infections, eczema and very high IgE concentrations in serum. While transcription factor *STAT3* gene mutations cause autosomal dominant (AD-HIES) form of this disease, mutations in other genes lead to autosomal recessive hyper IgE syndrome (AR-HIES) (Q. Zhang et al., 2018). Majority of patients with AR-HIES carry mutations in the *DOCK8* (Dedicator of Cytokinesis 8) gene. AR-HIES caused by mutations in the *DOCK8* gene is classified as combined immunodeficiency since both cellular and humoral immunity are affected. Unlike other inborn errors that cause HIES, *DOCK8* mutation leads to persistent viral infections, severe allergies and asthma (Su, 2010). The DOCK8 protein is an atypical guanine nucleotide exchange factor (GEF) highly expressed in immune cells. Due to GEF activity, DOCK8 protein is involved in many important cellular events such as migration, phagocytosis and adhesion (Su et al., 2011). Apart from its role associated with GEF activity, the DOCK8 protein was shown to act as an adaptor in the TLR9-MyD88 signaling pathway in B-cells (Jabara et al., 2012). However, DOCK8 gene mutation-related pathological mechanism underlying the persistent viral infections seen in these patients remain largely unexplored. Although it is a rare genetic disease, DOCK8 mutation frequency in our country is quite high compared to other countries due to consanguineous marriages (Engelhardt et al., 2009). Hematopoietic stem cell transplantation is the only treatment available for these patients. Given the role of serious infections in transplant rejection, investigating the role of DOCK8 protein in viral infections would expand our understanding of the disease and contribute to finding new treatment options.

4.1 Assessment of Anti-viral Responses from PBMCs of Healthy Controls and Patients with DOCK8 Deficiency

Our initial aim was to investigate a potential defect in the anti-viral mechanism. For this, with the first patient that we worked on, we checked the STAT1 and STAT3 phosphorylation in response to interferon stimulation. It was previously shown that the DOCK8 protein has a regulatory role in STAT3 activation and translocation in response to IL-6 or IL-21 stimulation (Keles et al., 2016b). It is also known that STAT1 and STAT3 signaling are closely linked and cross-regulate each other (Schindler et al., 2007). Our preliminary findings showed that IFN-β-mediated STAT1 phosphorylation in helper T-cells of the patient was more robust whereas STAT3 phosphorylation was reduced when compared to healthy controls (Figure 4-1). Similarly, IFNβ-induced pSTAT1 levels in patient B cells was higher than healthy controls but pSTAT3 levels were lower (Figure 4-2).
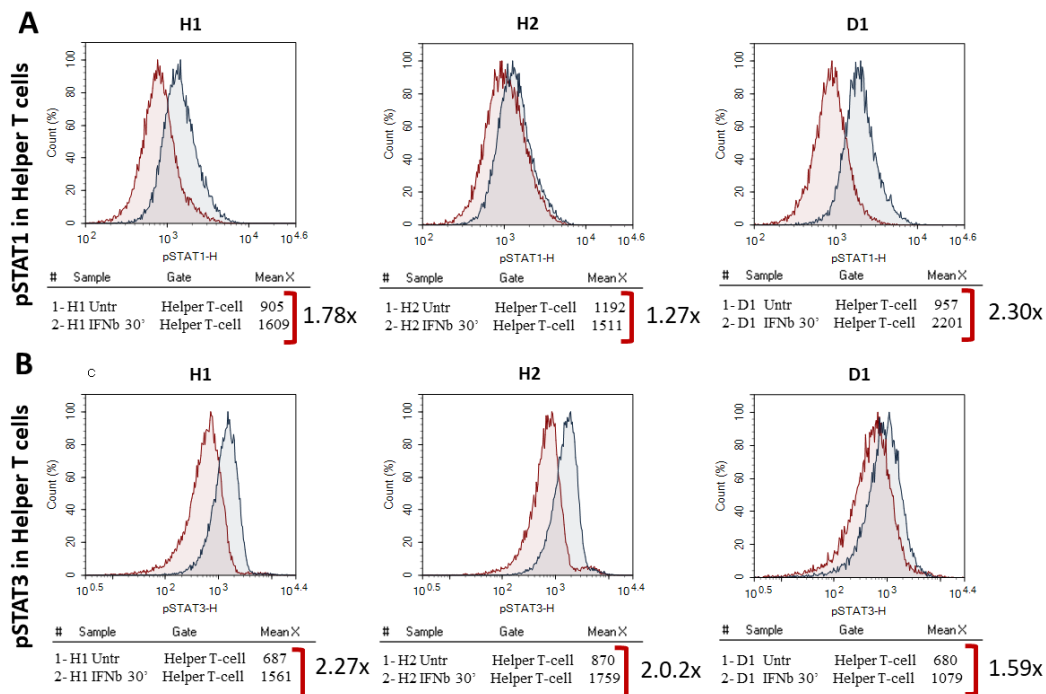
Figure 4-1: Determination of STAT1 and STAT3 phosphorylation in helper T-cells of patient D1 and healthy controls.

PBMCs (1x10^6) were stimulated with IFN-β (100ng/ml) for 30 minutes. Phosphorylated STAT1 (A) and STAT3 (B) levels in untreated or IFNβ treated CD3/CD4 double-positive cells were analyzed. Fold change in response values are indicated on each histogram. (Patient: D1, Healthy Controls: H1 & H2)
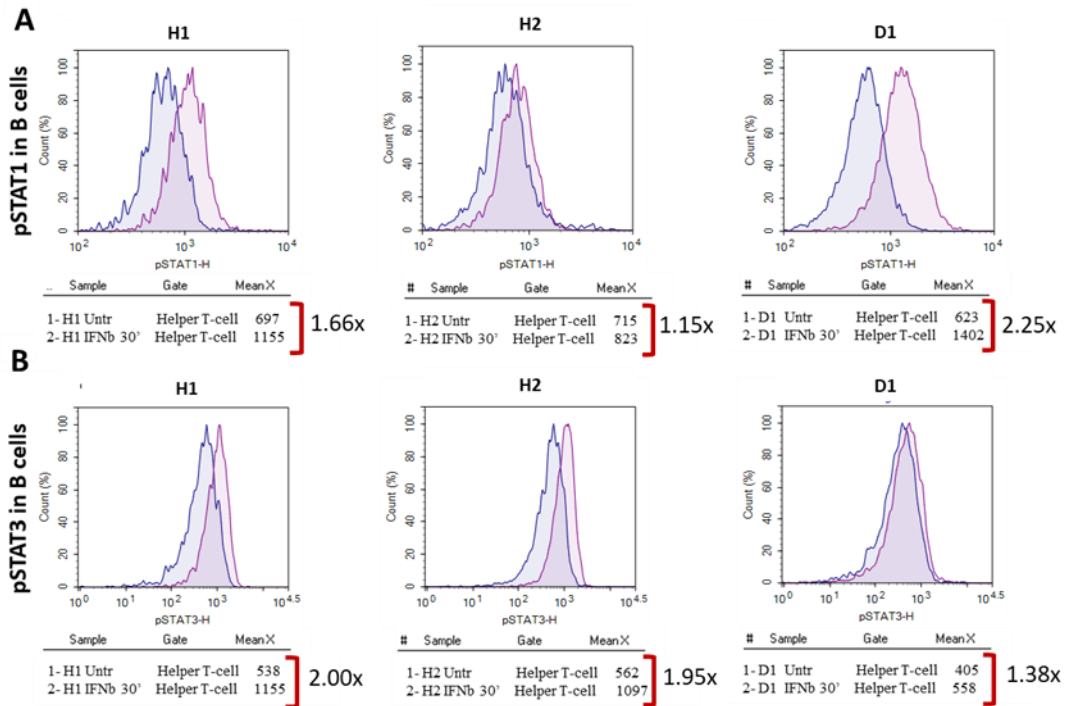
Figure 4-2: Determination of STAT1 and STAT3 phosphorylation in the B-cells of patient D1 and healthy controls.

PBMCs (1x10^6) were stimulated with IFN-β (100ng/ml) for 30 minutes. Phosphorylated STAT1 (A) and STAT3 (B) levels in untreated and IFNβ treated CD19le-positive cells were analyzed. Fold changes were indicated on each histogram. (Patient: D1, Healthy Controls: H1 & H2)

Phospho STAT1 and STAT3 levels are is strongly cross-regulated in immune cells. Any possible dysregulation on one pathway is counteracted by an enhanced or diminished response on the other pathway. In other words, if the STAT3 activation upon IFN-β stimulation is downmodulated in DOCK8-deficient cells due to the missing GEF activity of DOCK8 protein, then, IFN-β-induced STAT1 phosphorylation would increase. Such a mechanism is consistent with the enhanced phosphorylation of STAT1 observed in helper T- and B-cells of patient D1.

Next, we aimed to measure the amount of IFNα produced by PBMCs of DOCK8-deficient patients D1 and D2 following stimulation with various nucleic acid sensor agonists. Upon stimulation of patient and healthy cells with R484 (TLR7), D35 (TLR9), transfected polyI:C (RIG-I/MDA5) and HSV (cGAS) for 24 hours, cytokine amounts in cell culture medium was measured. Interestingly, type I interferon responses triggered by these nucleic acid ligands were significantly diminished in both patients (D1 & D2) compared to healthy controls (Figure 4-3).
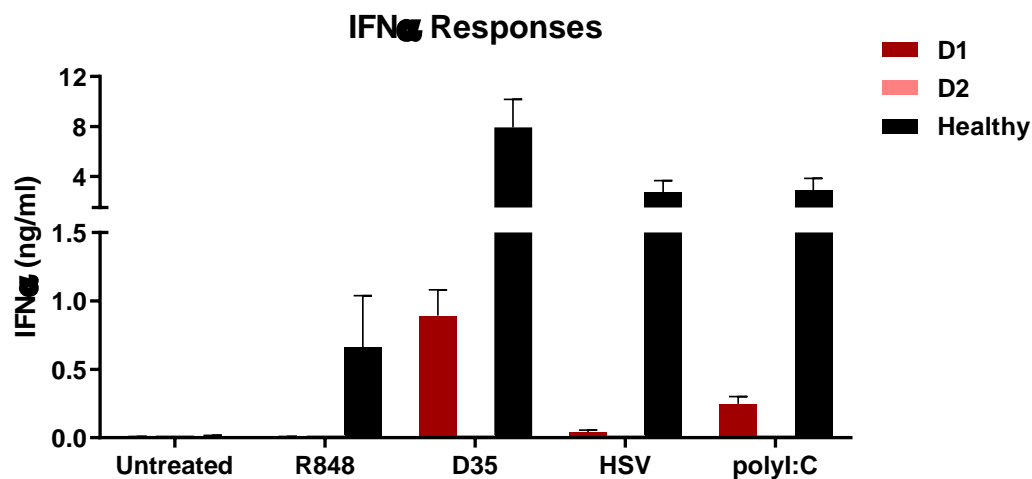
Figure 4-3: IFN-α responses to nucleic acid ligands in PBMCs of patients (D1 & D2) and healthy controls

PBMCs (0.4x10^6/well) were stimulated with various nucleic acid ligands and cell culture supernatant was collected after 24 hours. IFN-α amounts in supernatants were determined by sandwich ELISA.

To confirm that patient-derived cells are capable of responding to activating stimuli and are still viable, we next assessed the proinflammatory cytokine production in response to R848. The TNF-α and IL-1β production from R848 stimulated PBMCs were similar for both patients and healthy controls (Figure 4-4).
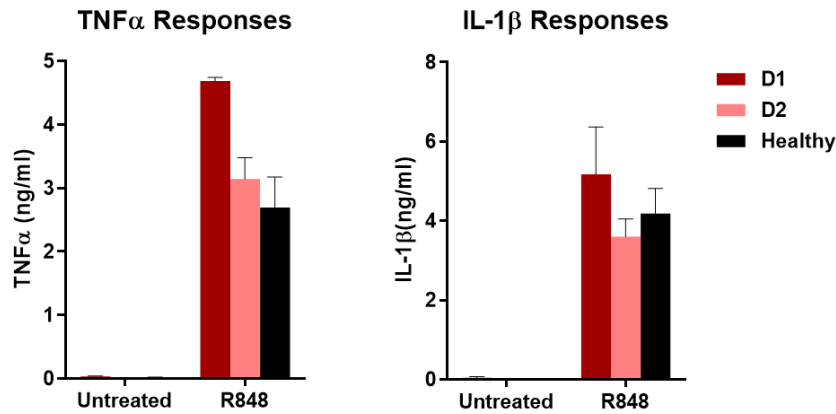
Figure 4-4 : R848-induced TNF-α and IL-1β production in PBMCs of patients (D1 & D2) and healthy controls

PBMCs (0.4x10^6/well) were stimulated with R848, a synthetic TLR7/8 agonis,t and cell culture supernatant was collected 24 hours later. TNF- α and IL-1β amounts in supernatants were determined by sandwich ELISA.

Previous reports showed a similar decrease in type I IFN production in response to TLR9 stimulation in patient PBMCs. The suggested explanation for impaired type I IFN response to CpG-ODNs in DOCK8 immunodeficiency syndrome (DIDS) was the decreased number of plasmacytoid dendritic cells (pDC), which are considered as professional type I interferon producers (Al-Zahrani et al., 2014, Keles et al., 2014). The hypothesis was based on the fact that pDCs are the major producers of type I IFNs. They selectively express nucleic acid sensors TLR7 and TLR9 that can recognize viral nucleic acids in the endosomal compartments and consequently secrete type I IFNs (Haeryfar, 2005). However, herein, we have investigated RIG-I/MDA5-mediated type I interferon production, which is not restricted to plasmacytoid dendritic cells. Type I IFN production in response to transfected dsRNA (RIG-I/MDA5) and viral DNA (cGAS) was also impaired in these patients. Moreover, when we evaluated the number of pDCs in six DOCK8 patients, only three of them (D2, D3 & D4) exhibited a reduced number of pDCs while the other three patients (D1, D5 & D6) had normal pDCs counts (Figure 4-5).
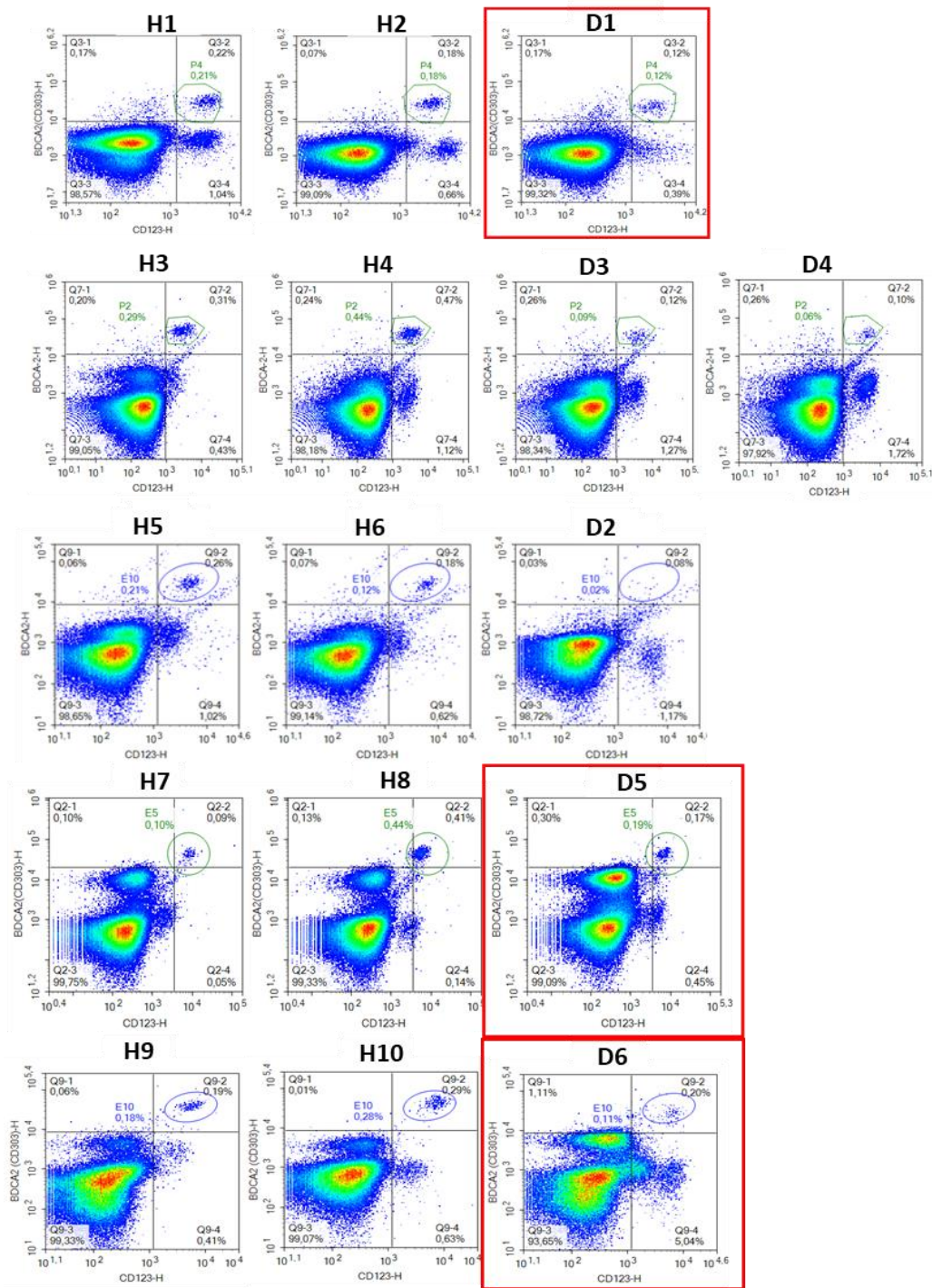
Figure 4-5: Determination of the pDC percentages in PBMCs of patients and healthy controls.

pDC population was determined as CD123 and BDCA2(CD303) co-expressing cells via flow cytometry. Patient samples (D) were presented in each row with corresponding healthy controls (H). Red squares indicate the patient samples with normal pDC count.

Of interest, although a decrease in interferon responses was observed in the patients D1 and D2, the pDC percent of patient D1 was normal whereas the pDC population was significantly reduced in patient D2. Therefore, we speculated that a possible defect in the downstream nucleic acid sensing pathways likely exists rather than a pDC-related reduction.

To further assess response of cells to nucleic acid sensor ligands, we investigated the capability of IP-10 production in monocytes of two DOCK8-deficient patients (D3 & D4) upon transfection with HSV-DNA which activates the cGAS-STING pathway. IP-10 production in response to transfected HSV-DNA was normal in monocytes of both patients (Figure 4-6). In order words, the signaling pathway involved in sensing of dsDNA in the cytosol (cGAS-STING pathway) was intact in the monocytes of the patients. Typically, IFN-α production from pDCs in response to dsDNA stimulation may contribute to IP-10 production from monocytes. Although pDC percentages in PBMCs of patients D3 and D4 were lower than healthy controls, IP-10 production in their monocytes were comparable to healthy controls.
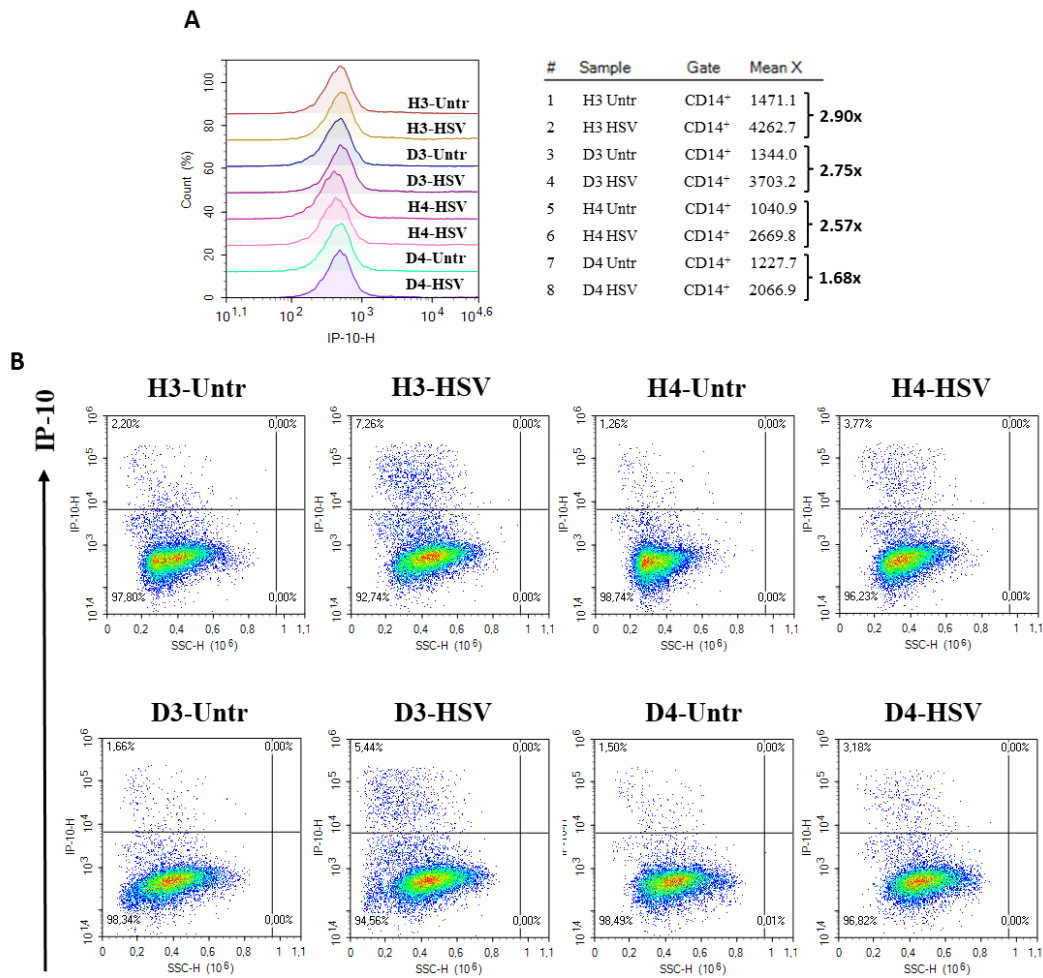
Figure 4-6: IP-10 production in the monocytes of patients and controls upon HSV-DNA stimulation.

PBMCs ($1x10^6$) were stimulated with Lipofectamine 2000 transfected HSV-DNA for 5 hours. Following 5-hour incubation, cells were treated with Brefeldin A and incubated further for 3 hours. IP-10 production was determined via intracellular cytokine staining within the $CD14^+$ cell gate. (A) Mean fluorescence intensities (MFI) in each sample and fold changes in MFI upon stimulation were presented in the figure. (B) Percent of IP-10 positive monocytes before and after stimulations were given on dot plots. (Patients: D3 & D4, Healthy Controls: H3 &H4)

IP-10 production from monocytes might be considered an indirect interferon response triggered by nucleic acid ligands. To confirm our previous finding that DOCK8-deficienct monocytes can can respond to nucleic acid ligands, we evaluated

the total ISG15 levels in the monocytes as a proxy to type I IFN signaling. Stimulation of PBMC of patient D7 and healthy control H11 with TLR4 (LPS), TLR7/8 (R848), TLR9 (D35 ODN), RIG-I (5'pppRNA) or cGAS (HSV DNA) ligands resulted in comparable levels of total intracellular ISG15 upregulation in monocytes of both subjects (Figure 4-7A) and within limits of between-subject variability, a similar pattern of response was also observed for the T-cells (Figure 4-7B). Almost all of the T-cells of the patient and healthy control were ISG15 positive upon stimulation with D35-ODN, R848, 5'pppRNA and HSV-DNA. These results indicate that the patient's monocytes and T-cells were not compromised in their response to various nucleic acid ligands .
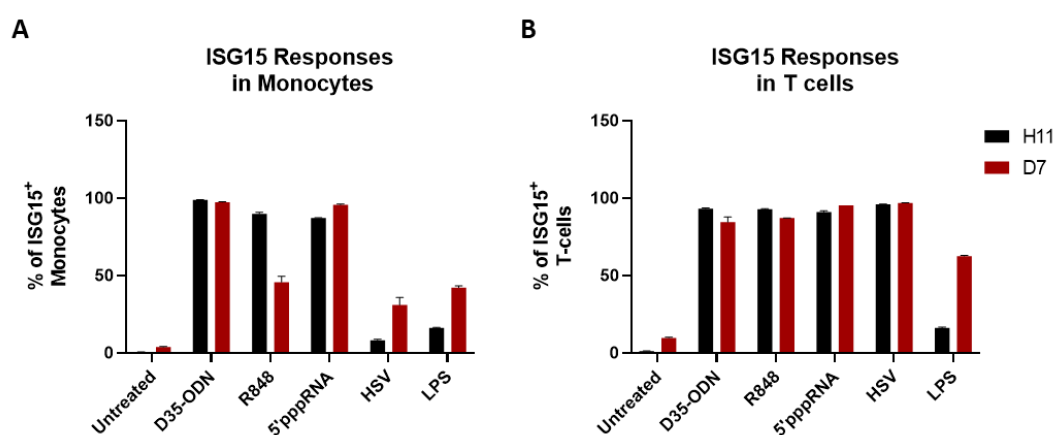
Figure 4-7: Percent of ISG15-producing cells upon stimulation with various PRR ligands.

PBMCs ($0.5x10^6$) were stimulated with several PRR ligands for 18 hours. Following overnight incubation, the percent of ISG positive Monocytes (A) and T-cells (B) were determined via intracellular cytokine staining. (Patient: D7, Healthy Control:H11)

In summary, the functional assays conducted on a very limited number of DOCK8 deficient patient samples generated contradictory data, showing either compromised or normal response to stimulation with nucleic acid ligands.

4.2 Assessment of The Gene Expression Profiles of DOCK8-Deficient Patients

To gain further insight as to why DOCK8 deficiency is often accompanied by recurrent viral infections, we decided to investigate gene expression profiles of patients with DOCK8 deficiency. For this, we performed a transcriptome analysis for PBMCs of 15 DOCK8-deficient patients (D1 to D15) using the nCounter Host Response Panel in comparison to samples collected from 24 healthy individuals selected from different age groups.

4.2.1 Principle Component Analysis (PCA) and Clustering

Firstly, we investigated the gene expression levels of patients in comparison to healthy controls using the nSolver Analysis Software version 4.0 and nCounter Advanced Analysis Software 2.0. Then, we performed principal component analysis (PCA) on log-transformed data to observe the spatial distribution of patients based on the differential expressions of 770 genes found in the panel. The findings suggested that these 15 patients were clustered into 2 distinct groups according to their gene expression profiles (Figure 4-8). Group1 includes patients coded by D2, D5, D6, D7, D8, D9, D10, D11 and D12 while Group2 covers the patients coded by D1, D3, D4, D13, D14 and D15.
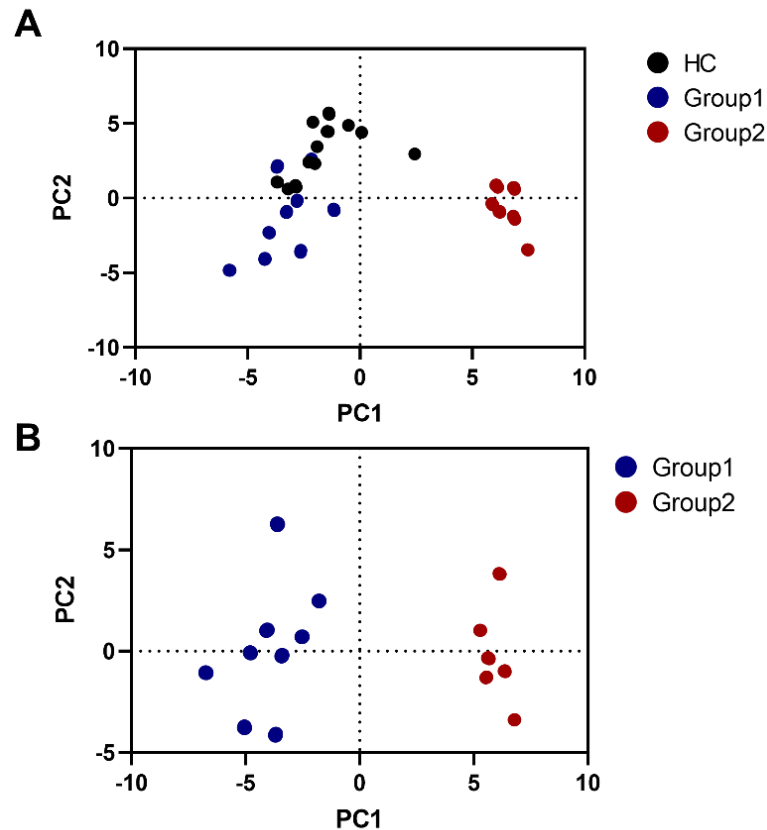
Figure 4-8: The principal component analysis (PCA) score plot of the first two PCs of differentially expressed genes in DOCK8-deficient patients in comparison to healthy controls (A) and within two groups (B).

Differential expression data from the comparison between DOCK8-deficient patients and healthy controls were log transformed. PCA was performed on log-transformed data. The score plot of PC1 and PC2 shows a clear separation of patients into 2 groups; Group1 (blue dots), Group2 (red dots) and Healthy Controls (HC: black dots).

When we compared the clinical presentations of these two groups of patients, the most apparent difference was the incidence of infections. In Group2, viral and bacterial infections were observed in 5 out of 6 patients whereas half of the patients were suffering from fungal infections. In Group1, the percentages of viral, bacterial and fungal infections were 55%, 78% and 11%, respectively. Therefore, the overall incidence of infections was higher in Group2 patients, especially those of viral and fungal origin. Moreover, all the patients in Group2 were suffering from eczema

whereases 67% of patients in Group1 had eczema. The incidence of food allergies was similar in both groups (~50%) and autoimmune manifestations were not observed in the patient cohort.

The genes that contributed to the clustering are mostly chemokines including *CCL2*, *CXCL3*, *CCL7* and *CXCL10*. These chemokines are mainly expressed in monocytes within the PBMC population. Furthermore, *ALPL* and *CSF3R* genes were identified as two of the top contributors to this clustering, which are known to be expressed specifically in neutrophils. Therefore, we next assessed the cell type scores of these patient groups compared to healthy controls. Neutrophil scores of patients in Group1 were found to be significantly higher than patients in Group2 and healthy controls (Figure 4-9A). In contrast, macrophage scores of group1 and group2 were not statistically different but were significantly higher for both patient groups compared to healthy controls (Figure 4-9B). Macrophage score calculation depends on the expression of *CD68*, *CD84*, *CD163* and *MS4A4A* genes which are differentially expressed in monocyte/macrophages. Even though the cell type scores analysis demonstrated similar macrophage scores for both groups, the clustering of the patients mainly originated from monocyte-specific chemokine encoding genes. Upregulated expression of monocyte-specific chemokines in the Group2 patients could be related to activation status of monocytes/macrophages.
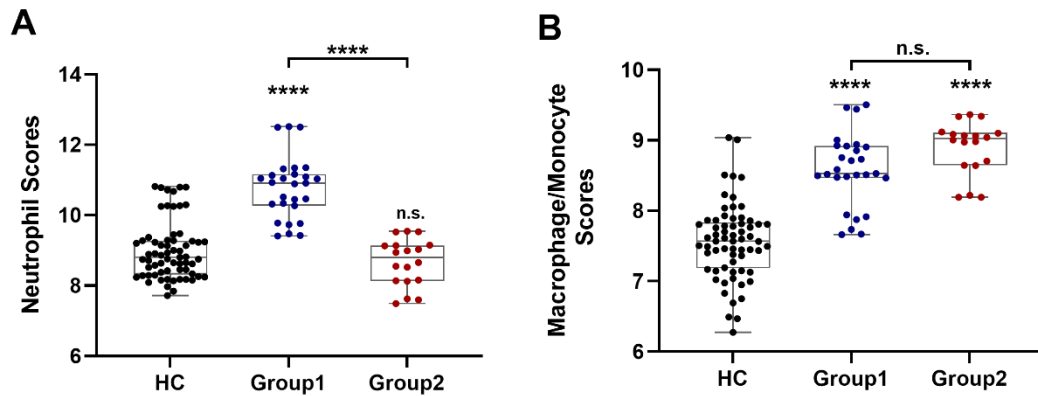
Figure 4-9: Neutrophil and Macrophage scores of Group1 and Group2 compared to Healthy Controls.

Neutrophil (A) and Macrophage/Monocyte (B) scores were calculated via nSolver advanced analysis software. One-way ANOVA with Tukey's posttest was used for the comparison of patient groups and healthy controls. Comparison between Group1 and Group2 was indicated on bars. (n.s., Not significant, *p <0.05, **p <0.01 ***p<0.001 and ****p<0.0001)

4.2.2   Assessment of Differential Gene Expression

Volcano plots were generated to visualize the differentially expressed genes in Group1 and Group2 patients in comparison to healthy controls (Figure 4-10A and B). Comparison of the two volcano plots using the same scale reveals that differential expression in Group2 versus healthy controls was more striking than in Group1 versus healthy controls. Some of the most upregulated genes in Group2 were interferon stimulated genes (ISG) such as *MX1*, *OAS1*, *IFI16*, *RSAD2* and *CXCL10*, which implies an elevated interferon signature for these patients (Figure 4-10B). Furthermore, the genes encoding the AP-1 transcription factor subunits including *JUN*, *JUNB* and *FOS* were found to be downregulated in Group2 patients (Figure 4-10B). The importance of upregulation of ISGs and downregulation of AP-1 subunit genes in disease progression will be discussed later in detail.

ALOX5 and *ALOX5AP*, required for the synthesis of leukotrienes, were significantly upregulated in Group1 patients. Both of these enzymes are expressed by all leukocytes, however, the level of expression changes according to the type of cell.

The expression levels of ALOX5 and ALOX5AP are higher in granulocytes and upregulated during inflammation (Bonyek-Silva et al., 2021). These results are consistent with the elevated neutrophil score observed in group1.
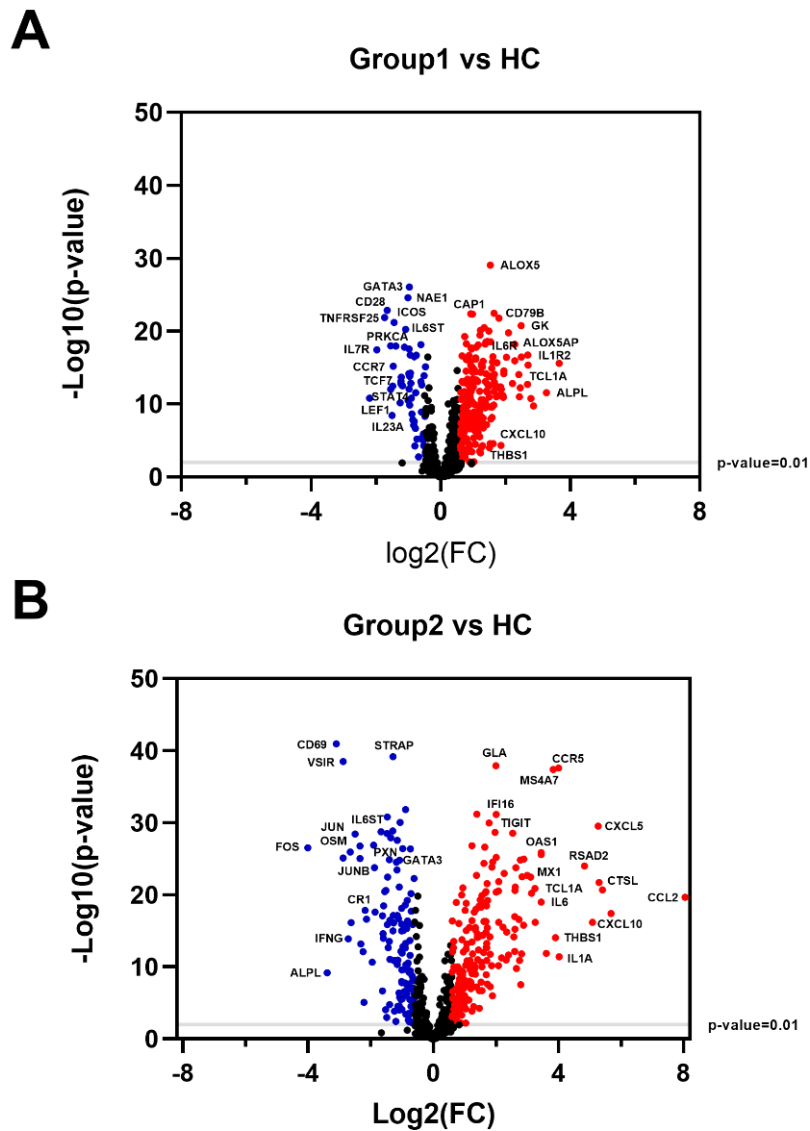
Figure 4-10: Volcano plots illustrating differentially expressed Host Response panel genes in (A) Group1(n=9) and (B) Group2(n=6) in comparison to healthy controls (n=24)

Upregulated genes with log2(fold change) ≥ 0.6 and p-value < 0.01 (red) and downregulated genes with log2(fold change) ≤ -0.6 and p-value<0.01 (blue) are shown. Identities of the most differentially expressed genes are given on the plot.

Of note, two genes; *IL6ST* and *GATA3* were downregulated in both patient groups (Figure 4-10A and B). *IL6ST* gene encodes for Glycoprotein 130 (also known as gp130, IL6ST, UL6R-beta or CD130) which is the signaling co-receptor of IL-6 family of cytokines (Hunter & Jones, 2015). Upon IL-6 family of cytokine binding to its corresponding receptor, gp130 dimerizes with this specific receptor, which consequently activates the JAK/STAT signaling pathway (Regis et al., 2008). Gp130 signaling is involved in a wide range of cellular processes, including T-cell differentiation and regulation of inflammatory responses (Nishihara et al., 2007). It is interesting that dominant negative and biallelic loss-of-function mutations in *IL6ST* gene encoding for gp130, result in different forms of hyper IgE syndrome (Shahin et al., 2019, Béziat et al., 2020). In fact, DOCK8 deficiency and gp130 deficiency share several clinical symptoms including elevated IgE levels, eczema, food allergies and most importantly higher incidence of respiratory tract infections (Shahin et al., 2019, Béziat et al., 2020). Interestingly, there are no previous reports showing a decreased expression of gp130 in DOCK8 deficiency. However, Keles et al.(2016) state that gp130 expression was normal in these patients and the defect in STAT3 phosphorylation was not due to a deficiency in this co-receptor. In contrast, our findings suggest that *IL6ST* downregulation was consistently observed in all patients in Group1 and 2, and further studies are required to verify this result at protein level. Of interest, the pivotal role of gp130 in helper T-cell dependent anti-viral immunity has been reported previously (Harker et al., 2013, Harker et al., 2015). Therefore, the investigation of *IL6ST* downregulation in DOCK8 deficiency could be a promising future perspective.

It was unexpected to observe a consistent downregulation of *GATA3* gene within the DOCK8 cohort since this gene encodes for the well-known transcription factor GATA3, involved in Th2 differentiation. Therefore, this finding paradoxical in view of the fact that DOCK8 deficiency characterized by a Th2 skewed response (Zhou & Ouyang, 2003, Tangye et al., 2017). One possible explanation for GATA3

downregulation might be the use of intravenous immunoglobulin (IVIG) replacement therapy that all the patients were receiving (Bozza et al., 2019).

In addition to these common downregulated genes, patients in both groups had upregulated expression of *CAP1, CD79B* and *TCL1A* genes. Adenylate cyclase-associated protein 1 (CAP1) is involved in the regulation of actin filament organization and facilitates actin filament turnover (H. Zhang et al., 2013). Depletion of CAP1 induces the accumulation of F-actin and lamellipodia formation. DOCK8 plays a pivotal role in actin cytoskeleton organization through the activation of CDC42. The absence of DOCK8 protein results in defective F-actin polymerization during immunological synapse formation and migration (Q. Zhang et al., 2016). The defect in actin filament formation in DOCK8-deficient cells might induce *CAP1* expression to facilitate the F-actin turnover.

CD79B was one of the most significantly upregulated genes in both patient groups. Additionally, the signaling partner of *CD79B*, *CD79A*, was also upregulated in both patient groups. Together, these molecules act as a signaling unit of the BCR complex for the maturation and activation of B cells (Burger & Wiestner, 2018). In DOCK8 deficiency, B cell maturation and memory B cell formation are impaired due to the defects in immunological synapse formation and TLR/MyD88 signaling (Randall et al., 2009, Jabara et al., 2012). Therefore, the upregulation of CD79 could be a compensatory mechanism for B-cell activation.

Another gene that is upregulated in both patient groups is *TCL1A*. Under normal circumstances, the expression of *TCL1A* is restricted to embryonic stages and pre-mature T- and B-cells. However, certain conditions such as malignancies and viral infections may induce the expression of *TCL1A* in mature T- and B-cells (Aggarwal et al., 2008). Overexpression of *TCL1A* has been shown to result in enhanced ROS production and consequently induce genomic instability in the context of malignancies (Stachelscheid et al., 2021, 2022). The overexpression of proto-oncogene *TCL1A* may be related to the increased risk of cancer observed in DOCK8 patients (Biggs et al., 2017). Of note, somatic reversion is a common phenomenon

72

observed in certain primary immunodeficiency diseases including DOCK8 deficiency (Pillay et al., 2021b; Revy et al., 2019). It has been stated that genomic instability would increase the chance of somatic reversion in PIDs which results in a milder clinical outcome (Miyazawa & Wada, 2021). Therefore, the upregulated expression of *TCL1A* might be important to understand the high frequency of somatic reversions observed in DOCK8 deficiency.

4.2.3 Assessment of Upregulated and Downregulated Pathways in Two Patient Groups

The clustering of two groups was also observed with the heatmap of pathway scores for the comparison of the patient groups with healthy controls (Figure 4-11). While all the patients in Group2 clustered together, some patients in Group1 were located within health controls in the heatmap of pathway scores. Two patients in Group1 clustered differently than the other patients within the heatmap of pathway scores, which could affect the pathway scores of this group. Additionally, pathways upregulated in Group2 were generally downregulated in Group1 or vice versa. It was interesting to observe a reverse pattern between patient groups. With the inverse gene expression profiles of two patient groups, it would be difficult to study all the patients as one group. Thus, in line with our initial findings, it would be more beneficial to evaluate the patients as two groups to find clues on molecular mechanisms underlying DIDS.
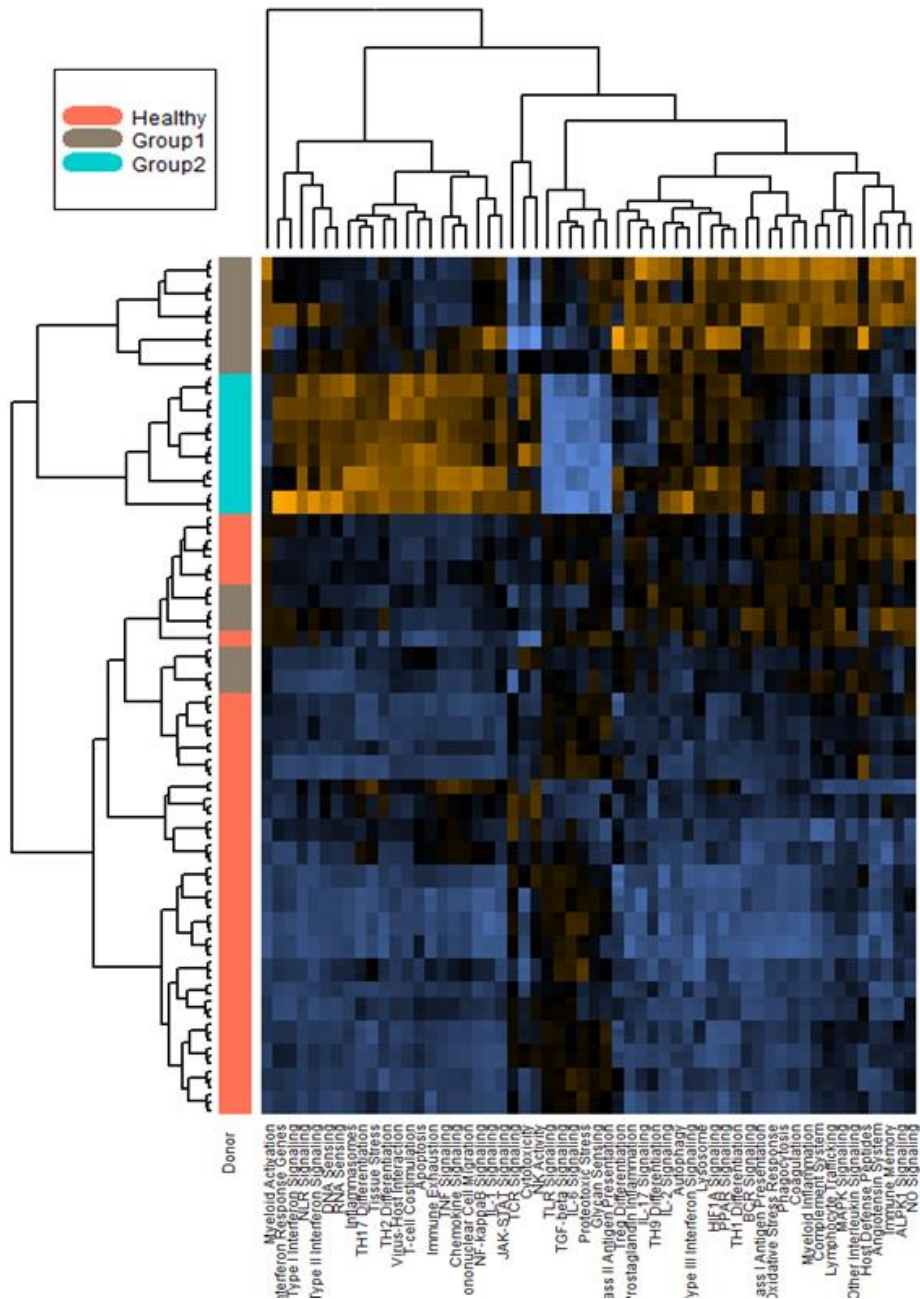
Figure 4-11: Heatmap of pathway scores for the comparison of two patient groups and healthy controls.

The heatmap shows the clustering of patient groups according to their pathway score profiles. Blue indicates a low score while orange indicates a high score (Group 1: D2, D5, D6, D7, D8, D9, D10, D11 and D12; Group2: D1, D3, D4, D13, D14 and D15). Scores are displayed on the same scale via a Z-transformation.

74

4.2.3.1 Assessment of Dysregulated Pathways Related to Viral Immunity in DOCK8-deficient Patients

The heatmap showed a general upregulation in Group2 for the pathways related to viral immunity including, Interferon Response Genes, Interferon Type I, II & III signaling, DNA and RNA sensing pathways. Therefore, we next, compared the z-scores of patient groups and healthy controls for each viral immunity-related pathway. The z-score of Interferon Response Genes were significantly higher for both patient groups when compared to healthy controls (Figure 4-12A). Furthermore, Group2 patient scores were strikingly higher than Group1. Consistently, most of the interferon response gene members were significantly upregulated in this group. A similar pattern was observed for the Type I, II and III Interferon signaling pathways. Compared to healthy controls, z-scores for Interferon signaling pathways were higher for both patient groups and Group2 scores were consistently higher than Group1 (Figure 4-12B, C and D).

The overall increase in expression of type I interferon associated genes in both group of patients could stem from the recurrent viral infections, particularly those commonly caused by HSV. Although interferon stimulated gene signature was elevated, our preliminary results indicate that type I interferon secretion is compromised. Evidence suggests that following an initial viral infection, innate immune cells robustly respond to this insult by producing large amounts of type I interferons. However, after this initial wave, the cells tune down this response, producing lower levels of type I interferons in response to both the ongoing infection and to unrelated secondary stimuli (Greene et al., 2021). This exhausted state, favors virus persistence and is associated with decreased response to PRR agonists. This "exhausted phenotype" is in line with our findings
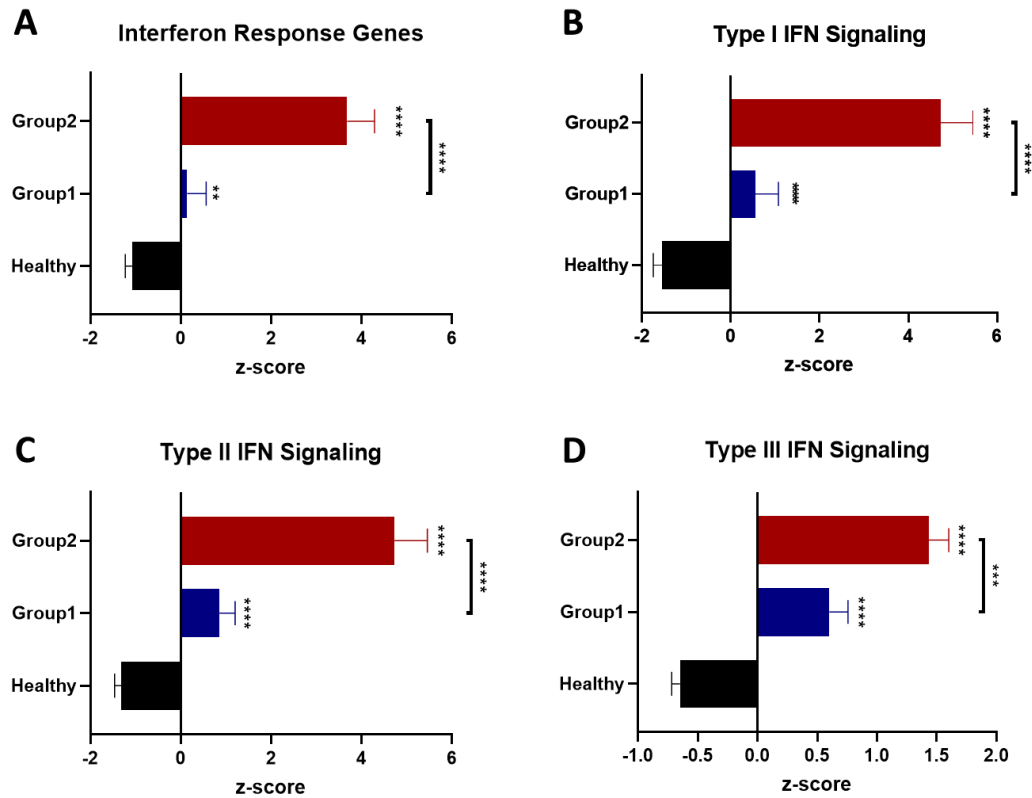
Figure 4-12: Bar graphs illustrating the Interferon Response Genes, Type I, II & III Signaling pathway z-scores in groups and healthy controls.

The z-scores of Interferon Response Genes (A), Type I (B), II (C) and III (D) IFN signaling were calculated via nSolver advanced analysis software. One-way ANOVA with Tukey's posttest was used for the comparison of patient groups and healthy controls. Comparison between Group1 and Group2 was indicated on bars. (n.s., Not significant, *p <0.05, **p <0.01 ***p<0.001 and ****p<0.0001)

However, to confirm that the diminished response we observed at the protein level does not stem from a reduction in expression of nucleic sensors, we next analyzed the z-scores for DNA and RNA sensing pathways to see if there is any downregulation that may cause a diminished interferon response to nucleic acid ligands in these patients. The results showed that z-scores of both DNA and RNA sensing pathways were significantly higher than that of healthy controls in both patient groups and greatly elevated in Group2 (Figure 4-13).

Figure 4-13: The comparison of z-scores of the DNA & RNA Sensing pathways for the patient groups and healthy controls.

The z-scores of DNA (A) and RNA (B) sensing pathways were calculated via nSolver advanced analysis software. One-way ANOVA with Tukey's posttest was used for the comparison of patient groups and healthy controls. Comparison between Group1 and Group2 was indicated on bars. (n.s., Not significant, *p <0.05, **p <0.01 ***p<0.001 and ****p<0.0001)

We also investigated the differential expression of each sensor for both patient groups (Figure 4-14). The expression of DNA sensor cGAS was similar to healthy controls for both group of patients (Figure 4-14A). The expression of other DNA sensors *ZBP1* (DAI), *IFI16* and *AIM2* were upregulated in both groups. Specifically, *IFI16* and *AIM2* expressions in Group2 were ~4-fold higher than healthy controls. The expression of these sensors are known to be upregulated with interferon signaling (Kumari et al., 2020, Karki et al., 2021). The enhanced interferon signaling in these patients may explain the upregulation of these genes. In conclusion, these findings favor the exhausted phenotype mechanism and rules out the possibility that the diminished interferon production stems from a decreased expression of cytosolic DNA sensors.

However, our findings also revealed a significant downregulation in *STING1* gene in Group2 patients. STING is a central molecule for the inhibition of HSV replication (Sharma et al., 2021). As mentioned above, most of the DOCK8 patients suffer from infections caused by HSV, which is a double-stranded DNA (dsDNA) virus.

Decreased expression of *STING1* might accounts for the persistent HSV infections observed in these patients. Of interest, HSV infection itself can also downmodulate STING expression. HSV evades anti-viral response by preventing STING protein translation through the induction of miR-24 expression, which binds to the 3'UTR region of *STING1* mRNA and causes translational repression (Sharma et al., 2021).

Figure 4-14: Differential expression of the cytosolic DNA and RNA sensing molecules in patient groups.

Change in gene expression was calculated as Log2(Fold Change) of healthy controls and presented with lower and upper limits. Dotted lines indicate log2(Fold Change) =0.6 for upregulated genes and log2(Fold Change) =-0.6 for downregulated genes (n.s., Not significant, *q<0.05, **q <0.01 ***q<0.001 and ****q<0.0001)

.

The expressions of RIG-I-like receptors (RLR) and their adaptor protein MAVS were also upregulated in Group2 patients. *DDX58* (RIG-I) and *IFIH* (MDA5) are the two major RNA sensors responsible for the recognition of viral RNA and the generation of anti-viral immune response. They are not only responsible for the detection of ssRNA and dsRNA viruses, but also play role in recognition of DNA viruses like HSV. Since their expression are dependent on interferon signaling pathway, their upregulation in this patient group is expected due to the enhanced interferon signature. In summary, our findings suggest once again that the reduced

type I interferon secretion in response to cytosolic polyI:C, does not stem from a reduced expression of RNA sensors, but is consistent with the exhausted phenotype view.

The type I IFN production in response to R848 (TLR7/TLR8) and D35 (TLR9) was also lower in patients compared to healthy controls. Therefore, we also compared the expression of endosomal TLRs in the patient groups relative to healthy controls. In Group2, there was no significant change in the expression of endosomal TLRs (Figure 4-15). The expression of TLR8 was upregulated ~2.4-fold in Group1 compared to healthy controls. Therefore, we can conclude that the aberrant interferon response to these nucleic acid ligands is not due to the decreased expression of their cognate sensors but is consistent with the exhausted state of responding cells.
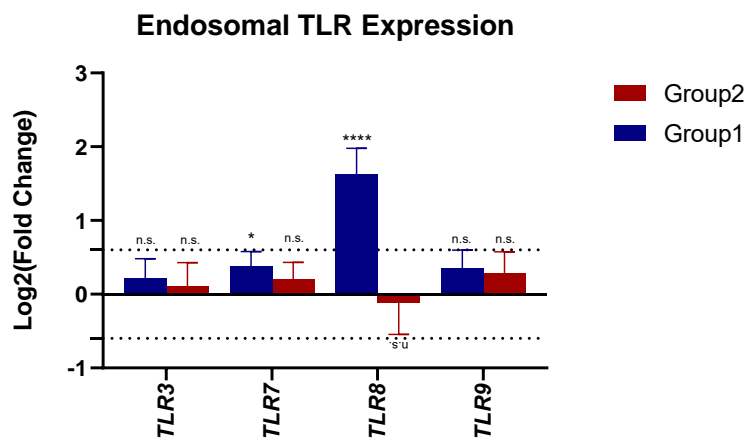
Figure 4-15 Differential expression of the endosomal TLRs in patient groups.

Change in gene expression was calculated as Log2(Fold Change) of healthy controls and presented with lower and upper limits. Dotted lines indicate log2(Fold Change) =0.6 for upregulated genes and log2(Fold Change) =-0.6 for downregulated genes (n.s., Not significant, *q<0.05, **q <0.01 ***q<0.001 and ****q<0.0001)

4.2.3.2   Assessment of Dysregulated Pathways Related to MAPK and AP-1 signaling in DOCK8-deficient Patients

Most of the immune related pathways were upregulated in Group2 patients whereas a few pathways were observed to be downregulated. Particularly, the MAPK signaling pathway was found to be downregulated only in the Group2 patients. The z-scores of MAPK signaling in both patient groups in comparison to healthy controls showed a significant downregulation in Group2 but a significant upregulation in Group1 (Figure 4-16). MAP kinases are activated by phosphorylation following cellular stimulation and phosphorylate transcription factors to regulate gene expression (Qi & Elion, 2005). MAP kinases are divided into three subfamilies; ERK, JNK and p38. Certain cytokines and/or stress, generally induces the activation of JNK and p38 cascades, whereas ERK signaling is initiated by growth factors and mitogens ERK signaling is associated with cell growth and differentiation whereas, JNK and p38 signaling pathways primarily induce cytokine production, inflammation and apoptosis (Morrison, 2012).
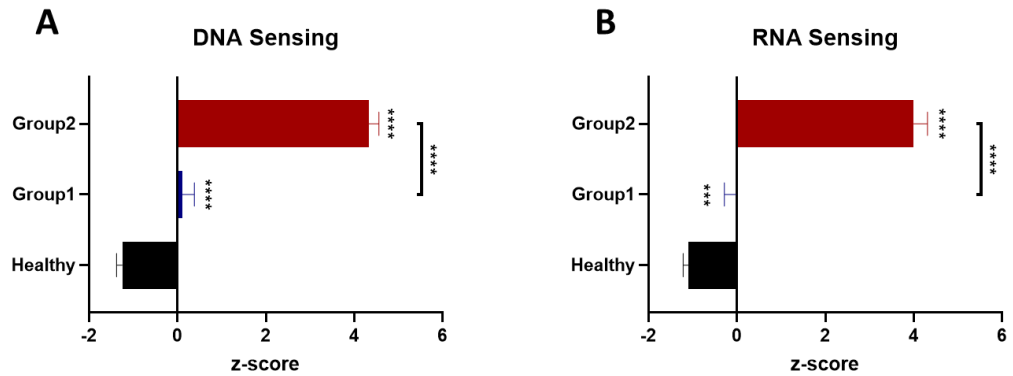

Figure 4-16: The comparison of z-scores of the MAPK signaling pathway for the patient groups and healthy controls.

The z-scores of the MAPK signaling pathway were calculated via nSolver advanced analysis software. One-way ANOVA with Tukey's posttest was used for the comparison of patient groups and healthy controls. Comparison between Group1 and Group2 was indicated on bars. (n.s., Not significant, *p <0.05, **p <0.01 ***p<0.001 and ****p<0.0001)

80

To gain further insight into which components are responsible for this dysregulated MAPK signaling, we evaluated the most differentially expressed genes related to the MAPK signaling pathway for both patient groups. Results showed that *JUN* (~5.2 fold), *JUNB* (~4.8 fold) and *FOS* (~15.4 fold) genes were significantly downregulated in Group2 patients (Figure 4-17). These genes encode for a family of DNA binding proteins that function as the subunits of the AP-1 complex. Upon activation of JUN and FOS protein by certain MAP kinases, AP-1 complex regulates the expression of inflammatory genes in response to a variety of stimuli, including growth factors, cytokines and stress signals (Gazon et al., 2018). The well-known functions of AP-1 signaling in the immune system are the regulation of cytokine production and T-cell activation (Katagiri et al., 2021a). For example, upon activation of MAPK cascade with a certain stimulus, MAP kinase JNK (*MAPK8*) phosphorylates JUN and activated JUN dimerizes with FOS to promote transcription of target genes including, IL-2 which is required for T cell activation and its effector function (Murphy & Weaver, 2016a). Although *MAPK8* is not differentially expressed in these patients, upstream of *MAPK8*, *MAP3K1* (MEKK1) was also ~2 fold downregulated in Group2 patients (Figure 4-17). Decreased expression of AP-1 subunit genes and *MAP3K1* are consistent with the defect of T cell activation and differentiation observed in DOCK8 deficiency (Lambe et al., 2011, Randall et al., 2011). Furthermore, it has been shown that JUNB, one of the subunits of AP-1 complex, plays a pivotal role in T-cell differentiation, especially the Treg subset (Katagiri et al., 2021). In fact, the absence of JUNB, the expression of certain effector molecules of Tregs such as *CTLA4* and *ICOS* is downregulated, which restricts the suppressive function of regulatory T-cells. Both *CTLA4* (~2.3 fold in Group1 and ~1.6 fold in Group2) and *ICOS* (~2.7 fold in Group1 and ~2. 6 fold in Group2) were also downregulated in both patient groups, which is consistent with the impaired suppressive ability of regulatory T-cells in DOCK8 deficiency (Singh et al., 2017).
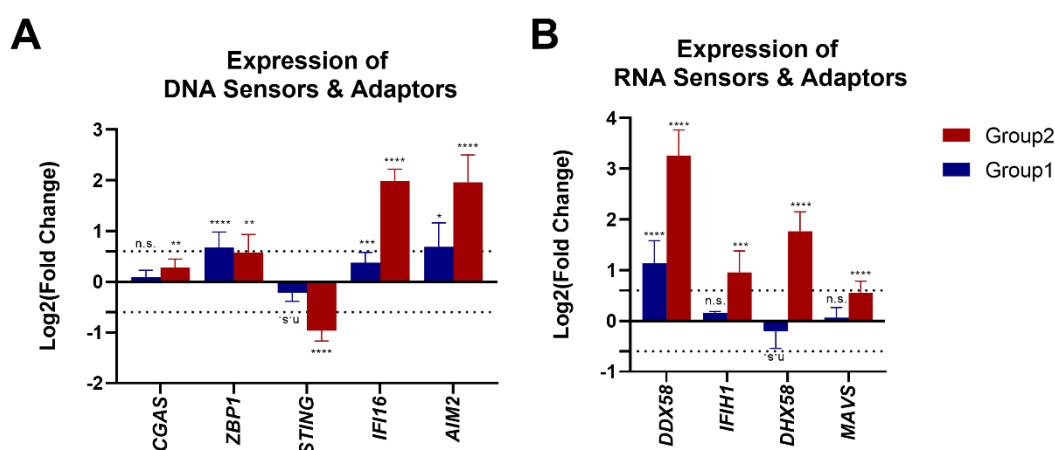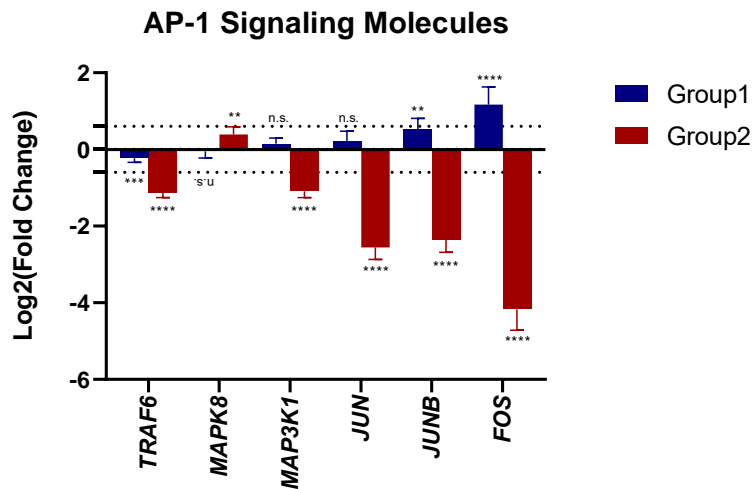
Figure 4-17: Differential expression of the AP-1 signaling molecules in patient groups.

Change in gene expression was calculated as Log2(Fold Change) of healthy controls and presented with lower and upper limits. Dotted lines indicate log2(Fold Change) =0.6 for upregulated genes and log2(Fold Change) =-0.6 for downregulated genes (n.s., Not significant, *q<0.05, **q <0.01 ***q<0.001 and ****q<0.0001)

TRAF6/MEKK1-mediated signaling also plays a pivotal role in the production of type I IFNs in response to viral infections and dsRNA ligands (Yoshida et al., 2008). Downregulated expressions of both *TRAF6* and *MAP3K1* (MEKK1) in Group2 patients may indicate a possible defect in the downstream of RLR/MAVS pathway (Figure 4-17). Another example of the involvement of AP-1 in anti-viral immunity is that Influenza A infections induce AP-1 dependent anti-viral cytokine production from infected cells through the activation of JNK signaling pathway (Ludwig et al., 2001). Furthermore, during viral infection, IFN-β transcription is activated and amplified by IFN-β enhanceosome, which consists of NF-κB, AP-1, IRFs and CBP, which is pivotal for the clearance of viral infection (Merika et al., 1998). Furthermore, it has been shown that TLR9 induced interferon response in pDCs is linked to the function of AP-1 transcription factors (Mann-Nüttel et al., 2021). Therefore, the consistent downregulation in AP-1 subunits in Group2 patients might be relevant to the aberrant type I interferon production from patient PBMCs and needs to be further investigation.

4.2.3.3 Assessment of Dysregulated Pathways Related to Immune Exhaustion and Apoptosis in DOCK8-deficient Patients

T-cell activation requires the combined effort of NFAT and AP-1 signaling. AP-1 and NFAT forms a heterodimer which binds to DNA for the promotion of target gene transcription (Murphy & Weaver, 2016a). In the absence of AP-1, signaling through the NFAT results in the suppression of target gene expression and impairment in T cell activation and proliferation, leading to T-cell exhaustion (Atsaves et al., 2019). T-cell exhaustion is a common phenomenon observed in the case of chronic viral infections. Exhaustion can be defined as the state of T-cells with decreased capacity of effector cytokine production and increased surface expression of inhibitory receptors (Wherry & Kurachi, 2015). Of note, the expression of AP-1 subunits has been reported to be downregulated in the context of T-cell exhaustion (Wherry et al., 2007). Due to the correlation between AP-1 signaling and T-cell exhaustion, we investigated the z-scores of the immune exhaustion pathway in patient groups compared to healthy controls. The z-score of the immune exhaustion pathway was found to be elevated in both group of patients compared to healthy controls and the z-score of Group2 was significantly higher than Group1 (Figure 4-18). Our findings are consistent with previous reports showing an increased percentages of exhausted effector memory T-cells (CD45^{+}CCR7^{-}) in DOCK8 deficiency (Janssen et al., 2014; Randall et al., 2011). Of interest, Pillay et al. have proposed that the exhausted phenotype is T-cell intrinsic and caused by DOCK8 deficiency. The exhausted phenotype possibly contributes to failure of the capability of viral clearance and results in persistent infections.

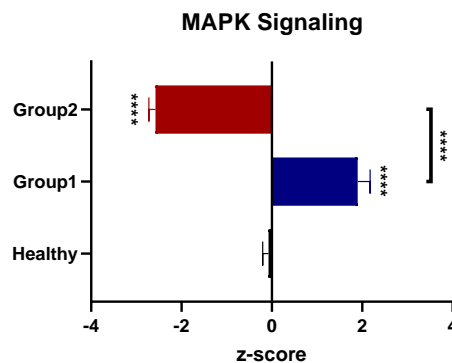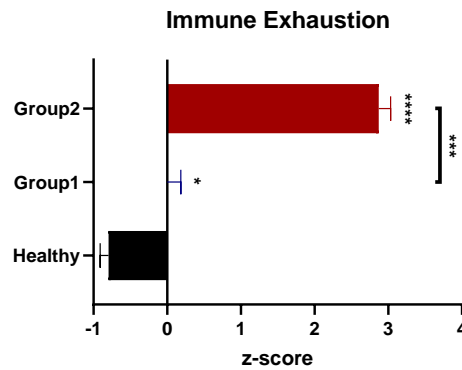*Figure 4-18: The comparison of z-scores of the immune exhaustion pathway for the patient groups and healthy controls.*

The z-scores of the immune exhaustion pathway were calculated via nSolver advanced analysis software. One-way ANOVA with Tukey's posttest was used for the comparison of patient groups and healthy controls. Comparison between Group1 and Group2 was indicated on bars. (n.s., Not significant, *p <0.05, **p <0.01 ***p<0.001 and ****p<0.0001)

In order to further evaluate the exhausted phenotype in the two patient groups, we next investigated the most differentially expressed immune exhaustion markers in both patient groups. The analysis revealed that three of the co-inhibitory receptors, *TIGIT*, *LAG3* and *HAVCR2* (TIM-3), were significantly upregulated in Group2 whereas only *HAVCR2* (TIM-3) was upregulated in Group1 patients (Figure 4-19). Interestingly, the major co-inhibitory receptor and exhaustion marker *CTLA4,* was downregulated in both patient groups, especially in Group1. Targeting the co-inhibitory receptors to overcome T-cell exhaustion and consequently clear persistent viral infections is a promising approach that multiple research groups have been working on (Pauken & Wherry, 2015). Our findings are significant in terms of identifying a possible target for the reversal of T-cell exhaustion in DOCK8 deficiency. Due to the decreased expression of CTLA4 in these patients, targeting other co-inhibitory receptors such as TIGIT could be of considerable interest. Ongoing trials in TIGIT blockage of human T-cells might be adapted for the management of DOCK8 deficiency in the future (Harjunpää & Guillerey, 2020).
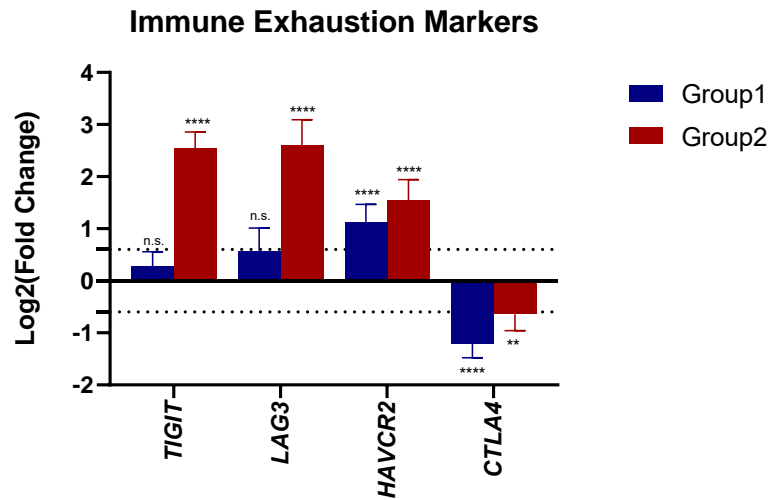
Figure 4-19:Differential expression of the immune exhaustion markers in patient groups.

Change in gene expression was calculated as Log2(Fold Change) of healthy controls and presented with lower and upper limits. Dotted lines indicate log2(Fold Change) =0.6 for upregulated genes and log2(Fold Change) =-0.6 for downregulated genes (n.s., Not significant, *q<0.05, **q <0.01 ***q<0.001 and ****q<0.0001)

Although immune exhaustion is generally used in the context of T-cells, it is known that increased expression of co-inhibitory receptors involved in exhaustion can also be observed in other immune cell types, including monocytes/macrophages and dendritic cells. For example, TIM-3 is expressed by multiple immune cells including, NK cells, Dendritic cells, monocytes and macrophages. TIM-3 has been shown to play a pivotal role in the regulation of innate immune responses to TLR stimulation (Yang et al., 2013). The upregulation of TIM-3 in DOCK8-deficient PBMCs is consistent with in the exhausted immune phenotype of innate immune cells, accounting for the decreased production of type I IFN in response to endosomal TLR stimulation.

Another gene product with a regulatory function is the lymphocyte activation gene 3 (LAG-3). Workman et al. have reported high expression of *LAG3* in plasmacytoid dendritic cells and demonstrated that deletion of LAG-3 resulted in increased proliferation and expansion of pDCs (Workman et al., 2009). Therefore, the

upregulated expression of *LAG3* in DOCK8-deficient PBMCs might be relevant to the decreased number and impaired function of pDCs in these patients.

Our data also revealed that apoptosis pathway was upregulated in Group2 but not Group1 patients (Figure 4-20). In Group2 patients, the most differentially expressed gene in the apoptosis pathway was *CSTL* (Cathepsin L), a cysteine protease, involved in antigen processing whose expression is upregulated in chronic inflammation (Cao et al., 2017). The expression of *CTSL* was ~36 fold upregulated in Group2 patients, possibly correlated with the recurrent chronic viral infections. Of note, DOCK8-deficient cells are known to be more prone to apoptosis than wild-type cells (Kearney et al., 2017). Therefore, targeting CTSL with specific inhibitors might be a viable treatment option for DOCK8 deficiency.
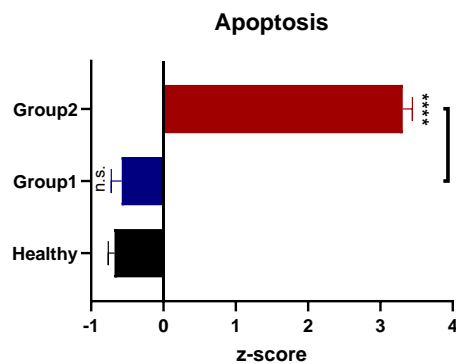
Figure 4-20:The comparison of z-scores of the apoptosis pathway for the patient groups and healthy controls.

The z-scores of the apoptosis pathway were calculated via nSolver advanced analysis software. One-way ANOVA with Tukey's posttest was used for the comparison of patient groups and healthy controls. Comparison between Group1 and Group2 was indicated on bars. (n.s., Not significant, *p <0.05, **p <0.01 ***p<0.001 and ****p<0.0001)

4.2.4 Assessment of Normalization in Dysregulated Gene Expression Profile of a Patient with DOCK8 Deficiency Following Hematopoietic Stem Cell Transplantation (HSCT)

Hematopoietic stem cell transplantation (HSCT) is the only curative treatment available for DOCK8-deficient patients (Haskologlu et al., 2020). One patient in the cohort that had clustered in Group2 underwent a successful bone marrow transplantation. Post-transplantation, patient's overall health improved and persistent viral infections were cleared. To investigate the impact of HSCT on the dysregulated gene expression profile of this DOCK8-deficient patient, RNA samples of the patient prior to and 1-year post-transplant were isolated from fresh PBMCs and gene expression analysis was performed simultaneously. Volcano plots were generated to visualize the differentially expressed genes in the patient prior to (D1) and 1 year after HSCT (D1-HSCT) in comparison to healthy controls (Figure 4-21A and B). The overall variation in gene expression profiles of patient in comparison to healthy controls significantly normalized after HSCT. Upregulated expressions of ISGs, chemokines and exhaustion markers were normalized post-HSCT. Furthermore, downregulated expressions of AP-1 subunit genes were upregulated and become similar to healthy controls.
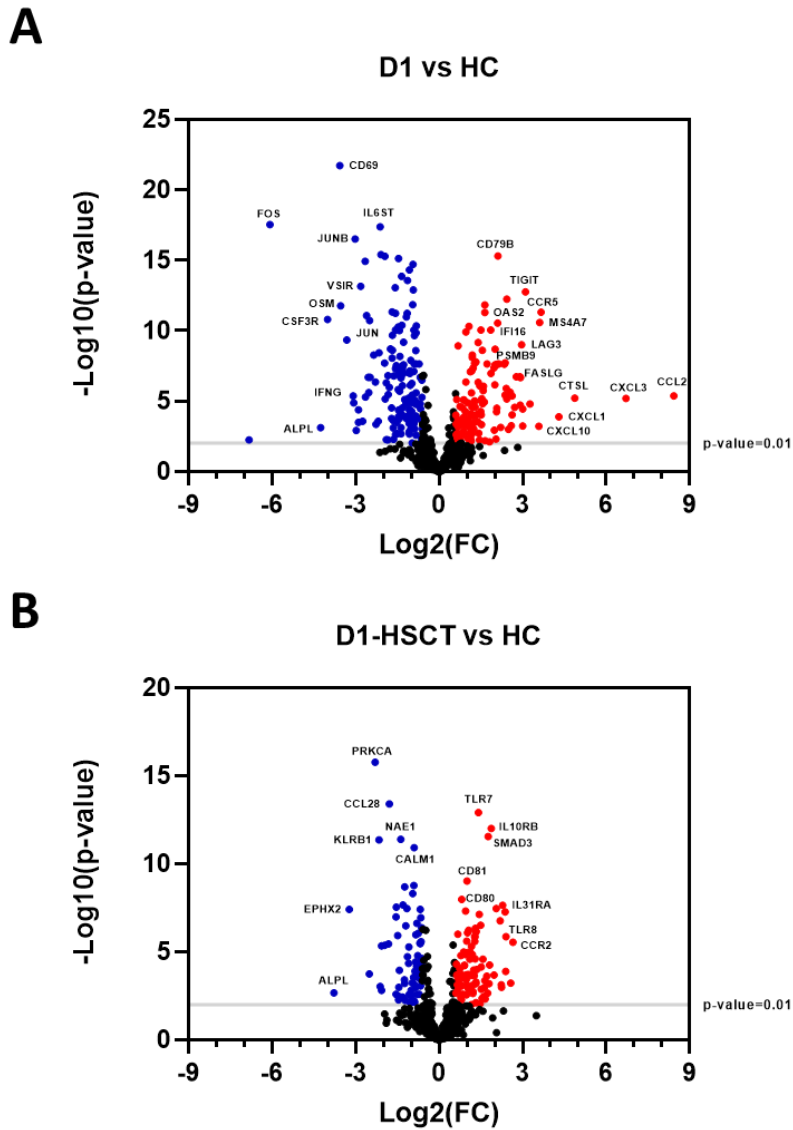
Figure 4-21: Volcano plots illustrating differentially expressed Host Response panel genes in the patient (A) prior to transplantation (D1) and (B) 1 year after HSCT (D1-HSCT) in comparison to healthy controls (n=24)

Upregulated genes with log2(fold change) ≥ 0.6 and p-value < 0.01 (red) and downregulated genes with log2(fold change) ≤ -0.6 and p-value<0.01 (blue) are shown. Identities of the most differentially expressed genes are given on the plot.

In Group2 patients, we previously showed that interferon-stimulated genes were upregulated, implying an elevated interferon signature. In order to investigate the effect of HSCT on this elevated interferon signature, we next evaluated the differential expression of interferon-stimulated genes in the patient before and after bone marrow transplant (Figure 4-22). The expression of most ISGs in the patient (D1) was found to be significantly upregulated and normalized following HSCT.
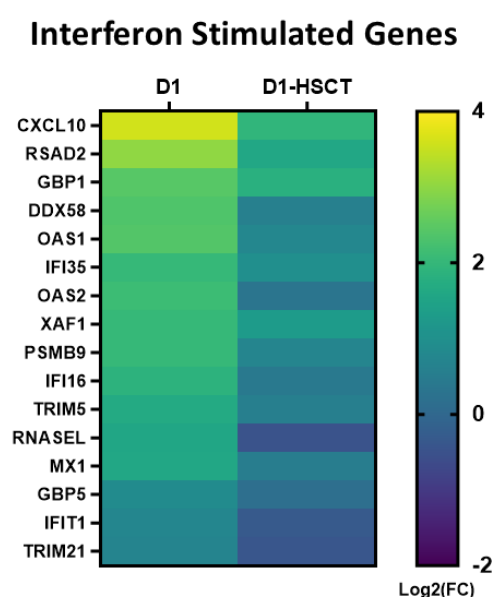
Figure 4-22: Heatmap illustrating the log2 (fold change) of Interferon-induced genes differentially expressed in the patient, prior to (D1) and 1-year post-transplantation (D1-HSCT) relative to healthy controls (n=24).

Furthermore, we also showed that the expression of genes associated with MAP kinase and AP-1 signaling pathways was decreased in Group 2 patients. Considering the clustering of patient D1 within Group2, we observed a similar degree of downregulation in these genes including *FOS*, *JUN*, *JUNB* and *MAP3K1* (MEKK1) in this patient, as expected (Figure 4-23A). The drastic downregulation in AP-1 subunit genes was normalized after HSCT. However, the *MAP3K1* expression, which was 2.2-fold lower before the transplant in comparison to healthy controls,

was partially normalized 1 year after the transplant. Additionally, our previous analysis revealed a significant upregulation in the expression of three immune exhaustion markers, TIGIT, LAG3 and HAVCR2 (TIM-3) in Group2 patients. In patient D1, similarly, TIGIT and LAG3 were significantly upregulated and normalized after the bone marrow transplant (Figure 4-23B).
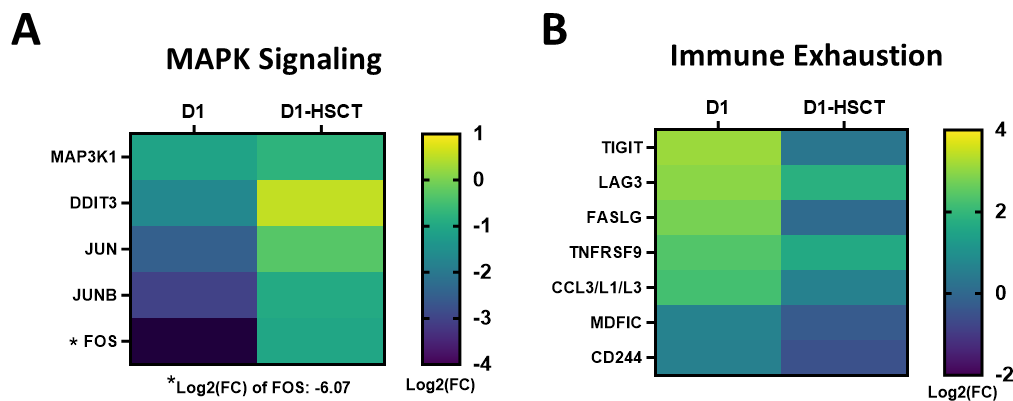
Figure 4-23: Heatmap illustrating the log2 (fold change) of differentially expressed MAPK signaling and Immune Exhaustion related genes in the patient, prior to (D1) and 1-year post-transplantation (D1-HSCT) relative to healthy controls (n=24).

Collectively, our results suggested that the dysregulated gene expression observed in the patient D1 clustered within Group2 was normalized 1-year after the successful bone marrow transplant, which is in line with the improved overall health of the patient post-HSCT.

CHAPTER 5

CONCLUSION

The scope of our lab is to gain insight on underlying mechanisms contributing to the progression of diseases associated with a variety of inborn errors of immunity. Our main focus in this study was the primary immunodeficiency diseases (PIDs) that lead to susceptibility to viral infections. First, we aimed to unravel the utilization of Ruxolitinib as a bridge therapy in a patient with a gain-of-function mutation in the DNA-binding domain of the *STAT1* gene to manage disease manifestations including viral and fungal infections. In line with this, we investigated the dysregulated gene expression profile of STAT1 GOF patient prior to, during Ruxolitinib and after HSCT. Secondly, in light of our preliminary findings suggesting the compromised type I IFN production in response to viral mimicry ligands, we investigated the deregulated immune-related pathways that can be associated with viral immunity in DOCK8 deficiency.

The primary immunodeficiency disease caused by the gain-of-function (GOF) mutations in the *STAT1* gene is characterized by chronic mucocutaneous candidiasis (CMC), chronic viral infections and autoimmunity. These gain-of-function mutations result in enhanced STAT1 phosphorylation and impaired dephosphorylation accompanied by defective Th17 differentiation. Herein, we confirmed the pre-defined cellular level defects in a patient with sporadic *STAT1* T385M mutation, who presented with CMC, recurrent respiratory tract infections and autoimmunity. The disease manifestations that the patient suffered from were resolved with the 6 months use of Ruxolitinib treatment. In line with the improved health status of the patient, impaired STAT1 phosphorylation dynamics were partially normalized following Ruxolitinib treatment. Interestingly, the Th17 deficiency persisted after Ruxolitinib treatment despite the clearance of CMC; this

may imply the involvement of pathways other than defective Th17 immunity in susceptibility to fungal infections for STAT1 GOF patients (Break et al., 2021b).

We also evaluated the gene expression profile of the patient in comparison to healthy controls to determine which pathways were dysregulated because of the gain-of-function mutation in the DNA binding domain of *STAT1* gene. Firstly, interferon-stimulated genes were found to be consistently upregulated in the patient, implying an interferon signature. Furthermore, the antigen processing, T- and B-cell function related genes were also significantly upregulated. The identification of these upregulated pathways has pivotal importance to uncover the underlying causes of autoimmune manifestations observed in STAT1 GOF patients. Autoimmune hemolytic anemia, the major manifestation of autoimmunity in the patient, has been shown to be triggered by interferon alpha/beta treatment as an adverse side effect (S. Wang et al., 2017). This may suggest that the elevated interferon signature has a role in the emergence of the patient's autoimmune manifestations. Consistent with this view, autoimmunity in the patient resolved following Ruxolitinib treatment, which resulted in partial downregulation of elevated interferon signature.

Viral infections are known to trigger elevated interferon signature. Interestingly, the elevated interferon signature in chronic viral infections results in an exhausted phenotype. With constant stimulation, exhausted cells exhibit a compromised interferon response to infections and unrelated secondary stimuli (Greene et al., 2021). The partial improvement in elevated interferon signature together with the clearance of persistent viral infections with Ruxolitinib treatment implies a role of overwhelming interferon signaling in the persistency of viral infections. Additionally, NK cell function and cytotoxicity pathways were found to be downregulated in the patient. The pivotal role of NK cells and its cytotoxicity function in the elimination of viral infections is well-known. The impaired cytotoxicity and NK cell functions have been speculated to lead to compromised viral clearance in STAT1 GOF patients (Tabellini et al., 2017). Of note, the perforin encoding gene *PRF1* was also downregulated and its expression was significantly elevated following Ruxolitinib treatment. The defective perforin function has been

shown to lead to susceptibility to respiratory viral infection (Cunningham et al., 2020). A modest downregulation in elevated ISG expression and partial improvement in reduced expression of cytotoxicity related genes including the *PRF1* can be speculated to aid in the clearance of chronic viral infections following Ruxolitinib treatment (Vargas-Hernández et al., 2018).

Collectively, our results indicate that the utilization of Ruxolitinib as a bridge therapy would reduce the risk of adverse outcome of HSCT through the improvement of disease management and dysregulated gene expression (Kayaoglu et al., 2021).

In the second part of our study, we aimed to investigate the underlying mechanisms that result in viral susceptibility in DOCK8 deficiency. Our preliminary results indicated that DOCK8-deficient PBMCs secreted lower levels of type I interferons following stimulation with various nucleic acid ligands. To gain further insight on this impaired interferon response, we performed gene expression analysis on RNA samples isolated from PBMCs of 15 DOCK8-deficient patients. The principal component analysis (PCA) conducted on differentially expressed genes in these patients in comparison to healthy controls revealed a clustering of patients into two distinct groups. The patients with PC1 smaller than zero were designated as Group1 whereas patients with PC1 larger than zero were assigned to Group2. Group2 patients were clustered together in a distant location than healthy controls and Group1 patients on the PCA plot whereas Group1 and healthy controls were located closely. Therefore, our analysis was mainly focused on Group2 patients in order to acquire new insights on defective pathways in DOCK8 deficiency. Among the most differentially expressed genes in Group2, interferon-stimulated genes predominated, indicative of an elevated interferon signature similar to that seen in the STAT1 GOF patient. Although an elevated interferon signature in these patients can be associated with chronic viral infections, the poor type I IFN response to nucleic acid ligands is more likely indicative of an "exhausted phenotype" in the innate immune cells with a role in type I interferon production. To further investigate the pathways involved in this impairment, we evaluated the MAPK and AP-1 signaling related gene expression in patient groups. The results showed that the MAPK signaling was

93

downregulated in Group2 patients and this downregulation mainly stemmed from the decreased expression of AP-1 subunit genes. The combined effort of NFAT and AP-1 is required for proper T-cell activation. In the absence of AP-1, NFAT signaling results in the expression of exhaustion-related genes, which mainly encode co-inhibitory receptors (Martinez et al., 2015). Therefore, the decreased expression of AP-1 subunit genes in these patients may induce exhaustion-related genes in T-cells. As expected, most of the co-inhibitory receptors *TIGIT*, *LAG3* and *HAVCR2* (TIM-3) were found to be upregulation in Group2 patients. Interestingly, the well-known exhaustion marker and co-inhibitory receptor *CTLA4*, was downregulated in both groups of patients. The downregulation in *CTLA4* can be associated with impaired regulatory T-cell differentiation and function observed in DOCK8 deficiency (Alroqi et al., 2017). Therefore, the speculated "exhausted phenotype" of the DOCK8 deficient cells should stem from co-inhibitory receptors with elevated expression. The term "exhaustion" is predominantly used in the context of T-cells. However, immune exhaustion can be observed in other immune cells, including those that are part of innate immunity. LAG-3, one of the upregulated co-inhibitory receptors, is known to be expressed by mainly T-cells and pDCs (Workman et al., 2009). The function of LAG3 expression in pDCs is to regulate proliferation and expansion in response to certain stimuli. Of note, depletion of LAG-3 has been shown to result in enhanced proliferation and expansion of pDCs (Workman et al., 2009). Furthermore, increased expression of *LAG3* in DOCK8-deficient patients can be associated with the reduced number of pDCs and compromised type I interferon production from pDCs in response to endosomal TLR ligand stimulation. Furthermore, TIM-3, another upregulated co-inhibitory receptor, can be expressed by a variety of immune cells including monocytes, macrophages, NK and T-cells. TIM-3 has been shown as the negative regulator of immune response to TLR stimulation (Yang et al., 2013).

Collectively, our findings suggest that impairment in type I interferon secretion in response to viral mimicry ligands can be explained by "exhausted phenotype" of innate immune cells as a consequence of chronically elevated interferon signature.

Furthermore, the identification of upregulated exhaustion markers in DOCK8 deficiency is pivotal in terms of proposing potential novel targets for therapeutic interventions to overcome chronic infection.

REFERENCES

Abbas, Y. M., Pichlmair, A., Górna, M. W., Superti-Furga, G., & Nagar, B. (2013). Structural basis for viral 5′-PPP-RNA recognition by human IFIT proteins. *Nature 2013 494:7435*, *494*(7435), 60–64. https://doi.org/10.1038/nature11783

Aggarwal, M., Villuendas, R., Gomez, G., Rodriguez-Pinilla, S. M., Sanchez-Beato, M., Alvarez, D., Martinez, N., Rodriguez, A., Castillo, M. E., Camacho, F. I., Montes-Moreno, S., Garcia-Marco, J. A., Kimby, E., Pisano, D. G., & Piris, M. A. (2008). TCL1A expression delineates biological and clinical variability in B-cell lymphoma. *Modern Pathology 2009 22:2*, *22*(2), 206–215. https://doi.org/10.1038/modpathol.2008.148

Al-Shaikhly, T., & Ochs, H. D. (2019). Hyper IgE syndromes: clinical and molecular characteristics. *Immunology and Cell Biology*, *97*(4), 368–379. https://doi.org/10.1111/IMCB.12209

Al-Zahrani, D., Raddadi, A., Massaad, M., Keles, S., Jabara, H. H., Chatila, T. A., & Geha, R. (2014). Successful Interferon–alpha 2b Therapy for Unremitting Warts in a Patient with DOCK8 Deficiency. *Clinical Immunology (Orlando, Fla.)*, *153*(1), 104. https://doi.org/10.1016/J.CLIM.2014.04.005

Alroqi, F. J., Charbonnier, L. M., Keles, S., Ghandour, F., Mouawad, P., Sabouneh, R., Mohammed, R., Almutairi, A., Chou, J., Massaad, M. J., Geha, R. S., Baz, Z., & Chatila, T. A. (2017). DOCK8 Deficiency Presenting as an IPEX-Like Disorder. *Journal of Clinical Immunology*, *37*(8), 811–819. https://doi.org/10.1007/S10875-017-0451-1

Atsaves, V., Leventaki, V., Rassidakis, G. Z., & Claret, F. X. (2019). AP-1 Transcription Factors as Regulators of Immune Responses in Cancer. *Cancers*, *11*(7). https://doi.org/10.3390/CANCERS11071037

Bailey, C. C., Zhong, G., Huang, I. C., & Farzan, M. (2014). IFITM-Family Proteins: The Cell's First Line of Antiviral Defense. *Annual Review of Virology*, *1*(1), 261. https://doi.org/10.1146/ANNUREV-VIROLOGY-031413-085537

Bengsch, B., & Wherry, E. J. (2015). The Importance of Cooperation: Partnerless NFAT Induces T Cell Exhaustion. *Immunity*, *42*(2), 203–205. https://doi.org/10.1016/J.IMMUNI.2015.01.023

Bergerson, J. R. E., & Freeman, A. F. (2019). An Update on Syndromes with a Hyper-IgE Phenotype. *Immunology and Allergy Clinics of North America*, *39*(1), 49–61. https://doi.org/10.1016/J.IAC.2018.08.007

Béziat, V., Tavernier, S. J., Chen, Y. H., Ma, C. S., Materna, M., Laurence, A., Staal, J., Aschenbrenner, D., Roels, L., Worley, L., Claes, K., Gartner, L., Kohn, L. A., De Bruyne, M., Schmitz-Abe, K., Charbonnier, L. M., Keles, S., Nammour, J., Vladikine, N., … Puel, A. (2020). Dominant-negative mutations in human IL6ST underlie hyper-IgE syndrome. *Journal of Experimental Medicine*, *217*(6). https://doi.org/10.1084/JEM.20191804/151577

Biggs, C. M., Keles, S., & Chatila, T. A. (2017). DOCK8 deficiency: Insights into pathophysiology, clinical features and management. *Clinical Immunology*, *181*, 75–82. https://doi.org/10.1016/J.CLIM.2017.06.003

Bonyek-Silva, I., Fernando Ara ujo Machado, onio, Cerqueira-Silva, T., Nunes, S., arcio Rivison Silva Cruz, M., essica Silva, J., Lima Santos, R., Barral, A., Rafael Silveira Oliveira, P., Khouri, R., Henrique Serezani, C., audia Brodskyn, C., Ribeiro Caldas, J., Barral-Netto, M., Boaventura, V., & Machado Tavares, N. (2021). *LTB 4-Driven Inflammation and Increased Expression of ALOX5/ACE2 During Severe COVID-19 in Individuals With Diabetes*. https://doi.org/10.2337/db20-1260

Bozza, S., Käsermann, F., Kaveri, S. V., Romani, L., & Bayry, J. (2019). Intravenous immunoglobulin protects from experimental allergic

bronchopulmonary aspergillosis via a sialylation-dependent mechanism. *European Journal of Immunology*, *49*(1), 195–198. https://doi.org/10.1002/EJI.201847774

Break, T. J., Oikonomou, V., Dutzan, N., Desai, J. V., Swidergall, M., Freiwald, T., Chauss, D., Harrison, O. J., Alejo, J., Williams, D. W., Pittaluga, S., Lee, C. C. R., Bouladoux, N., Swamydas, M., Hoffman, K. W., Greenwell-Wild, T., Bruno, V. M., Rosen, L. B., Lwin, W., … Lionakis, M. S. (2021a). Aberrant type 1 immunity drives susceptibility to mucosal fungal infections. *Science*, *371*(6526). https://doi.org/10.1126/SCIENCE.AAY5731/SUPPL_FILE/AAY5731_TABL E-S4.XLSX

Break, T. J., Oikonomou, V., Dutzan, N., Desai, J. V., Swidergall, M., Freiwald, T., Chauss, D., Harrison, O. J., Alejo, J., Williams, D. W., Pittaluga, S., Lee, C. C. R., Bouladoux, N., Swamydas, M., Hoffman, K. W., Greenwell-Wild, T., Bruno, V. M., Rosen, L. B., Lwin, W., … Lionakis, M. S. (2021b). Aberrant type 1 immunity drives susceptibility to mucosal fungal infections. *Science*, *371*(6526). https://doi.org/10.1126/SCIENCE.AAY5731/SUPPL_FILE/AAY5731_TABL E-S4.XLSX

Bruns, A. M., & Horvath, C. M. (2015). LGP2 synergy with MDA5 in RLR-mediated RNA recognition and antiviral signaling. *Cytokine*, *74*(2), 198–206. https://doi.org/10.1016/J.CYTO.2015.02.010

Burger, J. A., & Wiestner, A. (2018). Targeting B cell receptor signalling in cancer: preclinical and clinical advances. *Nature Reviews Cancer 2018 18:3*, *18*(3), 148–167. https://doi.org/10.1038/nrc.2017.121

Cao, Y., Liu, X., Li, Y., Lu, Y., Zhong, H., Jiang, W., Chen, A. F., Billiar, T. R., Yuan, H., & Cai, J. (2017). Cathepsin L activity correlates with proteinuria in chronic kidney disease in humans. *International Urology and Nephrology*,

49(8), 1409–1417. https://doi.org/10.1007/S11255-017-1626-7

Cervantes, J. L., Weinerman, B., Basole, C., & Salazar, J. C. (2012). TLR8: the forgotten relative revindicated. *Cellular & Molecular Immunology 2012 9:6*, *9*(6), 434–438. https://doi.org/10.1038/cmi.2012.38

Chen, Q., Sun, L., & Chen, Z. J. (2016). Regulation and function of the cGAS–STING pathway of cytosolic DNA sensing. *Nature Immunology 2016 17:10*, *17*(10), 1142–1149. https://doi.org/10.1038/ni.3558

Choudhury, S. M., Ma, X., Abdullah, S. W., & Zheng, H. (2021). Activation and Inhibition of the NLRP3 Inflammasome by RNA Viruses. *Journal of Inflammation Research*, *14*, 1145. https://doi.org/10.2147/JIR.S295706

Ciancanelli, M. J., Huang, S. X. L., Luthra, P., Garner, H., Itan, Y., Volpi, S., Lafaille, F. G., Trouillet, C., Schmolke, M., Albrecht, R. A., Israelsson, E., Lim, H. K., Casadio, M., Hermesh, T., Lorenzo, L., Leung, L. W., Pedergnana, V., Boisson, B., Okada, S., … Casanova, J. L. (2015). Life-threatening influenza and impaired interferon amplification in human IRF7 deficiency. *Science*, *348*(6233), 448–453. https://doi.org/10.1126/SCIENCE.AAA1578/SUPPL_FILE/CIANCANELLI.SM.PDF

Crosse, K. M., Monson, E. A., Beard, M. R., & Helbig, K. J. (2018). Interferon-Stimulated Genes as Enhancers of Antiviral Innate Immune Signaling. *Journal of Innate Immunity*, *10*(2), 85–93. https://doi.org/10.1159/000484258

Crow, Y. J., & Stetson, D. B. (2021). The type I interferonopathies: 10 years on. *Nature Reviews Immunology 2021 22:8*, *22*(8), 471–483. https://doi.org/10.1038/s41577-021-00633-9

Cunningham, L., Simmonds, P., Kimber, I., Basketter, D. A., & McFadden, J. P. (2020). Perforin and resistance to SARS coronavirus 2. *The Journal of Allergy and Clinical Immunology*, *146*(1), 52. https://doi.org/10.1016/J.JACI.2020.05.007

Cushing, L., Winkler, A., Jelinsky, S. A., Lee, K., Korver, W., Hawtin, R., Rao, V. R., Fleming, X. M., & Lin, L. L. (2017). IRAK4 kinase activity controls Toll-like receptor-induced inflammation through the transcription factor IRF5 in primary human monocytes. *The Journal of Biological Chemistry*, *292*(45), 18689–18698. https://doi.org/10.1074/JBC.M117.796912

Dropulic, L. K., & Cohen, J. I. (2011). Severe Viral Infections and Primary Immunodeficiencies. *Clinical Infectious Diseases: An Official Publication of the Infectious Diseases Society of America*, *53*(9), 897. https://doi.org/10.1093/CID/CIR610

Duan, T., Du, Y., Xing, C., Wang, H. Y., & Wang, R. F. (2022). Toll-Like Receptor Signaling and Its Role in Cell-Mediated Immunity. *Frontiers in Immunology*, *13*, 747. https://doi.org/10.3389/FIMMU.2022.812774/BIBTEX

Engelhardt, K. R., Gertz, M. E., Keles, S., Schäffer, A. A., Sigmund, E. C., Glocker, C., Saghafi, S., Pourpak, Z., Ceja, R., Sassi, A., Graham, L. E., Massaad, M. J., Mellouli, F., Ben-Mustapha, I., Khemiri, M., Kilic, S. S., Etzioni, A., Freeman, A. F., Thiel, J., … Grimbacher, B. (2015). The extended clinical phenotype of 64 patients with DOCK8 deficiency. *The Journal of Allergy and Clinical Immunology*, *136*(2), 402. https://doi.org/10.1016/J.JACI.2014.12.1945

Engelhardt, K. R., McGhee, S., Winkler, S., Sassi, A., Woellner, C., Lopez-Herrera, G., Chen, A., Sook Kim, H., Garcia Lloret, M., Schulze, I., Ehl, S., Thiel, J., Pfeifer, D., Veelken, H., Niehues, T., Siepermann, K., Weinspach, S., Reisli, I., Keles, S., … Chatila, T. (2009). Large Deletions and Point Mutations Involving DOCK8 in the Autosomal Recessive Form of the Hyper-IgE Syndrome. *J Allergy Clin Immunol. J Allergy Clin Immunol*, *124*(6). https://doi.org/10.1016/j.jaci.2009.10.038

Fond, A. M., & Ravichandran, K. S. (2016). Clearance of dying cells by phagocytes: mechanisms and implications for disease pathogenesis. *Advances*

in Experimental Medicine and Biology, *930*, 25. https://doi.org/10.1007/978-3-319-39406-0_2

García, M. A., Gil, J., Ventoso, I., Guerra, S., Domingo, E., Rivas, C., & Esteban, M. (2006). Impact of Protein Kinase PKR in Cell Biology: from Antiviral to Antiproliferative Action. *Microbiology and Molecular Biology Reviews*, *70*(4), 1032. https://doi.org/10.1128/MMBR.00027-06

Gazon, H., Barbeau, B., Mesnard, J. M., & Peloponese, J. M. (2018). Hijacking of the AP-1 signaling pathway during development of ATL. *Frontiers in Microbiology*, *8*(JAN), 2686. https://doi.org/10.3389/FMICB.2017.02686/BIBTEX

Gellert, M. (1992). Molecular analysis of V(D)J recombination. *Annual Review of Genetics*, *26*, 425–446. https://doi.org/10.1146/ANNUREV.GE.26.120192.002233

Goraya, M. U., Zaighum, F., Sajjad, N., Anjum, F. R., Sakhawat, I., & Rahman, S. ur. (2020). Web of interferon stimulated antiviral factors to control the influenza A viruses replication. *Microbial Pathogenesis*, *139*, 103919. https://doi.org/10.1016/J.MICPATH.2019.103919

Greene, T. T., Zuniga, E. I., Oldstone, A., & De La Torre, J. C. (2021). Type I Interferon Induction and Exhaustion during Viral Infection: Plasmacytoid Dendritic Cells and Emerging COVID-19 Findings. *Viruses 2021, Vol. 13, Page 1839*, *13*(9), 1839. https://doi.org/10.3390/V13091839

Guéguen, M., & Long, E. O. (1996). Presentation of a cytosolic antigen by major histocompatibility complex class II molecules requires a long-lived form of the antigen. *Proceedings of the National Academy of Sciences of the United States of America*, *93*(25), 14692. https://doi.org/10.1073/PNAS.93.25.14692

Gui, X., Yang, H., Li, T., Tan, X., Shi, P., Li, M., Du, F., & Chen, Z. J. (2019). Autophagy induction via STING trafficking is a primordial function of the cGAS pathway. *Nature 2019 567:7747*, *567*(7747), 262–266.

https://doi.org/10.1038/s41586-019-1006-9

Haeryfar, S. M. M. (2005). The importance of being a pDC in antiviral immunity:
The IFN mission versus Ag presentation? *Trends in Immunology*, *26*(6), 311–
317. https://doi.org/10.1016/j.it.2005.04.002

Harjunpää, H., & Guillerey, C. (2020). TIGIT as an emerging immune checkpoint.
Clinical & Experimental Immunology, *200*(2), 108–119.
https://doi.org/10.1111/CEI.13407

Harker, J. A., Dolgoter, A., & Zuniga, E. I. (2013). Cell-intrinsic interleukin-27 and
gp130 cytokine receptor signaling regulates virus specific CD4+ T cell
responses and viral control during chronic infection. *Immunity*, *39*(3), 548.
https://doi.org/10.1016/J.IMMUNI.2013.08.010

Harker, J. A., Wong, K. A., Dolgoter, A., & Zuniga, E. I. (2015). Cell-Intrinsic
gp130 Signaling on CD4+ T Cells Shapes Long-Lasting Antiviral Immunity.
Journal of Immunology (Baltimore, Md. : 1950), *195*(3), 1071–1081.
https://doi.org/10.4049/JIMMUNOL.1402402

Haskologlu, S., Kostel Bal, S., Islamoglu, C., Aytekin, C., Guner, S., Sevinc, S.,
Keles, S., Kendirli, T., Ceylaner, S., Dogu, F., & Ikinciogullari, A. (2020).
Clinical, immunological features and follow up of 20 patients with dedicator
of cytokinesis 8 (DOCK8) deficiency. *Pediatric Allergy and Immunology*,
31(5), 515. https://doi.org/10.1111/PAI.13236

Hornung, V., Ablasser, A., Charrel-Dennis, M., Bauernfeind, F., Horvath, G.,
Caffrey, D. R., Latz, E., & Fitzgerald, K. A. (2009). AIM2 recognizes
cytosolic dsDNA and forms a caspase-1-activating inflammasome with ASC.
Nature, *458*(7237), 514–518. https://doi.org/10.1038/nature07725

Hornung, V., Hartmann, R., Ablasser, A., & Hopfner, K.-P. (2014). OAS proteins
and cGAS: unifying concepts in sensing and responding to cytosolic nucleic
acids. *Nature Reviews Immunology*, *14*(8), 521–528.
https://doi.org/10.1038/nri3719

Huang, X., & Yang, Y. (2010). Targeting the TLR9-MyD88 pathway in the
regulation of adaptive immune responses. *Expert Opinion on Therapeutic Targets*, *14*(8), 787. https://doi.org/10.1517/14728222.2010.501333

Hunter, C. A., & Jones, S. A. (2015). IL-6 as a keystone cytokine in health and
disease. *Nature Immunology*, *16*(5), 448–457. https://doi.org/10.1038/NI.3153

Huppler, A. R., Bishu, S., & Gaffen, S. L. (2012). Mucocutaneous candidiasis: The
IL-17 pathway and implications for targeted immunotherapy. *Arthritis Research and Therapy*, *14*(4). https://doi.org/10.1186/ar3893

Jabara, H. H., McDonald, D. R., Janssen, E., Massaad, M. J., Ramesh, N.,
Borzutzky, A., Rauter, I., Benson, H., Schneider, L., Baxi, S., Recher, M.,
Notarangelo, L. D., Wakim, R., Dbaibo, G., Dasouki, M., Al-Herz, W.,
Barlan, I., Baris, S., Kutukculer, N., … Geha, R. S. (2012). DOCK8 functions
as an adaptor that links TLR-MyD88 signaling to B cell activation. *Nature Immunology*, *13*(6), 612–620. https://doi.org/10.1038/ni.2305

Jamilloux, Y., El Jammal, T., Vuitton, L., Gerfaud-Valentin, M., Kerever, S., &
Sève, P. (2019). JAK inhibitors for the treatment of autoimmune and
inflammatory diseases. *Autoimmunity Reviews*, *18*(11), 102390.
https://doi.org/10.1016/J.AUTREV.2019.102390

Jang, M. A., Kim, E. K., Now, H., Nguyen, N. T. H., Kim, W. J., Yoo, J. Y., Lee,
J., Jeong, Y. M., Kim, C. H., Kim, O. H., Sohn, S., Nam, S. H., Hong, Y., Lee,
Y. S., Chang, S. A., Jang, S. Y., Kim, J. W., Lee, M. S., Lim, S. Y., … Ki, C.
S. (2015). Mutations in DDX58, which Encodes RIG-I, Cause Atypical
Singleton-Merten Syndrome. *The American Journal of Human Genetics*,
96(2), 266–274. https://doi.org/10.1016/J.AJHG.2014.11.019

Janssen, E., Tsitsikov, E., Al-Herz, W., Lefranc, G., Megarbane, A., Dasouki, M.,
Bonilla, F. A., Chatila, T., Schneider, L., & Geha, R. S. (2014). Flow
cytometry biomarkers distinguish DOCK8 deficiency from severe atopic
dermatitis. *Clinical Immunology (Orlando, Fla.)*, *150*(2), 220.

https://doi.org/10.1016/J.CLIM.2013.12.006

Jouanguy, E., Béziat, V., Mogensen, T. H., Casanova, J.-L., Tangye, S. G., & Zhang, S.-Y. (2020). Human inborn errors of immunity to herpes viruses HHS Public Access. *Curr Opin Immunol*, *62*, 106–122. https://doi.org/10.1016/j.coi.2020.01.004

Kailasan Vanaja, S., Rathinam, V. A. K., Atianand, M. K., Kalantari, P., Skehan, B., Fitzgerald, K. A., & Leong, J. M. (2014). Bacterial RNA:DNA hybrids are activators of the NLRP3 inflammasome. *Proceedings of the National Academy of Sciences*, *111*(21), 7765–7770. https://doi.org/10.1073/pnas.1400075111

Karki, R., Sundaram, B., Raj Sharma, B., Lee, S., Subbarao Malireddi, R., Nhat Nguyen, L., Christgen, S., Zheng, M., Wang, Y., Samir, P., Neale, G., Vogel, P., & Kanneganti, T.-D. (2021). ADAR1 restricts ZBP1-mediated immune response and PANoptosis to promote tumorigenesis. *CellReports*, *37*, 109858. https://doi.org/10.1016/j.celrep.2021.109858

Katagiri, T., Kameda, H., Nakano, H., & Yamazaki, S. (2021a). Regulation of T cell differentiation by the AP-1 transcription factor JunB. *Immunological Medicine*, *44*(3), 197–203. https://doi.org/10.1080/25785826.2021.1872838

Katagiri, T., Kameda, H., Nakano, H., & Yamazaki, S. (2021b). Regulation of T cell differentiation by the AP-1 transcription factor JunB. *Https://Doi.Org/10.1080/25785826.2021.1872838*, *44*(3), 197–203. https://doi.org/10.1080/25785826.2021.1872838

Kawai, T., & Akira, S. (2006). TLR signaling. *Cell Death & Differentiation 2006 13:5*, *13*(5), 816–825. https://doi.org/10.1038/sj.cdd.4401850

Kawasaki, T., & Kawai, T. (2014). Toll-like receptor signaling pathways. *Frontiers in Immunology*, *5*(SEP). https://doi.org/10.3389/FIMMU.2014.00461

Kayaoglu, B., Kasap, N., Yilmaz, N. S., Charbonnier, L. M., Geckin, B., Akcay,

A., Eltan, S. B., Ozturk, G., Ozen, A., Karakoc-Aydiner, E., Chatila, T. A., Gursel, M., & Baris, S. (2021). Stepwise Reversal of Immune Dysregulation Due to STAT1 Gain-of-Function Mutation Following Ruxolitinib Bridge Therapy and Transplantation. *Journal of Clinical Immunology*, *41*(4), 769–779. https://doi.org/10.1007/S10875-020-00943-Y/FIGURES/3

Kearney, C. J., Randall, K. L., & Oliaro, J. (2017). DOCK8 regulates signal transduction events to control immunity. *Cellular & Molecular Immunology*, *14*(5), 406–411. https://doi.org/10.1038/cmi.2017.9

Keles, S., Charbonnier, L. M., Kabaleeswaran, V., Reisli, I., Genel, F., Gulez, N., Al-Herz, W., Ramesh, N., Perez-Atayde, A., Karaca, N. E., Kutukculer, N., Wu, H., Geha, R. S., & Chatila, T. A. (2016a). Dedicator of cytokinesis 8 regulates signal transducer and activator of transcription 3 activation and promotes TH17 cell differentiation. *The Journal of Allergy and Clinical Immunology*, *138*(5), 1384-1394.e2. https://doi.org/10.1016/j.jaci.2016.04.023

Keles, S., Charbonnier, L. M., Kabaleeswaran, V., Reisli, I., Genel, F., Gulez, N., Al-Herz, W., Ramesh, N., Perez-Atayde, A., Karaca, N. E., Kutukculer, N., Wu, H., Geha, R. S., & Chatila, T. A. (2016b). Dedicator of cytokinesis 8 regulates signal transducer and activator of transcription 3 activation and promotes TH17 cell differentiation. *Journal of Allergy and Clinical Immunology*, *138*(5), 1384-1394.e2. https://doi.org/10.1016/j.jaci.2016.04.023

Keles, S., Jabara, H. H., Reisli, I., McDonald, D. R., Barlan, I., Hanna-Wakim, R., Dbaibo, G., Lefranc, G., Al-Herz, W., Geha, R. S., & Chatila, T. A. (2014). Plasmacytoid Dendritic Cell Depletion in DOCK8 Deficiency: Rescue of Severe Herpetic Infections with Interferon Alpha-2b Therapy. *The Journal of Allergy and Clinical Immunology*, *133*(6), 1753. https://doi.org/10.1016/J.JACI.2014.03.032

Kerur, N., Veettil, M. V., Sharma-Walia, N., Bottero, V., Sadagopan, S., Otageri, P., & Chandran, B. (2011). IFI16 Acts as a Nuclear Pathogen Sensor to Induce

the Inflammasome in Response to Kaposi Sarcoma-Associated Herpesvirus Infection. *Cell Host & Microbe*, *9*(5), 363–375. https://doi.org/10.1016/j.chom.2011.04.008

Keskinen, P., Ronni, T., Matikainen, S., Lehtonen, A., & Julkunen, I. (1997). Regulation of HLA class I and II expression by interferons and influenza A virus in human peripheral blood mononuclear cells. *Immunology*, *91*(3), 421. https://doi.org/10.1046/J.1365-2567.1997.00258.X

Krämer, B., Knoll, R., Bonaguro, L., ToVinh, M., Raabe, J., Astaburuaga-García, R., Schulte-Schrepping, J., Kaiser, K. M., Rieke, G. J., Bischoff, J., Monin, M. B., Hoffmeister, C., Schlabe, S., De Domenico, E., Reusch, N., Händler, K., Reynolds, G., Blüthgen, N., Hack, G., … Nattermann, J. (2021). Early IFN-α signatures and persistent dysfunction are distinguishing features of NK cells in severe COVID-19. *Immunity*, *54*(11), 2650-2669.e14. https://doi.org/10.1016/J.IMMUNI.2021.09.002

Kumagai, Y., Takeuchi, O., & Akira, S. (2008). TLR9 as a key receptor for the recognition of DNA. *Advanced Drug Delivery Reviews*, *60*(7), 795–804. https://doi.org/10.1016/J.ADDR.2007.12.004

Kumari, P., Russo, A. J., Shivcharan, S., & Rathinam, V. A. (2020). AIM2 in health and disease: inflammasome and beyond. *Immunological Reviews*, *297*(1), 83. https://doi.org/10.1111/IMR.12903

Lambe, T., Crawford, G., Johnson, A. L., Crockford, T. L., Bouriez-Jones, T., Smyth, A. M., Pham, T. H. M., Zhang, Q., Freeman, A. F., Cyster, J. G., Su, H. C., & Cornall, R. J. (2011). DOCK8 is essential for T-cell survival and the maintenance of CD8+ T-cell memory. *European Journal of Immunology*, *41*(12), 3423–3435. https://doi.org/10.1002/EJI.201141759

Leiding, J. W., Okada, S., Hagin, D., Abinun, M., Shcherbina, A., Balashov, D. N., Kim, V. H. D., Ovadia, A., Guthery, S. L., Pulsipher, M., Lilic, D., Devlin, L. A., Christie, S., Depner, M., Fuchs, S., van Royen-Kerkhof, A., Lindemans,

C., Petrovic, A., Sullivan, K. E., … Torgerson, T. R. (2018). Hematopoietic stem cell transplantation in patients with gain-of-function signal transducer and activator of transcription 1 mutations. *Journal of Allergy and Clinical Immunology*, *141*(2), 704-717.e5. https://doi.org/10.1016/j.jaci.2017.03.049

Li, X., Ranjith-Kumar, C. T., Brooks, M. T., Dharmaiah, S., Herr, A. B., Kao, C., & Li, P. (2009). The RIG-I-like Receptor LGP2 Recognizes the Termini of Double-stranded RNA. *The Journal of Biological Chemistry*, *284*(20), 13881. https://doi.org/10.1074/JBC.M900818200

Liau, N. P. D., Laktyushin, A., Lucet, I. S., Murphy, J. M., Yao, S., Whitlock, E., Callaghan, K., Nicola, N. A., Kershaw, N. J., & Babon, J. J. (2018). The molecular basis of JAK/STAT inhibition by SOCS1. *Nature Communications*, *9*(1), 1–14. https://doi.org/10.1038/s41467-018-04013-1

Liu, L., Okada, S., Kong, X. F., Kreins, A. Y., Cypowyj, S., Abhyankar, A., Toubiana, J., Itan, Y., Audry, M., Nitschke, P., Masson, C., Toth, B., Flatot, J., Migaud, M., Chrabieh, M., Kochetkov, T., Bolze, A., Borghesi, A., Toulon, A., … Casanova, J. L. (2011). Gain-of-function human STAT1 mutations impair IL-17 immunity and underlie chronic mucocutaneous candidiasis. *Journal of Experimental Medicine*, *208*(18), 1635–1648. https://doi.org/10.1084/jem.20110958

Ludwig, S., Ehrhardt, C., Neumeier, E. R., Kracht, M., Rapp, U. R., & Pleschka, S. (2001). Influenza Virus-induced AP-1-dependent Gene Expression Requires Activation of the JNK Signaling Pathway*. *Journal of Biological Chemistry*, *276*, 10990–10998. https://doi.org/10.1074/jbc.M009902200

Lurie, R. H., & Platanias, L. C. (2005). Mechanisms of type-I- and type-II-interferon-mediated signalling. *Nature Reviews Immunology 2005 5:5*, *5*(5), 375–386. https://doi.org/10.1038/nri1604

Madera, S., Rapp, M., Firth, M. A., Beilke, J. N., Lanier, L. L., & Sun, J. C. (2016). Type I IFN promotes NK cell expansion during viral infection by protecting

NK cells against fratricide. *The Journal of Experimental Medicine*, *213*(2), 225. https://doi.org/10.1084/JEM.20150712

Mann-Nüttel, R., Ali, S., Petzsch, P., Köhrer, K., Alferink, J., & Scheu, S. (2021). The transcription factor reservoir and chromatin landscape in activated plasmacytoid dendritic cells. *BMC Genomic Data*, *22*(1). https://doi.org/10.1186/S12863-021-00991-2

Marshall, J. S., Warrington, R., Watson, W., & Kim, H. L. (2018). An introduction to immunology and immunopathology. *Allergy, Asthma and Clinical Immunology*, *14*(2), 1–10. https://doi.org/10.1186/S13223-018-0278-1/TABLES/4

Martinez, G. J., Pereira, R. M., Äijö, T., Kim, E. Y., Marangoni, F., Pipkin, M. E., Togher, S., Heissmeyer, V., Zhang, Y. C., Crotty, S., Lamperti, E. D., Ansel, K. M., Mempel, T. R., Lähdesmäki, H., Hogan, P. G., & Rao, A. (2015). The Transcription Factor NFAT Promotes Exhaustion of Activated CD8+ T Cells. *Immunity*, *42*(2), 265–278. https://doi.org/10.1016/J.IMMUNI.2015.01.006

Mascarenhas, J., & Hoffman, R. (2012). Ruxolitinib: The first FDA approved therapy for the treatment of myelofibrosis. *Clinical Cancer Research*, *18*(11), 3008–3014. https://doi.org/10.1158/1078-0432.CCR-11-3145/84811/AM/RUXOLITINIB-THE-FIRST-FDA-APPROVED-THERAPY-FOR-THE

Merika, M., Williams, A. J., Chen, G., Collins, T., & Thanos, D. (1998). Recruitment of CBP/p300 by the IFN beta enhanceosome is required for synergistic activation of transcription. *Molecular Cell*, *1*(2), 277–287. https://doi.org/10.1016/S1097-2765(00)80028-3

Mistry, P., Nakabo, S., O'Neil, L., Goel, R. R., Jiang, K., Carmona-Rivera, C., Gupta, S., Chan, D. W., Carlucci, P. M., Wang, X., Naz, F., Manna, Z., Dey, A., Mehta, N. N., Hasni, S., Dell'Orso, S., Gutierrez-Cruz, G., Sun, H. W., & Kaplan, M. J. (2019). Transcriptomic, epigenetic, and functional analyses

implicate neutrophil diversity in the pathogenesis of systemic lupus erythematosus. *Proceedings of the National Academy of Sciences of the United States of America*, *116*(50), 25222–25228. https://doi.org/10.1073/pnas.1908576116

Miyazawa, H., & Wada, T. (2021). Reversion Mosaicism in Primary Immunodeficiency Diseases. *Frontiers in Immunology*, *12*, 4816. https://doi.org/10.3389/FIMMU.2021.783022/BIBTEX

Mizoguchi, Y., & Okada, S. (2021). Inborn errors of STAT1 immunity. *Current Opinion in Immunology*, *72*, 59–64. https://doi.org/10.1016/J.COI.2021.02.009

Morrison, D. K. (2012). MAP Kinase Pathways. *Cold Spring Harbor Perspectives in Biology*, *4*(11). https://doi.org/10.1101/CSHPERSPECT.A011254

Müller, L., Aigner, P., & Stoiber, D. (2017). Type I Interferons and Natural Killer Cell Regulation in Cancer. *Frontiers in Immunology*, *8*(MAR), 304. https://doi.org/10.3389/FIMMU.2017.00304

Murphy, K., & Weaver, C. (2016a). *Janeway's immunobiology*. https://www.google.com/books?hl=tr&lr=&id=GmPLCwAAQBAJ&oi=fnd&pg=PP2&dq=janeway+immunobiology+murphy&ots=69xd56x4vi&sig=APMq9dX-OrjYkYm7upQ21M9E_hI

Murphy, K., & Weaver, C. (2016b). *Janeway's immunobiology*. https://www.google.com/books?hl=tr&lr=&id=GmPLCwAAQBAJ&oi=fnd&pg=PP2&dq=janeway%27s+immunobiology&ots=69xc9bs3ql&sig=Vk5cBVXzPnYIkqc8xN11LFY8qDw

Nguyen, L. T., & Ohashi, P. S. (2014). Clinical blockade of PD1 and LAG3 — potential mechanisms of action. *Nature Reviews Immunology 2015 15:1*, *15*(1), 45–56. https://doi.org/10.1038/nri3790

Nikolakopoulou, C., Willment, J. A., & Brown, G. D. (2020). C-Type Lectin

Receptors in Antifungal Immunity. *Advances in Experimental Medicine and Biology*, *1204*, 1–30. https://doi.org/10.1007/978-981-15-1580-4_1

Nishihara, M., Ogura, H., Ueda, N., Tsuruoka, M., Kitabayashi, C., Tsuji, F., Aono, H., Ishihara, K., Huseby, E., Betz, U. A. K., Murakami, M., & Hirano, T. (2007). IL-6-gp130-STAT3 in T cells directs the development of IL-17+ Th with a minimum effect on that of Treg in the steady state. *International Immunology*, *19*(6), 695–702. https://doi.org/10.1093/INTIMM/DXM045

O'Neill, L. A. J., & Bowie, A. G. (2007). The family of five: TIR-domain-containing adaptors in Toll-like receptor signalling. *Nature Reviews Immunology 2007 7:5*, *7*(5), 353–364. https://doi.org/10.1038/nri2079

O'Shea, J. J., Gadina, M., & Siegel, R. M. (2019). Cytokines and Cytokine Receptors. *Clinical Immunology: Principles and Practice*, 127-155.e1. https://doi.org/10.1016/B978-0-7020-6896-6.00009-0

O'Shea, J. J., Holland, S. M., & Staudt, L. M. (2013a). JAKs and STATs in immunity, immunodeficiency, and cancer. *The New England Journal of Medicine*, *368*(2), 161–170. https://doi.org/10.1056/NEJMRA1202117

O'Shea, J. J., Holland, S. M., & Staudt, L. M. (2013b). JAKs and STATs in Immunity, Immunodeficiency, and Cancer. *New England Journal of Medicine*, *368*(2), 161–170. https://doi.org/10.1056/NEJMra1202117

Olbrich, P., & Freeman, A. F. (2018). STAT1 and STAT3 mutations: important lessons for clinical immunologists. *Expert Review of Clinical Immunology*, *14*(12), 1029–1041. https://doi.org/10.1080/1744666X.2018.1531704

Pauken, K. E., & Wherry, E. J. (2015). Overcoming T cell exhaustion in infection and cancer. *Trends in Immunology*, *36*(4), 265–276. https://doi.org/10.1016/J.IT.2015.02.008

Peisley, A., Lin, C., Wu, B., Orme-Johnson, M., Liu, M., Walz, T., & Hur, S. (2011). Cooperative assembly and dynamic disassembly of MDA5 filaments

for viral dsRNA recognition. *Proceedings of the National Academy of Sciences of the United States of America*, *108*(52), 21010–21015. https://doi.org/10.1073/PNAS.1113651108/SUPPL_FILE/PNAS.1113651108 _SI.PDF

Perng, Y. C., & Lenschow, D. J. (2018). ISG15 in antiviral immunity and beyond. *Nature Reviews. Microbiology*, *16*(7), 423. https://doi.org/10.1038/S41579-018-0020-5

Pestka, S., Krause, C. D., & Walter, M. R. (2004). Interferons, interferon-like cytokines, and their receptors. *Immunological Reviews*, *202*(1), 8–32. https://doi.org/10.1111/J.0105-2896.2004.00204.X

Pillay, B. A., Fusaro, M., Gray, P. E., Statham, A. L., Burnett, L., Bezrodnik, L., Kane, A., Tong, W., Abdo, C., Winter, S., Chevalier, S., Levy, R., Masson, C., Schmitt, Y., Bole, C., Malphettes, M., Macintyre, E., de Villartay, J. P., Ziegler, J. B., … Ma, C. S. (2021a). Somatic reversion of pathogenic DOCK8 variants alters lymphocyte differentiation and function to effectively cure DOCK8 deficiency. *Journal of Clinical Investigation*, *131*(3). https://doi.org/10.1172/JCI142434

Pillay, B. A., Fusaro, M., Gray, P. E., Statham, A. L., Burnett, L., Bezrodnik, L., Kane, A., Tong, W., Abdo, C., Winter, S., Chevalier, S., Levy, R., Masson, C., Schmitt, Y., Bole, C., Malphettes, M., Macintyre, E., de Villartay, J. P., Ziegler, J. B., … Ma, C. S. (2021b). Somatic reversion of pathogenic DOCK8 variants alters lymphocyte differentiation and function to effectively cure DOCK8 deficiency. *The Journal of Clinical Investigation*, *131*(3). https://doi.org/10.1172/JCI142434

Qi, M., & Elion, E. A. (2005). MAP kinase pathways. *Journal of Cell Science*, *118*(16), 3569–3572. https://doi.org/10.1242/JCS.02470

Randall, K. L., Chan, S. S. Y., Ma, C. S., Fung, I., Mei, Y., Yabas, M., Tan, A., Arkwright, P. D., Suwairi, W. Al, Reyes, S. O. L., Yamazaki-Nakashimada,

M. A., Garcia-Cruz, M. de la L., Smart, J. M., Picard, C., Okada, S., Jouanguy, E., Casanova, J. L., Lambe, T., Cornall, R. J., … Goodnow, C. C. (2011a). DOCK8 deficiency impairs CD8 T cell survival and function in humans and mice. *The Journal of Experimental Medicine*, *208*(11), 2305–2320. https://doi.org/10.1084/JEM.20110345

Randall, K. L., Chan, S. S. Y., Ma, C. S., Fung, I., Mei, Y., Yabas, M., Tan, A., Arkwright, P. D., Suwairi, W. Al, Reyes, S. O. L., Yamazaki-Nakashimada, M. A., Garcia-Cruz, M. de la L., Smart, J. M., Picard, C., Okada, S., Jouanguy, E., Casanova, J. L., Lambe, T., Cornall, R. J., … Goodnow, C. C. (2011b). DOCK8 deficiency impairs CD8 T cell survival and function in humans and mice. *Journal of Experimental Medicine*, *208*(11), 2305–2320. https://doi.org/10.1084/JEM.20110345

Randall, K. L., Lambe, T., Johnson, A., Treanor, B., Kucharska, E., Domaschenz, H., Whittle, B., Tze, L. E., Enders, A., Crockford, T. L., Bouriez-Jones, T., Alston, D., Cyster, J. G., Lenardo, M. J., Mackay, F., Deenick, E. K., Tangye, S. G., Chan, T. D., Camidge, T., … Goodnow, C. C. (2009). Dock8 mutations cripple B cell immunological synapses, germinal centers and long-lived antibody production. *Nature Immunology*, *10*(12), 1283–1291. https://doi.org/10.1038/NI.1820

Raulet, D. H. (2006). Missing self recognition and self tolerance of natural killer (NK) cells. *Seminars in Immunology*, *18*(3), 145–150. https://doi.org/10.1016/j.smim.2006.03.003

Regis, G., Pensa, S., Boselli, D., Novelli, F., & Poli, V. (2008a). Ups and downs: The STAT1:STAT3 seesaw of Interferon and gp130 receptor signalling. *Seminars in Cell & Developmental Biology*, *19*(4), 351–359. https://doi.org/10.1016/J.SEMCDB.2008.06.004

Regis, G., Pensa, S., Boselli, D., Novelli, F., & Poli, V. (2008b). Ups and downs: The STAT1:STAT3 seesaw of Interferon and gp130 receptor signalling.

Seminars in Cell & Developmental Biology, *19*(4), 351–359.
https://doi.org/10.1016/J.SEMCDB.2008.06.004

Rehwinkel, J., & Gack, M. U. (2020). RIG-I-like receptors: their regulation and
roles in RNA sensing. *Nature Reviews Immunology 2020 20:9*, *20*(9), 537–
551. https://doi.org/10.1038/s41577-020-0288-3

Reikine, S., Nguyen, J. B., & Modis, Y. (2014). Pattern recognition and signaling
mechanisms of RIG-I and MDA5. *Frontiers in Immunology*, *5*(JUL), 342.
https://doi.org/10.3389/FIMMU.2014.00342/BIBTEX

Reiner, S. L. (2007). Development in Motion: Helper T Cells at Work. *Cell*,
129(1), 33–36. https://doi.org/10.1016/j.cell.2007.03.019

Revy, P., Kannengiesser, C., & Fischer, A. (2019). Somatic genetic rescue in
Mendelian haematopoietic diseases. *Nature Reviews Genetics 2019 20:10*,
20(10), 582–598. https://doi.org/10.1038/s41576-019-0139-x

Rice, G. I., Del Toro Duany, Y., Jenkinson, E. M., Forte, G. M. A., Anderson, B.
H., Ariaudo, G., Bader-Meunier, B., Baildam, E. M., Battini, R., Beresford,
M. W., Casarano, M., Chouchane, M., Cimaz, R., Collins, A. E., Cordeiro, N.
J. V., Dale, R. C., Davidson, J. E., De Waele, L., Desguerre, I., … Crow, Y. J.
(2014). Gain-of-function mutations in IFIH1 cause a spectrum of human
disease phenotypes associated with upregulated type I interferon signaling.
Nature Genetics 2014 46:5, *46*(5), 503–509. https://doi.org/10.1038/ng.2933

Ritz, U., & Seliger, B. (2001). The transporter associated with antigen processing
(TAP): Structural integrity, expression, function, and its clinical relevance.
Molecular Medicine, *7*(3), 149–158.
https://doi.org/10.1007/BF03401948/TABLES/1

Rodero, M. P., & Crow, Y. J. (2016a). Type I interferon–mediated monogenic
autoinflammation: The type I interferonopathies, a conceptual overview.
Journal of Experimental Medicine, *213*(12), 2527–2538.
https://doi.org/10.1084/JEM.20161596

Rodero, M. P., & Crow, Y. J. (2016b). Type I interferonâ-mediated monogenic autoinflammation: The type i interferonopathies, a conceptual overview. *Journal of Experimental Medicine*, *213*(12), 2527–2538. https://doi.org/10.1084/JEM.20161596

Roh, J. S., & Sohn, D. H. (2018). Damage-Associated Molecular Patterns in Inflammatory Diseases. *Immune Network*, *18*(4). https://doi.org/10.4110/IN.2018.18.E27

Saeidi, A., Zandi, K., Cheok, Y. Y., Saeidi, H., Wong, W. F., Lee, C. Y. Q., Cheong, H. C., Yong, Y. K., Larsson, M., & Shankar, E. M. (2018). T-cell exhaustion in chronic infections: Reversing the state of exhaustion and reinvigorating optimal protective immune responses. *Frontiers in Immunology*, *9*(NOV), 2569. https://doi.org/10.3389/FIMMU.2018.02569/BIBTEX

Sampaio, E. P., Hsu, A. P., Pechacek, J., Bax, H. I., Dias, D. L., Paulson, M. L., Chandrasekaran, P., Rosen, L. B., Carvalho, D. S., Ding, L., Vinh, D. C., Browne, S. K., Datta, S., Milner, J. D., Kuhns, D. B., Long Priel, D. A., Sadat, M. A., Shiloh, M., De Marco, B., … Holland, S. M. (2013). Signal transducer and activator of transcription 1 (STAT1) gain-of-function mutations and disseminated coccidioidomycosis and histoplasmosis. *The Journal of Allergy and Clinical Immunology*, *131*(6). https://doi.org/10.1016/J.JACI.2013.01.052

Satoh, J. I., & Tabunoki, H. (2013). A comprehensive profile of ChIP-Seq-based STAT1 target genes suggests the complexity of STAT1-mediated gene regulatory mechanisms. *Gene Regulation and Systems Biology*, *2013*(7), 41–56. https://doi.org/10.4137/GRSB.S11433

Saxena, M., & Yeretssian, G. (2014). NOD-like receptors: Master regulators of inflammation and cancer. *Frontiers in Immunology*, *5*(JUL), 327. https://doi.org/10.3389/FIMMU.2014.00327/BIBTEX

Schindler, C., Levy, D. E., & Decker, T. (2007). JAK-STAT Signaling: From

Interferons to Cytokines. *Journal of Biological Chemistry*, *282*(28), 20059–20063. https://doi.org/10.1074/JBC.R700016200

Schlee, M., & Hartmann, G. (2016). Discriminating self from non-self in nucleic acid sensing. *Nature Reviews Immunology 2016 16:9*, *16*(9), 566–580. https://doi.org/10.1038/nri.2016.78

Schneider, W. M., Chevillotte, M. D., & Rice, C. M. (2014a). Interferon-Stimulated Genes: A Complex Web of Host Defenses. *Annual Review of Immunology*, *32*(1), 513–545. https://doi.org/10.1146/annurev-immunol-032713-120231

Schneider, W. M., Chevillotte, M. D., & Rice, C. M. (2014b). Interferon-Stimulated Genes: A Complex Web of Host Defenses. *Https://Doi.Org/10.1146/Annurev-Immunol-032713-120231*, *32*, 513–545. https://doi.org/10.1146/ANNUREV-IMMUNOL-032713-120231

Sha, W., Mitoma, H., Hanabuchi, S., Bao, M., Weng, L., Sugimoto, N., Liu, Y., Zhang, Z., Zhong, J., Sun, B., & Liu, Y. J. (2014). Human NLRP3 Inflammasome senses multiple types of bacterial RNAs. *Proceedings of the National Academy of Sciences of the United States of America*, *111*(45), 16059–16064. https://doi.org/10.1073/PNAS.1412487111/SUPPL_FILE/PNAS.201412487SI.PDF

Shahin, T., Aschenbrenner, D., Cagdas, D., Bal, S. K., Conde, C. D., Garncarz, W., Medgyesi, D., Schwerd, T., Karaatmaca, B., Cetinkaya, P. G., Esenboga, S., Twigg, S. R. F., Cant, A., Wilkie, A. O. M., Tezcan, I., Uhlig, H. H., & Boztug, K. (2019). Selective loss of function variants in IL6ST cause Hyper-IgE syndrome with distinct impairments of T-cell phenotype and function. *Haematologica*, *104*(3), 609–621. https://doi.org/10.3324/HAEMATOL.2018.194233

Sharma, N., Wang, C., Kessler, P., & Sen, G. C. (2021). Herpes simplex virus 1

evades cellular antiviral response by inducing microRNA-24, which attenuates STING synthesis. *PLoS Pathogens*, *17*(9), e1009950. https://doi.org/10.1371/JOURNAL.PPAT.1009950

Singh, A. K., Eken, A., Hagin, D., Komal, K., Bhise, G., Shaji, A., Arkatkar, T., Jackson, S. W., Bettelli, E., Torgerson, T. R., & Oukka, M. (2017). DOCK8 regulates fitness and function of regulatory T cells through modulation of IL-2 signaling. *JCI Insight*, *2*(19). https://doi.org/10.1172/JCI.INSIGHT.94275

Stachelscheid, J., Jiang, Q., Aszyk, C. M., Warner, K., Bley, N., Müller, T. A., Vydzhak, O., Symeonidis, K., Crispatzu, G., Mayer, P., Blakemore, S. J., Goehring, G., Newrzela, S., Hippler, S., Robrecht, S., Kreuzer, K.-A., Pallasch, C. P., Krüger, M., Lechner, A., … Herling, M. (2022). The proto-oncogene TCL1A deregulates cell cycle and genomic stability in CLL. *Blood*. https://doi.org/10.1182/BLOOD.2022015494

Stachelscheid, J., Jiang, Q., & Herling, M. (2021). The Modes of Dysregulation of the Proto-Oncogene T-Cell Leukemia/Lymphoma 1A. *Cancers 2021, Vol. 13, Page 5455*, *13*(21), 5455. https://doi.org/10.3390/CANCERS13215455

Stritesky, G. L., Jameson, S. C., & Hogquist, K. A. (2012). Selection of self-reactive T cells in the thymus. *Annual Review of Immunology*, *30*, 95. https://doi.org/10.1146/ANNUREV-IMMUNOL-020711-075035

Su, H. C. (2010). Dedicator of cytokinesis 8 (DOCK8) deficiency. *Current Opinion in Allergy and Clinical Immunology*, *10*(6), 515–520. https://doi.org/10.1097/ACI.0b013e32833fd718

Su, H. C., Jing, H., Angelus, P., & Freeman, A. F. (2019). Insights into immunity from clinical and basic science studies of DOCK8 immunodeficiency syndrome. *Immunological Reviews*, *287*(1), 9–19. https://doi.org/10.1111/IMR.12723

Su, H. C., Jing, H., & Zhang, Q. (2011). DOCK8 deficiency. *Annals of the New York Academy of Sciences*, *1246*(1), 26–33. https://doi.org/10.1111/j.1749-

6632.2011.06295.x

Swiecki, M., Wang, Y., Gilfillan, S., & Colonna, M. (2013). Plasmacytoid dendritic cells contribute to systemic but not local antiviral responses to HSV infections. *PLoS Pathogens*, *9*(10). https://doi.org/10.1371/JOURNAL.PPAT.1003728

Tabellini, G., Vairo, D., Scomodon, O., Tamassia, N., Ferraro, R. M., Patrizi, O., Gasperini, S., Soresina, A., Giardino, G., Pignata, C., Lougaris, V., Plebani, A., Dotta, L., Cassatella, M. A., Parolini, S., & Badolato, R. (2017). Impaired natural killer cell functions in patients with signal transducer and activator of transcription 1 (STAT1) gain-of-function mutations. *Journal of Allergy and Clinical Immunology*, *140*(2), 553-564.e4. https://doi.org/10.1016/j.jaci.2016.10.051

Takeuchi, O., & Akira, S. (2010). Pattern recognition receptors and inflammation. *Cell*, *140*(6), 805–820. https://doi.org/10.1016/J.CELL.2010.01.022

Tangye, S. G., Al-Herz, W., Bousfiha, A., Cunningham-Rundles, C., Franco, J. L., Holland, S. M., Klein, C., Morio, T., Oksenhendler, E., Picard, C., Puel, A., Puck, J., Seppänen, M. R. J., Somech, R., Su, H. C., Sullivan, K. E., Torgerson, T. R., & Meyts, I. (2022). Human Inborn Errors of Immunity: 2022 Update on the Classification from the International Union of Immunological Societies Expert Committee. *Journal of Clinical Immunology*, *42*(7). https://doi.org/10.1007/S10875-022-01289-3

Tangye, S. G., Pillay, B., Randall, K. L., Avery, D. T., Phan, T. G., Gray, P., Ziegler, J. B., Smart, J. M., Peake, J., Arkwright, P. D., Hambleton, S., Orange, J., Goodnow, C. C., Uzel, G., Casanova, J. L., Lugo Reyes, S. O., Freeman, A. F., Su, H. C., & Ma, C. S. (2017). Dedicator of cytokinesis 8–deficient CD4+ T cells are biased to a TH2 effector fate at the expense of TH1 and TH17 cells. *Journal of Allergy and Clinical Immunology*, *139*(3), 933–949. https://doi.org/10.1016/J.JACI.2016.07.016

Ting, J. P. Y., Willingham, S. B., & Bergstralh, D. T. (2008). NLRs at the intersection of cell death and immunity. *Nature Reviews Immunology 2008 8:5*, *8*(5), 372–379. https://doi.org/10.1038/nri2296

Tolomeo, M., Cavalli, A., & Cascio, A. (2022). STAT1 and Its Crucial Role in the Control of Viral Infections. *International Journal of Molecular Sciences*, *23*(8). https://doi.org/10.3390/IJMS23084095

Toubiana, J., Okada, S., Hiller, J., Oleastro, M., Lagos Gomez, M., Aldave Becerra, J. C., Ouachée-Chardin, M., Fouyssac, F., Girisha, K. M., Etzioni, A., Van Montfrans, J., Camcioglu, Y., Kerns, L. A., Belohradsky, B., Blanche, S., Bousfiha, A., Rodriguez-Gallego, C., Meyts, I., Kisand, K., … International STAT1 Gain-of-Function Study Group. (2016). Heterozygous STAT1 gain-of-function mutations underlie an unexpectedly broad clinical phenotype. *Blood*, *127*(25), 3154–3164. https://doi.org/10.1182/blood-2015-11-679902

Tripathi, S. C., Peters, H. L., Taguchi, A., Katayama, H., Wang, H., Momin, A., Jolly, M. K., Celiktas, M., Rodriguez-Canales, J., Liu, H., Behrens, C., Wistuba, I. I., Ben-Jacob, E., Levine, H., Molldrem, J. J., Hanash, S. M., & Ostrin, E. J. (2016). Immunoproteasome deficiency is a feature of non-small cell lung cancer with a mesenchymal phenotype and is associated with a poor outcome. *Proceedings of the National Academy of Sciences of the United States of America*, *113*(11), E1555–E1564. https://doi.org/10.1073/PNAS.1521812113/SUPPL_FILE/PNAS.1521812113.SD07.XLSX

Van De Veerdonk, F. L., Plantinga, T. S., Hoischen, A., Smeekens, S. P., Joosten, L. A. B., Gilissen, C., Arts, P., Rosentul, D. C., Carmichael, A. J., Smits-van Der Graaf, C. A. A., Kullberg, B. J., Van Der Meer, J. W. M., Lilic, D., Veltman, J. A., & Netea, M. G. (2011). STAT1 mutations in autosomal dominant chronic mucocutaneous candidiasis. *New England Journal of Medicine*, *365*(1), 54–61. https://doi.org/10.1056/NEJMoa1100102

Vargas-Hernández, A., Mace, E. M., Zimmerman, O., Zerbe, C. S., Freeman, A. F., Rosenzweig, S., Leiding, J. W., Torgerson, T., Altman, M. C., Schussler, E., Cunningham-Rundles, C., Chinn, I. K., Carisey, A. F., Hanson, I. C., Rider, N. L., Holland, S. M., Orange, J. S., & Forbes, L. R. (2018). Ruxolitinib partially reverses functional natural killer cell deficiency in patients with signal transducer and activator of transcription 1 (STAT1) gain-of-function mutations. *Journal of Allergy and Clinical Immunology*, *141*(6), 2142-2155.e5. https://doi.org/10.1016/j.jaci.2017.08.040

Verhelst, J., Hulpiau, P., & Saelens, X. (2013). Mx Proteins: Antiviral Gatekeepers That Restrain the Uninvited. *Microbiology and Molecular Biology Reviews : MMBR*, *77*(4), 551. https://doi.org/10.1128/MMBR.00024-13

Wang, S., Qin, E., Zhi, Y., & Hua, R. (2017). Severe autoimmune hemolytic anemia during pegylated interferon plus ribavirin treatment for chronic hepatitis C: a case report. *Clinical Case Reports*, *5*(9), 1490. https://doi.org/10.1002/CCR3.1098

Wang, W., Xu, L., Su, J., Peppelenbosch, M. P., & Pan, Q. (2017). Transcriptional Regulation of Antiviral Interferon-Stimulated Genes. *Trends in Microbiology*, *25*(7), 573–584. https://doi.org/10.1016/J.TIM.2017.01.001

Weinacht, K. G., Charbonnier, L. M., Alroqi, F., Plant, A., Qiao, Q., Wu, H., Ma, C., Torgerson, T. R., Rosenzweig, S. D., Fleisher, T. A., Notarangelo, L. D., Hanson, I. C., Forbes, L. R., & Chatila, T. A. (2017). Ruxolitinib reverses dysregulated T helper cell responses and controls autoimmunity caused by a novel signal transducer and activator of transcription 1 (STAT1) gain-of-function mutation. *Journal of Allergy and Clinical Immunology*, *139*(5), 1629-1640.e2. https://doi.org/10.1016/j.jaci.2016.11.022

Wherry, E. J. (2011). T cell exhaustion. *Nature Immunology 2011 12:6*, *12*(6), 492–499. https://doi.org/10.1038/ni.2035

Wherry, E. J., Ha, S. J., Kaech, S. M., Haining, W. N., Sarkar, S., Kalia, V.,

Subramaniam, S., Blattman, J. N., Barber, D. L., & Ahmed, R. (2007). Molecular Signature of CD8+ T Cell Exhaustion during Chronic Viral Infection. *Immunity*, *27*(4), 670–684. https://doi.org/10.1016/j.immuni.2007.09.006

Wherry, E. J., & Kurachi, M. (2015). Molecular and cellular insights into T cell exhaustion. *Nature Reviews. Immunology*, *15*(8), 486. https://doi.org/10.1038/NRI3862

Workman, C. J., Wang, Y., El Kasmi, K. C., Pardoll, D. M., Murray, P. J., Drake, C. G., & Vignali, D. A. A. (2009). LAG-3 Regulates Plasmacytoid Dendritic Cell Homeostasis. *Journal of Immunology (Baltimore, Md. : 1950)*, *182*(4), 1885. https://doi.org/10.4049/JIMMUNOL.0800185

Yang, X., Jiang, X., Chen, G., Xiao, Y., Geng, S., Kang, C., Zhou, T., Li, Y., Guo, X., Xiao, H., Hou, C., Wang, R., Lin, Z., Li, X., Feng, J., Ma, Y., Shen, B., Li, Y., & Han, G. (2013). T cell Ig mucin-3 promotes homeostasis of sepsis by negatively regulating the TLR response. *Journal of Immunology (Baltimore, Md. : 1950)*, *190*(5), 2068–2079. https://doi.org/10.4049/JIMMUNOL.1202661

Yoshida, R., Takaesu, G., Yoshida, H., Okamoto, F., Yoshioka, T., Choi, Y., Akira, S., Kawai, T., Yoshimura, A., & Kobayashi, T. (2008). TRAF6 and MEKK1 play a pivotal role in the RIG-I-like helicase antiviral pathway. *Journal of Biological Chemistry*, *283*(52), 36211–36220. https://doi.org/10.1074/jbc.M806576200

Zhang, H., Ghai, P., Wu, H., Wang, C., Field, J., & Zhou, G. L. (2013). Mammalian adenylyl cyclase-associated protein 1 (CAP1) regulates cofilin function, the actin cytoskeleton, and cell adhesion. *Journal of Biological Chemistry*, *288*(29), 20966–20977. https://doi.org/10.1074/JBC.M113.484535

Zhang, Q., Boisson, B., Béziat, V., Puel, A., & Casanova, J. L. (2018). Human hyper-IgE syndrome: singular or plural? *Mammalian Genome 2018 29:7*,

29(7), 603–617. https://doi.org/10.1007/S00335-018-9767-2

Zhang, Q., Dove, C. G., Hor, J. L., Murdock, H. M., Strauss-Albee, D. M., Garcia, J. A., Mandl, J. N., Grodick, R. A., Jing, H., Chandler-Brown, D. B., Lenardo, T. E., Crawford, G., Matthews, H. F., Freeman, A. F., Cornall, R. J., Germain, R. N., Mueller, S. N., & Su, H. C. (2014). DOCK8 regulates lymphocyte shape integrity for skin antiviral immunity. *Journal of Experimental Medicine*, *211*(13), 2549–2566. https://doi.org/10.1084/jem.20141307

Zhang, Q., Jing, H., & Su, H. C. (2016). Recent Advances in DOCK8 Immunodeficiency Syndrome. *Journal of Clinical Immunology*, *36*(5), 441–449. https://doi.org/10.1007/S10875-016-0296-Z/FIGURES/3

Zhang, Y., Ma, C. A., Lawrence, M. G., Break, T. J., O'Connell, M. P., Lyons, J. J., López, D. B., Barber, J. S., Zhao, Y., Barber, D. L., Freeman, A. F., Holland, S. M., Lionakis, M. S., & Milner, J. D. (2017). PD-L1 up-regulation restrains Th17 cell differentiation in STAT3 loss- and STAT1 gain-of-function patients. *Journal of Experimental Medicine*, *214*(9), 2523–2533. https://doi.org/10.1084/jem.20161427

Zhou, M., & Ouyang, W. (2003). The function role of GATA-3 in Th1 and Th2 differentiation. *Immunologic Research*, *28*(1), 25–37. https://doi.org/10.1385/IR:28:1:25

Zimmerman, O., Rösler, B., Zerbe, C. S., Rosen, L. B., Hsu, A. P., Uzel, G., Freeman, A. F., Sampaio, E. P., Rosenzwieg, S. D., Kuehn, H. S., Kim, T., Brooks, K. M., Kumar, P., Wang, X., Netea, M. G., van de Veerdonk, F. L., & Holland, S. M. (2017). Risks of Ruxolitinib in STAT1 Gain-of-Function-Associated Severe Fungal Disease. *Open Forum Infectious Diseases*, *4*(4), 1–5. https://doi.org/10.1093/ofid/ofx202

APPENDICES

A. Culture Media, Buffers and Solutions

RPMI-1640 (Gibco) supplemented with L-Glutamine

2 % :10 ml heat-inactivated FBS

10 %: 50 ml heat-inactivated FBS

5 ml Penicillin/Streptomycin (final concentration: 50μg/ml)

5 ml HEPES (final concentration: 10mM)

5 ml Na Pyruvate, (final concentration: 0,11 mg/ml)

5 ml Non-Essential Amino Acids Solution, (diluted into 1x from 100x stock)

FACS Buffer

500 ml 1x PBS

5g BSA (1%)

125mg (0,25%)

Blocking Buffer (ELISA)

500ml 1x PBS

25 grams BSA (5%)

250μl Tween20 (0,025%)

Wash Buffer (ELISA)

500 ml 10x PBS

2,5 ml Tween20

4,5lt ddH2O

B. Gating Strategies for Flow Cytometric Analysis

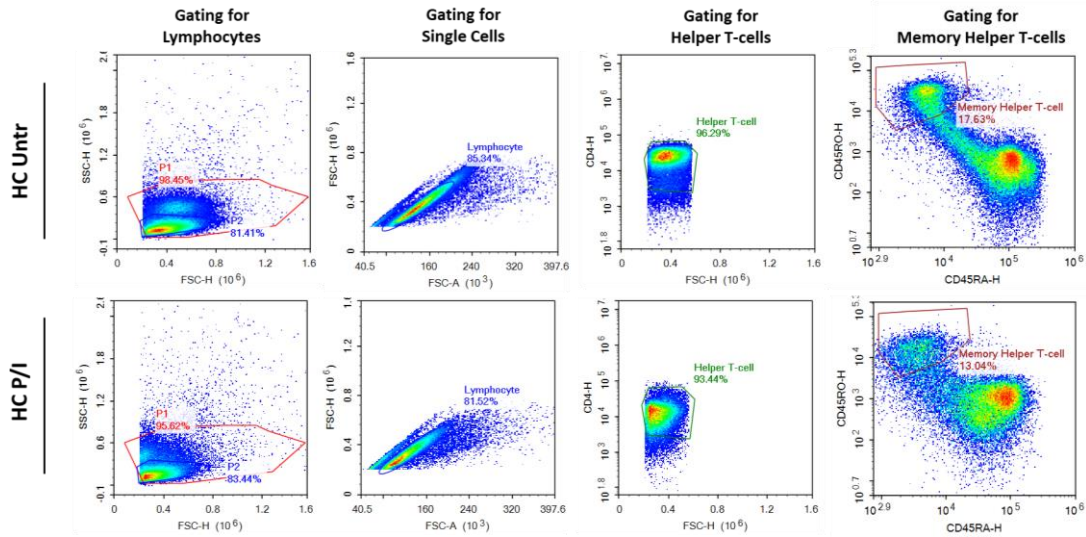*Figure B-1: Gating Strategies for Memory Helper T-cells used in intracellular IL-17A vs IFN-γ staining for STAT1 GOF patient and corresponding healthy controls.*
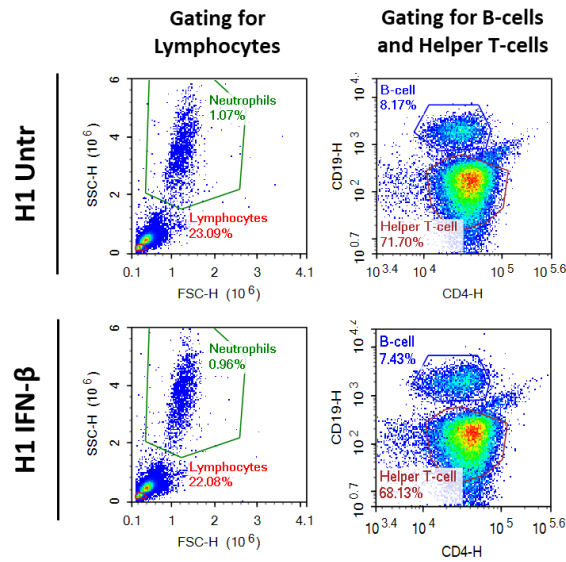

Figure B-2: Gating strategies for B-cells and Helper T-cells used in IFN-β induced STAT1 and STAT3 phosphorylation analysis in DOCK8 deficient patient (D1) and corresponding healthy controls (H1 & H2).

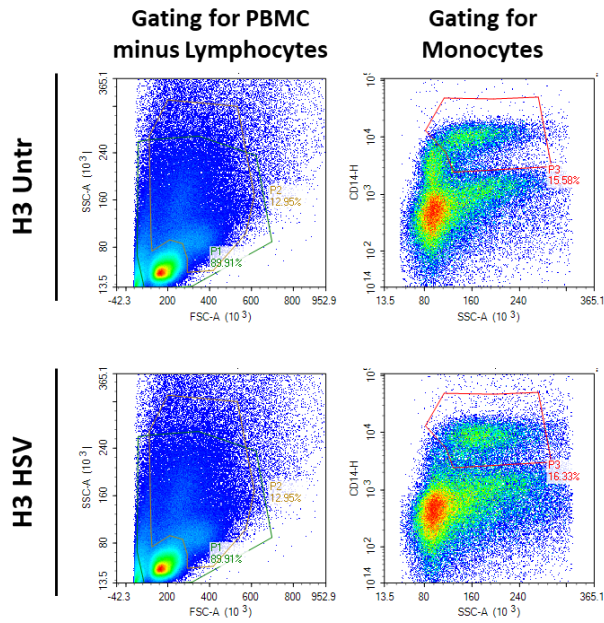*Figure B-3: Gating strategies for Monocytes used in intracellular IP-10 staining upon stimulation with transfected HSV in DOCK8 deficient patients (D3 & D4) and corresponding healthy controls (H3 & H4).*
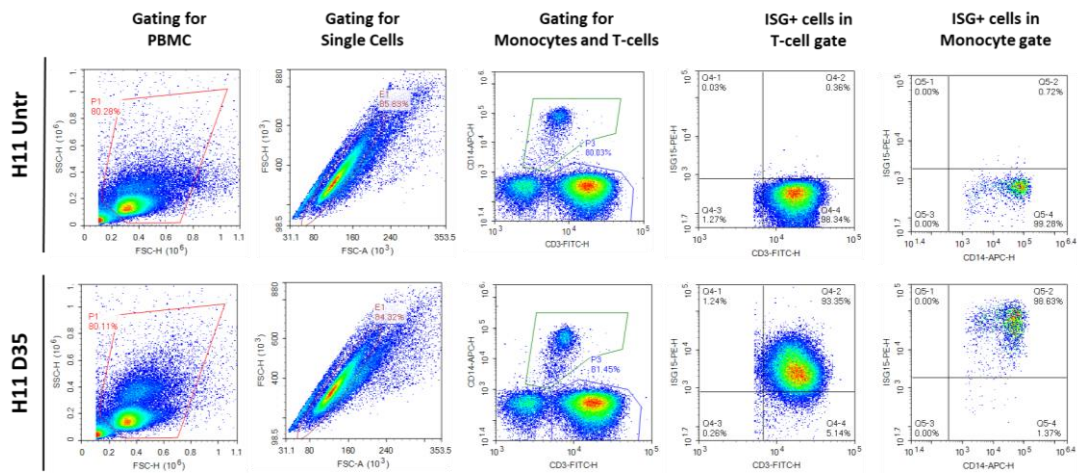

Figure B-4:Gating strategies for Monocytes and T-cells used in intracellular ISG15 staining upon stimulation with a variety of ligands (e.g., D35) in DOCK8 deficient patient (D7) and corresponding healthy control (H11).

C. Supplementary Table

Table B. 1 Clinical Presentations of DOCK8 Deficient Patients

	Mutation	Sex	Age(y)	Clinical Onset	Viral infections	Bacterial infections	Fungal infections	Eczema	Food allergies	Failure to thrive	HSCT	Status
D2	X	Female	9	3 years	HSV	skin abscess, Staph. Aureus	X	✓	✓	✓	X	Dead
D5	c.528G	Female	17	6 months	HSV, poxvirus	recurrent pneumonia, skin abscess	moniliasis, onychomycosis	✓	✓	✓	X	Alive
D6	ex25_46del	Female	11	8 years	X	LRTI	X	X	X	X	✓	Alive
D7	c.850_851delCT	Female	11	2 years	X	LRTI	X	✓	X	X	✓	Alive
D8	C.1422+1G>C	Male	10	4 years	HSV, VZV	X	X	✓	X	X	X	Alive
D9	c.1010C>T, C5809A>G (compound)	Male	5	1 year	X	LRTI	X	X	X	X	✓	Alive
D10	c.3067_3068du pAT	Male	8	2 years	EBV, CMV, Adeno	Pseudomonas aeruginosa, Staph. aureus	X	✓	✓	✓	✓	Alive
D11	ex2,28,31,32,38 and 42del	Male	5	2 years	X	X	X	X	X	X	✓	Alive
D12	X	Female	4	8 months	CMV	recurrent pneumonia, otitis media, TB	PCP	✓	✓	✓	✓	Alive
D1	ex28_48del	Female	6	3 months	HSV, CMV	LRTI	X	✓	✓	✓	✓	Alive
D3	c.555T>G	Male	3	1 month	X	LRTI	X	✓	✓	X	X	Alive
D4	c.555T>G missense	Male	2	6 months	CMV, RSV, Adeno, HMPV	Stenotro-phomonas maltophilia	galactomannan (+)	✓	X	✓	✓	Dead
D13	ex1_19del	Male	17	2 years	HSV, VZV	skin abscess	moniliasis, PCP	✓	✓	✓	✓	Alive
D14	ex1_14del	Male	8	6 months	HSV	X	galactomannan (+)	✓	X	✓	X	Alive
D15	c.2997_2998ln AA	Female	9	6 months	HSV	LRTI	galactomannan (+), aspergillosis	✓	X	✓	✓	Alive

CURRICULUM VITAE

PERSONAL INFORMATION

Surname, Name: Kayaoğlu, Başak
Nationality: Turkish (TC)

EDUCATION

Degree	Institution	Year of Graduation
MS	METU Biology	2017
BS	METU Molecular Biology and Genetics	2014
High School	Bornova Anadolu High School	2009

WORK EXPERIENCE

Year	Institution	Enrollment
2014-present	METU Biological Sciences	Teaching Asistant
2014-present	METU Biological Scineces	MS & PhD Student

FOREIGN LANGUAGES

Advanced English

PUBLICATIONS

1. Gul, E., Sayar, E. H., Gungor, B., Eroglu, F. K., Surucu, N., Keles, S., Guner, S. N., Findik, S., Alpdundar, E., Ayanoglu, I. C., Kayaoglu, B., Geckin, B. N., Sanli, H. A., Kahraman, T., Yakicier, C., Muftuoglu, M., Oguz, B., Cagdas Ayvaz, D. N., Gursel, I., Ozen, S., Reisli, I., & Gursel, M. (2018). Type I IFN–related NETosis in ataxia telangiectasia and Artemis deficiency. J. Allergy Clin. Immunol., 142(1), 246–257

2. Çağdaş, D., Sürücü, N., Tan, Ç., Kayaoğlu, B., Özgül, R. K., Akkaya-Ulum, Y. Z., Aydınoğlu, A. T., Aytaç, S., Gümrük, F., Balci-Hayta, B., Balci88 Peynircioğlu, B., Özen, S., Gürsel, M., & Tezcan, İ. (2020) Autoinflammation in addition to combined immunodeficiency: SLC29A3 gene defect. Mol. Immunol., 121, 28–37.

3. Kayaoglu, B., Kasap, N., Yilmaz, N. S., Charbonnier, L. M., Geckin, B., Akcay, A., Eltan, S. B., Ozturk, G., Ozen, A., Karakoc-Aydiner, E., Chatila, T. A., Gursel, M., & Baris, S. (2021). Stepwise Reversal of Immune Dysregulation Due to STAT1 Gain-of-Function Mutation Following Ruxolitinib Bridge Therapy and Transplantation. J. Clin. Immunol.

4. Yilmaz, IC; Ipekoglu, EM; Bulbul, A; Turay, N; Yildirim, M; Evcili, I; Surucu Yilmaz, Naz; Guvencli, N; Aydin, Y; Gungor, B; Saraydar, B; Bartan, AG; Ibibik, B; Bildik, T; Baydemir, I; Sanli, HA; Kayaoglu, B; Ceylan, Y; Yildirim, T; Abras, I; Ayanoglu, IC; Cam, SB; Ciftci Dede, E; Gizer, M; Erganis, O; Sarac, F; Uzar, S; Enul, H; Adiay, C; Aykut, G; Polat, H; Yildirim, IS; Tekin, S; Korukluoglu, G; Zeytin, HE; Korkusuz, P; Gursel, I; Gursel, M. (2021) Development and preclinical evaluation of virus-like particle vaccine against COVID-19 infection. Allergy.

5. Yilmaz, NS; Eltan SB; Kayaoglu B; Geckin B; Heredia RJ; Sefer AP; Kiykim A; Nain E; Kasap N; Dogru O; Yucelten AD; Cinel L; Karasu G; Yesilipek A; Sozeri B; Kaya GG; Yilmaz IC; Baydemir I; Aydin Y; Kahraman DC; Haimel M; Boztug K; Aydiner EK; Gursel I; Ozen A; Baris S; Gursel M. (2022), Low Density Granulocytes and Dysregulated Neutrophils Driving Autoinflammatory Manifestations in NEMO Deficiency Journal of Clinical Immunology.

6. Asena Pinar Sefer, Hassan Abolhassani, Franziska Ober, Basak Kayaoglu, Sevgi Bilgic Eltan, Altan Kara, Baran Erman, Naz Surucu Yilmaz, Cigdem Aydogmus, Sezin Aydemir, Louis-Marie Charbonnier, Burcu Kolukisa, Gholamreza Azizi, Samaneh Delavari, Tooba Momen, Simuzar Aliyeva, Yasemin Kendir Demirkol, Saban Tekin, Ayca Kiykim, Omer Faruk Baser, Haluk Cokugras, Mayda Gursel, Elif Karakoc-Aydiner, Ahmet Ozen, Daniel Krappmann, Talal A. Chatila, Nima Rezaei & Safa Baris (2022), Expanding the Clinical and Immunological Phenotypes and Natural History of MALT1 Deficiency Journal of Clinical Immunology.